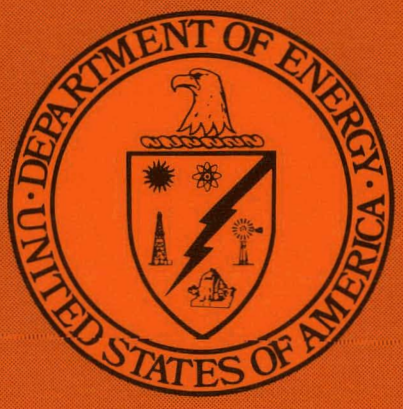

CW-WR-76-015.52A
(DE82007109)

ENGINEER, DESIGN, CONSTRUCT, TEST AND EVALUATE A PRESSURIZED FLUIDIZED BED PILOT PLANT USING HIGH SULFUR COAL FOR PRODUCTION OF ELECTRIC POWER

Phase I—Preliminary Engineering

Phase II—Final Design

Phase III—Construction

Annual Report for the Period March 1, 1979—February 29, 1980

Work Performed Under Contract No. AC21-76ET10417

Curtiss-Wright Corporation
Wood-Ridge, New Jersey

TECHNICAL INFORMATION CENTER
UNITED STATES DEPARTMENT OF ENERGY

DISCLAIMER

DISCLAIMER

This report has been reproduced directly from the best available copy.

Available from the National Technical Information Service, U. S. Department of Commerce, Springfield, Virginia 22161.

Price: Printed Copy A08
Microfiche A01

Codes are used for pricing all publications. The code is determined by the number of pages in the publication. Information pertaining to the pricing codes can be found in the current issues of the following publications, which are generally available in most libraries: *Energy Research Abstracts, (ERA); Government Reports Announcements* and Index (*GRA* and I); *Scientific and Technical Abstract Reports (STAR);* and publication, NTIS-PR-360 available from (NTIS) at the above address.

CW-WR-76-015.52A
(FE-1726-52A)
(DE82007109)
Distribution Category UC-90e

ENGINEER, DESIGN, CONSTRUCT, TEST AND EVALUATE A PRESSURIZED FLUIDIZED BED PILOT PLANT USING HIGH SULFUR COAL FOR PRODUCTION OF ELECTRIC POWER

PHASE I - PRELIMINARY ENGINEERING

PHASE II - FINAL DESIGN

PHASE III - CONSTRUCTION

Annual Report

March 1, 1979 Through February 29, 1980

Curtiss-Wright Corporation
Power Systems Division
Wood-Ridge, New Jersey 07075

Prepared for the United States
Department of Energy
Under Contract No. EX-76-C-01-1726

TABLE OF CONTENTS

TABLE OF CONTENTS (Continued)

LIST OF ILLUSTRATIONS

LIST OF ILLUSTRATIONS (Continued)

LIST OF ILLUSTRATIONS (Continued)

LIST OF ILLUSTRATIONS (Continued)

LIST OF TABLES

Section 1.0

INTRODUCTION AND SUMMARY

1.1 INTRODUCTION

Production of clean, cost-competitive electric power from coal requires advances in combustion and power conversion technology. One promising approach to improved power cycle efficiency involves application of a Pressurized Fluidized Bed (PFB) Combustor for combustion of high sulfur coal in the presence of a sulfur sorbent material. Bed temperature is controlled to maintain the bed temperature below 1750°F by removing heat from the PFB with heat exchanger tubes using a portion of incoming compressed air as coolant, while the balance of compressed air is used for combustion. The coolant air is heated substantially to bed gas temperature and mixes with the products of combustion after they are cleaned of particulates but prior to entering a gas turbine expander. The reduced percentage of turbine gas directly involved in coal combustion results in substantially less gas to be cleaned of particulates.

The most obvious application of the PFB combustor to commercial, base load power production is in a combined cycle system. The PFB combustor, in this concept, would supply energy to a gas turbine-generation unit, and a waste heat boiler at the exit of the gas turbine system would supply steam for a steam turbine-generator unit. A simplified flow diagram for the air-cooled PFB combined cycle system is shown in Figure 1.1.

The objective of this program is to evaluate the commercial potential of a power generating concept that includes the pressurized, fluidized bed combustion of coal in conjunction with a combined gas-steam turbine cycle. The capability to burn high sulfur coal in an environmentally acceptable manner is a major objective of the program. The program involves conceptual design of a 500 MW central station power plant, supporting experimental work to establish component and process operating characteristics, and the design, construction and operation of a PFB pilot plant at Wood-Ridge, New Jersey that can be used to evaluate the commercial concept.

PRESSURIZED FLUIDIZED BED/GAS TURBINE
HIGH SULFUR COAL COMBINED CYCLE PLANT

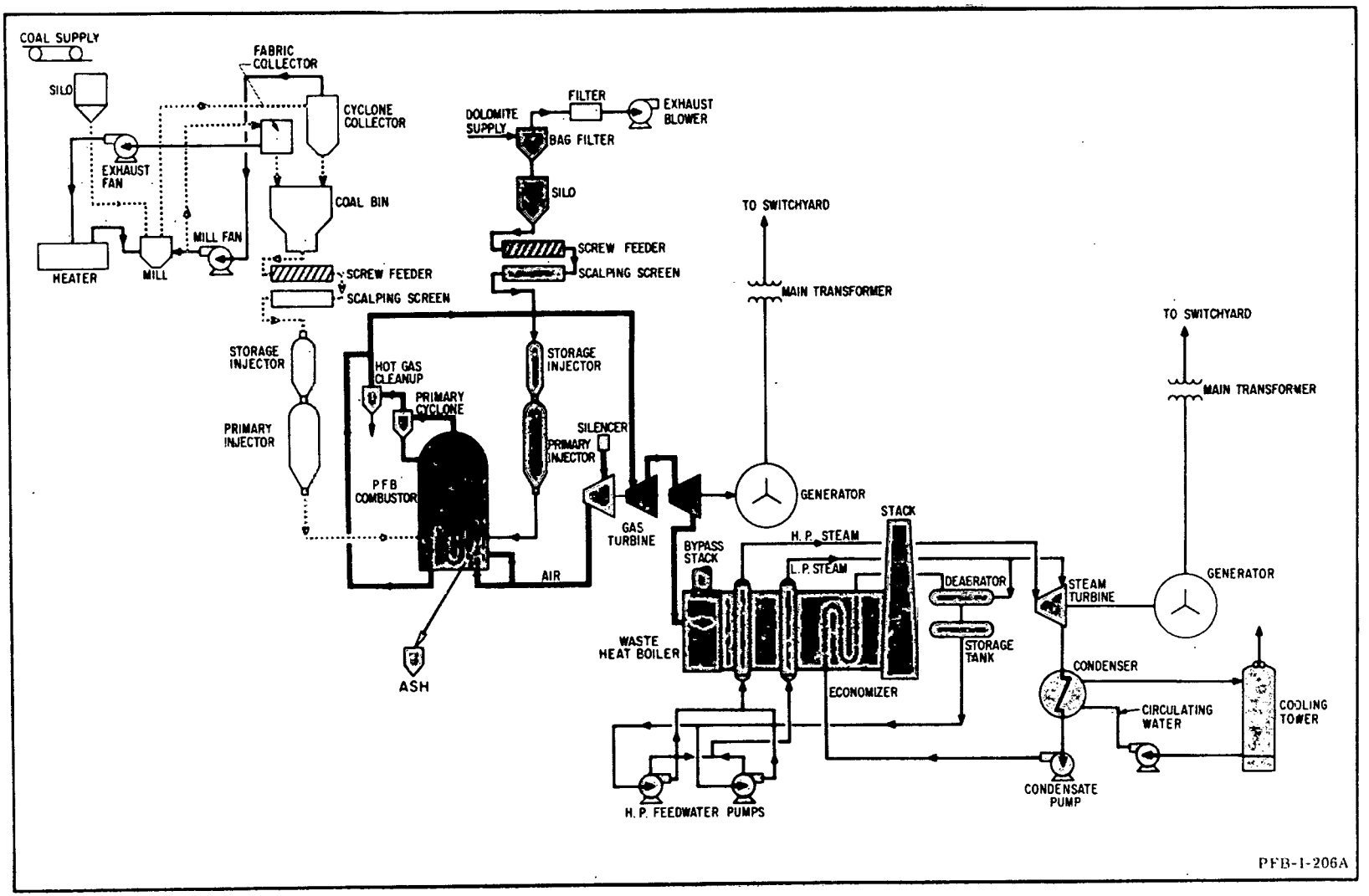

Figure 1.1
1-2

1.2 EXECUTIVE SUMMARY

The extended test program on the SGT/PFB Technology Unit, which was designed, erected and placed in operation during previous reporting periods, was completed. Total operating time is 3378 hours which includes 2681 hours burning coal and 1205 hours total turbine engine operation. Significant performance and operational milestones which have been completed during the past year are summarized below:

- Over 2000 Hours on Candidate Heat Exchanger Tube Materials at Design Temperature During Which Durability of Iron Base Alloy for PFB Heat Exchanger Tubes was Demonstrated

- Generated Electric Power with Gas Turbine Operating on PFB Coal Combustion Gas for 1000 Hours with no Appreciable Erosion or Corrosion of Turbine Rotor Blades and Stator Vanes

- Evaluated and Improved Hot Gas Cleanup System During Which Mean Particle Size of 1.3 Microns and a Loading of 0.054 Grains/Scf was Achieved

- Durability of Hot Ash Solids Lock Hopper Valves for Over 1000 Hours Without Leakage and Stellite Coated Butterfly Gas Valve Operating Successfully for Over 900 Hours in a Highly Erosive Environment was Demonstrated

Several heat exchanger materials, the best among them being Type 310 Stainless Steel, are suitable for use in the Pilot Plant. A corrosion rate of 0.001 inches/1000 hours of exposure was observed and is considered insignificant to tube life since the schedule 40 pipe has a wall thickness of .237 inches. This is based upon a tube fabricated from 4 inch schedule 40 pipe.

Heat transfer performance testing of a heat exchanger tube without external fins indicated that their arrangement can be almost equally effective to finned tubes at a lower cost.

The gaseous emission levels encountered were less than Federal and State of New Jersey emission regulations for the Pilot Plant. SO_2 level of $\leq$ 0.3 lb/10^6 Btu and NO_x level of $\leq$ 0.2 lb/10^6 Btu was observed. Sulfur capture efficiency of 95% with Ca/S mol ratio of 1.5 was achieved when operating on coal with a sulfur content of 3%. The utilization of dolomite was more efficient than other PFB investigations and is attributed to the low fluidized velocity, the deep bed and the recycle cyclone.

Significant results of the recently completed SGT/PFB Technology Unit test program indicate that the performance of the PFB process and the durability of the heat exchanger, turbine blades, and other hardware were satisfactory and support proceeding to the Pilot Plant phase.

The overall condition of both the Rover small gas turbine and the heat exchanger tube bundle after test indicates that the Pilot Plant can be constructed and operated for the required test period without corrosion/erosion failures on these components.

Corrosion potential of the PFB gas stream entering the turbine is lower than expected. Analysis of turbine fly ash deposits indicated alkali metal (sodium plus potassium) levels of 1%. Phase identification indicated high melting point complex sodium and potassium compounds. Sodium and potassium sulfates, if present, were below limits of detectability.

Several of the twelve alloy coating combinations evaluated in the turbine appear suitable for the Pilot Plant turbine, based upon corrosion/erosion penetration data obtained. The Fe-Cr-Al-Y vapor deposited (ATD-17) coating provided the greatest resistance to corrosion/erosion on the stator while the platinum-aluminide (RT-22) coating provided similar resistance on the rotor blade. The surface penetration or loss was $\leq$ 1 mil for these coatings.

The hot gas cleanup system operated at an overall efficiency of 97% and achieved an outlet loading of .046 to .056 grains/scf with a mean particle size of 1.4 micron and a maximum particle size below 10 micron.

The rate of attack on the alloys and coatings investigated for the heat exchanger in the bed falls within the range of results experienced previously by both Curtiss-Wright and other investigators. The corrosion atmosphere within the bed is quite uniform with respect to height and position relative to coal feed.

In addition to this testing, the Pilot Plant final design iterations were performed and preconstruction activities including the long lead procurement of equipment and raw materials proceeded.

Section 2.0

SGT/PFB TECHNOLOGY UNIT

2.1 PFB TECHNOLOGY UNIT DESCRIPTION

The configuration of the PFB Technology Rig for the extended test program is shown in Figure 2.1. The PFB combustor and recycle cyclone are supported within the structural tower. Coal and dolomite receiving storage silos and transport equipment, are shown to the right of the tower. The portion of the building between the silos at the right and the tower contains the coal milling and drying equipment and pneumatic coal and dolomite injection equipment. Modifications to the initial configuration included the addition of two new hot gas cleanup separators and sampling instrumentation, the addition of a re-heat system in the off-take piping to the turbine and the changes to the coal feed system.

A support structure was added to the left of the tower for installation of the modified hot gas cleanup system. During initial test evaluation reported earlier the hot gas cleanup system consisted of a two-stage cyclonic type Aerodyne SV separator. During this test phase the cleanup system was modified to include two additional cyclonic type separators. Gas leaving the recycle cyclone at the top of the PFB combustor enters a Dynatherm cleanup separator from which it flows through a Ducon separator prior to entering the last stage of hot gas cleanup train which is the Aerodyne unit. The cleaned up gas leaving the cleanup system then combines with the clean hot air from the in-bed heat exchanger. The gas mixture is cooled in a quench chamber and exhausted from the facility through a pressure let down valve, a backup exhaust particulate scrubber, a silencer and an exhaust stack (located in the background of Figure 2.1). Prior to reaching the cooling chamber a small portion of the mixed gas is withdrawn isokinetically and is used to power a small gas turbine. This turbine drives an electric generator. The facility components are fully instrumented with pressure and thermocouple probes, flow meters, and isokinetic particulate grab sample probes to provide performance and operating data.

SGT/PFB TECHNOLOGY UNIT

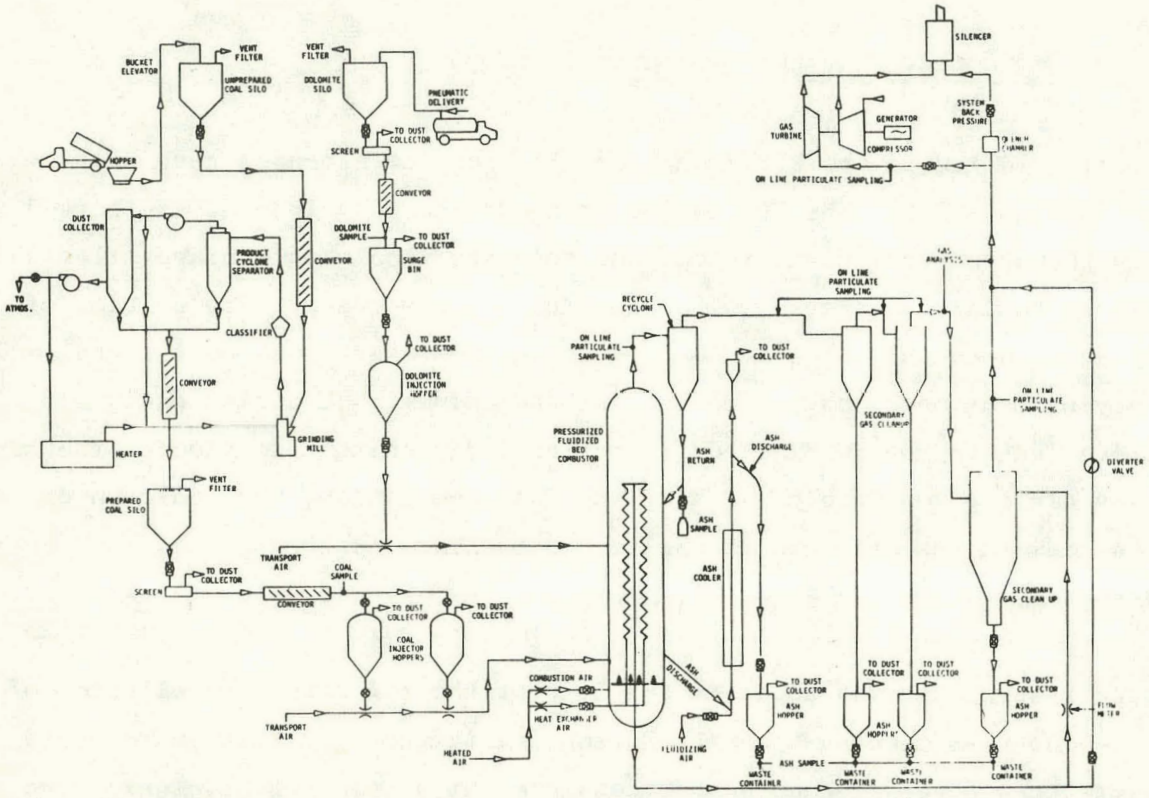

PFB-I-163C

PFB Technology Rig Flow Schematic

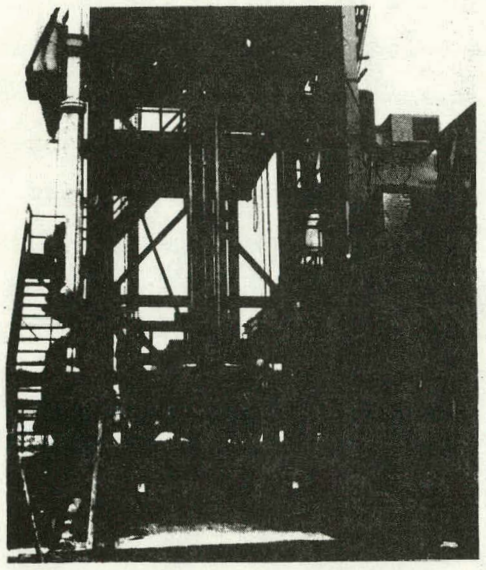

Heat Exchanger Installation in Combustor

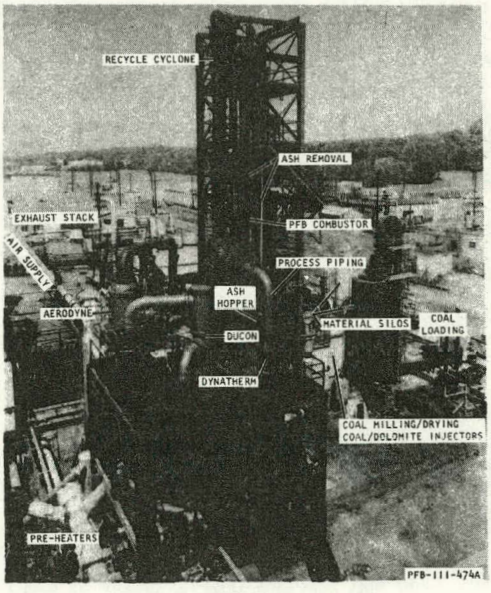

SGT/PFB Rig

Figure 2.1

A data logging, monitoring and limit alarming system and a computer control center is located in the control room. Also located in the control room is an on-line gas analysis system, the operators panel for coal milling and drying and the operators panel for the coal and dolomite feed systems.

2.2 TECHNOLOGY UNIT MODIFICATIONS

2.2.1 Hot Gas Cleanup System

Initial evaluation of the hot gas cleanup system performance indicated the need for improvement before the planned turbine materials test could proceed. Therefore, two additional cyclonic separator units were designed, fabricated and installed in series after the recycle cyclone and the existing Aerodyne separator was changed from a configuration which split the dirty gas into primary and secondary flow paths to a configuration that flows all the dirty gas in the primary path and uses clean air in the secondary path. This cleanup unit is shown in Figure 2.2.

Foundations, supporting structure and platforms to accommodate the two additional hot gas cleanup stages (Figure 2.2) were added as shown in Figure 2.1. Also added were process piping, ash lock hoppers and control panels. The ash lock hopper systems are similar to the design for the Aerodyne unit. Each ash hopper system is provided with a 55 gallon drum to receive the ash dump. During normal operation the hoppers are emptied periodically into the drums and the weight of ash content recorded. The sequence of ash hopper operation is fully automatic for both the dump and fill cycles and is controlled from a remote control panel.

2.2.2 Particulate Sampling

An isokinetic particulate grab sampling system was designed, fabricated and installed in the Technology Unit for evaluation of cleanup system performance.

HOT GAS CLEANUP SYSTEM

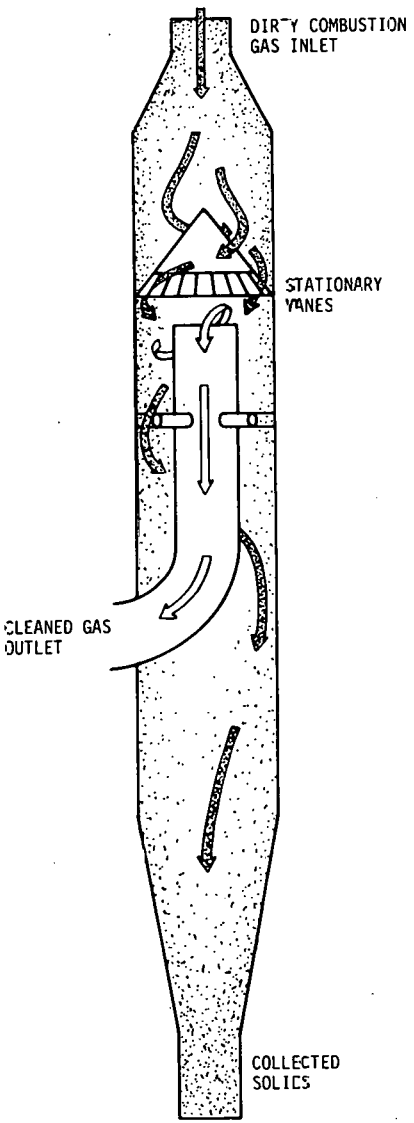

DYNATHERM "WHIRL-A-WAY"

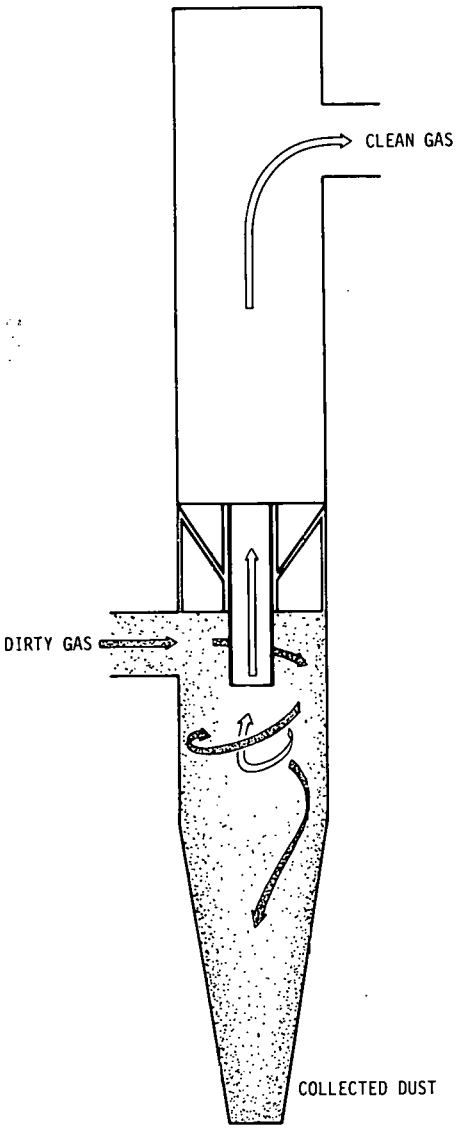

DUCON CYCLONE

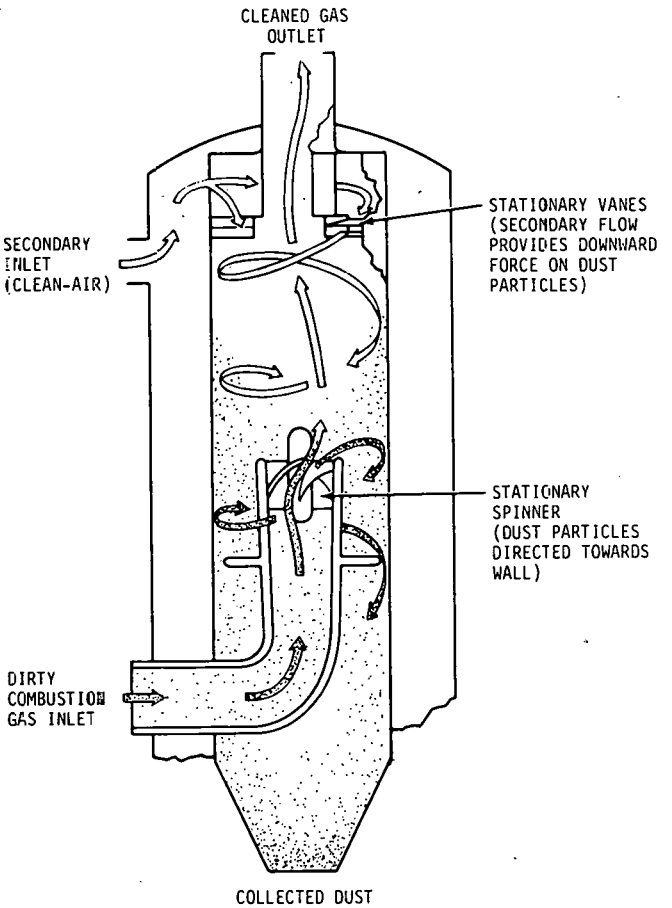

AERODYNE 2 STAGE SEPARATOR

PFB-III-390A

Figure 2.2

The system provides the capability of determining particulate loading at 6 locations in the PFB process piping. Samples can be taken upstream and downstream of each of the three hot gas cleanup cyclones, in the PFB combustor freeboard, and in the gas turbine inlet piping. Instrumentation needed to control particulate sample flow rate and monitor filtering temperature and filter pressure drop is included with each probe. The probes are located radially at the pipe center of area. Heat tracing is used to insure that sample temperature is always maintained above the point of H_2O condensation.

2.2.3 Turbine Inlet Gas Reheat

With the addition of the cleanup units to the hot gas cleanup system, loss in gas temperature through the small piping occurred. Thus the turbine engine inlet temperature would not meet design requirements. To obtain the additional heat required a kerosene reheat nozzle was installed in the off-take piping to the turbine. The flow of kerosene at the reheat nozzle was controlled by the gas temperature entering the turbine. Approximately 150°F manual reheat was required to achieve the gas turbine inlet temperature of 1550°-1600°F.

2.2.4 Coal Feed System

Modification to the coal feed lines and sequencing control logic of the coal feed system were made to maintain continuous mass flow and to assure smooth transfer between the two coal vessels which are alternately used for the feed and fill sequence. The dual coal feed lines (one from each of the 1-hour capacity coal injection vessels) to the injection nozzle at the PFB combustor were replaced by a single pipe connected to a "Y" joining the two coal injector vessels. A continuous air purge was provided in the coal transport line beneath each coal injector vessel to prevent migration of coal when the vessel was in the standby condition. Pressurization valves with metal seats were replaced with soft seated valves providing zero leakage in a closed position.

2.3 TEST PROGRAM

During previously reported testing of the PFB Technology Rig, test operations were directed towards the evaluation of the design and off-design performance characteristics of the pressurized fluidized bed combustor, the in-bed heat exchanger and hot gas cleanup equipment in support of Pilot Plant and Commercial Plant designs.

Testing continued during this reporting period with the primary objectives of the Extended Test Program as follows:

- Evaluation of Candidate Heat Exchanger Tube Materials to Determine Resistance to Corrosion and Erosion

- Evaluation of Candidate Turbine Blade and Vane Materials and Coatings to Determine Resistance to Corrosion, Erosion and Deposition

- Evaluation of Revised Hot Gas Particulate Cleanup Devices

A chronological summary of the test program through the current period is presented in Table 2.1. Tests 8 through 11 were conducted during this period, accumulating 1787 coal burning hours.

Prior to initiating an extended test of gas turbine rotor blade and stator vane for materials evaluation, the performance of the modified hot gas cleanup system was determined (Test 8). While operating at design conditions, the cleanup system was evaluated by taking particulate grab samples at the inlet and outlet of each gas cleanup unit over an extended period of time. The ash catch from each unit was also collected and weighed throughout the program testing.

During these tests the PFB Technology Unit was operated at the Pilot Plant 100% power simulated design point. Key operating parameters are shown in Table 2.2.

TABLE 2.1

SGT/PFB TECHNOLOGY UNIT TEST CHRONOLOGY

Test		Bed Temperature °F	Coal Fired Hours	Gas Turbine Hours	Total Air Blowing Hours
1	Functional and Leakage Checks	1000-1550	25		105
2	Shakedown	1400	25		55
3	Design Point Check	1665	66		179
4	Design Point and Off-Design	1400-1750	321		524
5	100-Hour Endurance	1650	108		121
6	Gas Turbine Checkout	1650	52		82
7	Extended Test Operation	1400-1650	297		360
8	Evaluate Added Separator Stages (1st Build Cleanup)	1650	196		215
9	150-Hour Gas Turbine Test	1650	284	150	321
10	Evaluate Separator Modifications (2nd Build Cleanup)	1650	98		124
11	1000-Hour Turbine Test (2nd and 3rd Build Cleanup)*	1650	1209	1056	1292
	Total		2681	1206	3378

* 720 Hours Coal Burning on 2nd Build Cleanup System

489 Hours on 3rd Build Cleanup System

TABLE 2.2

SGT/PFB TECHNOLOGY UNIT INTERNAL CONDITIONS

Space Velocity, fps	2.7
Bed Inlet	
Airflow, pps*	2.283
Temperature, °F	506.0
Pressure, psia	101.5
Coal Flow, pph	577.0
Sorbent Flow, pph	As Required
Coal/Air	.0702
Bed Outlet	
Gas Flow, pps	2.443
Temperature, °F	1650
Pressure, psia	94.95

* Includes Purge Air to Bed

A typical plot of key operating parameters for the PFB combustor is shown in Figure 2.3.

Initial performance evaluation of the as-designed first stage and second stage gas cleanup units utilized in the revised hot gas cleanup system, indicated the need for an improvement in performance prior to initiating long term operation (1000 hours) of the gas turbine engine. However, the turbine was operated for 150 hours to establish baseline blade and vane material data and to provide shakedown of the engine flow loop (Test 9). This testing also showed the need for improving the hot gas cleanup system.

The cyclone units were, therefore, partially disassembled and observed design deficiencies in flow capacity, structural integrity and sealing were corrected. Testing was again initiated to evaluate these design changes (Test 10). Test results indicated that although the first stage cyclone performance decreased, the second stage performance was significantly improved resulting in an overall improvement in hot gas cleanup system performance.

PHASE I OPERATION
100% DESIGN POWER

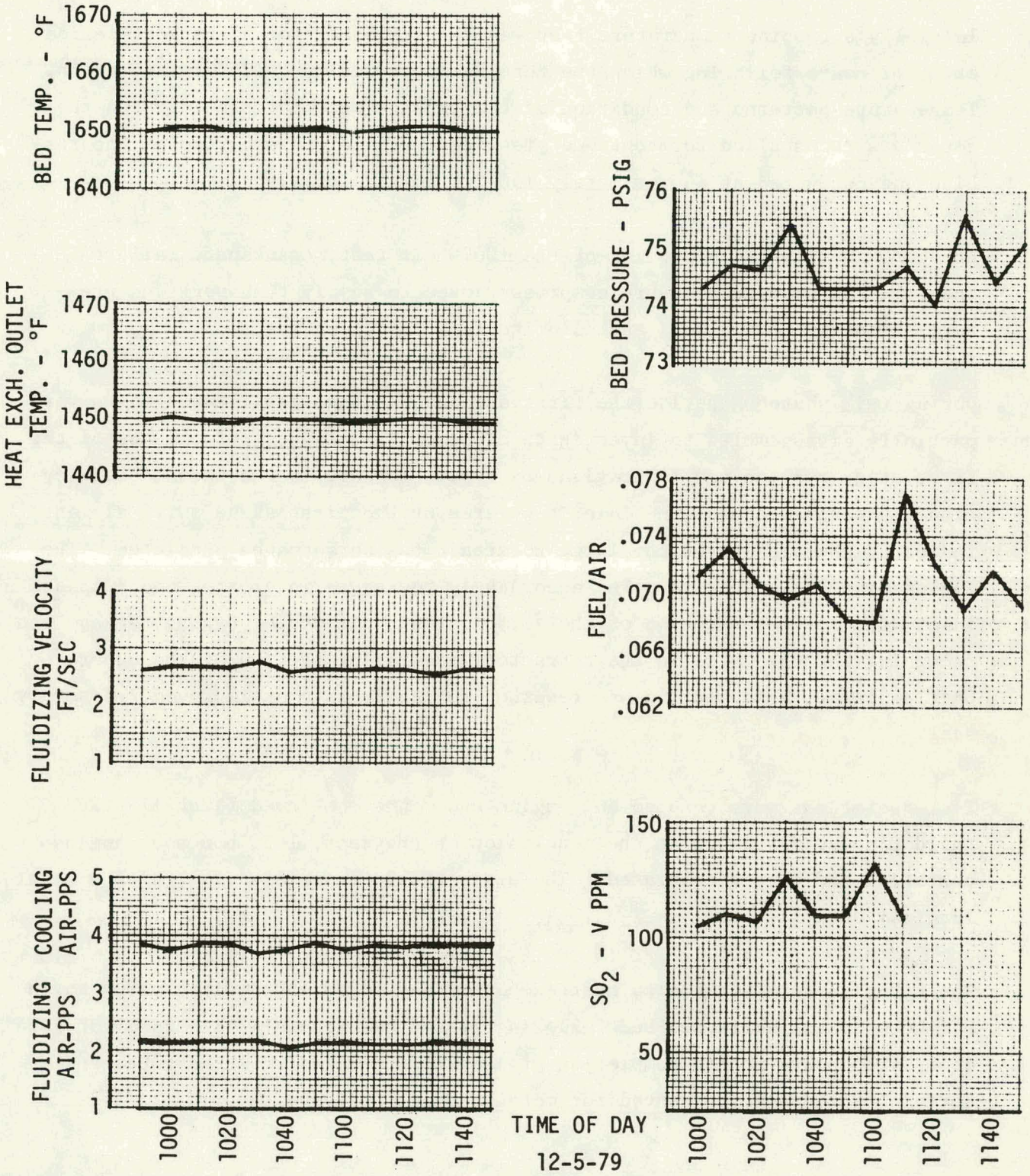

Figure 2.3

The gas turbine engine which had completed 150 hours of baseline testing was rebuilt with new turbine blades and vanes incorporating a variety of materials and coatings in preparation for the 1000-hour test (Test 11).

Initially a turbine temperature test was run at 1550°F for a checkout period of 1-1/2 hours following which the turbine rotor was removed for inspection. Temperature patterns and condition of the turbine were satisfactory and the rotor was reinstalled for continued testing. Periodic inspection of the turbine was conducted at approximately 150-200 hour intervals.

At approximately the mid-point of the 1000-hour test, crankshaft failure occurred on the high pressure compressor used to supply transport and pressurization air to the coal and dolomite feed injection system.

During this shutdown period the first and second stage gas cleanup units were partially disassembled to investigate cause of the reduced performance of the first stage cyclone and indications of bypass leakage in the second stage cyclone. Measurements of the inlet flow area of the first stage swirl element indicated the area to be too large to attain the performance predicted. The cyclone internals were reworked accordingly to reduce inlet area and increase inlet velocity. Inspection of the second stage unit showed bypass leakage was occurring through voids in the refractory insulating section of the upper baffle plate. This section was reworked to incorporate an improved refractory seal.

Test operations were resumed and engine endurance continued (Test 11 - 3rd Build Cleanup System). At the conclusion of the test, 1056 hours of engine operation had been accumulated. The engine was disassembled for turbine metallurgical analysis.

The PFB nine-tube air cooled heat exchanger and material specimen racks which had been installed in the bed following Test 6 had accumulated a total of 2084 coal fired hours at the completion of Test 11. Samples from the tubes and material specimens were removed for metallurgical analysis.

2.4 ANALYSIS OF RESULTS

During the period from Test 8 to Test 11, which comprises the evaluation of gas cleanup system modifications and the turbine 1000-hour endurance test, thirty-two test points were selected for analysis, based on stabilization of the operating conditions for one hour or more. A summary of the operating conditions for these points is shown in Tables 2.3, 2.4 and 2.5.

Periodically during the testing, samples of coal, dolomite, and bed material were taken for chemical analysis. The results are presented in Tables 2.6, 2.7 and 2.8.

For this test program, a Pittsburgh seam coal from West Virginia, Valley Camp Coal Company No. 3 mine, and Pfizer 1337 dolomite from Ohio were used.

2.4.1 Overall Heat Balance

Overall heat balances were calculated for the thirty-two test points and are presented in Table 2.9a and b. The heat loss to the outside through the combustor wall was estimated to be 90 Btu/sec based on outside combustor temperature readings taken during the running of a single point, which is equivalent to approximately 4.5% of the coal input. The variation in percentage unaccountable heat loss averaged 7%. The following factors were considered possible sources for the unaccounted heat loss:

1. Stabilization of bed and heat exchanger out temperatures, fluidizing airflow, cooling air tube flow and coal flow

2. Coal flow and airflow measuring system

3. Thermocouple correction

4. Combustion efficiency

Table 2.3

SGT/PFB RIG OPERATION CONDITIONS

1ST BUILD - TEST 8 & 9

COAL BURNING - HRS	10	54	104	148	175	212	303	374	453
DATE	5/31	6/2	6/4	6/6	6/8	6/19	6/29	7/13	7/17
TIME	9:49	8:05	9:45	23:00	1:40	14:37	13:00	4:00	7:58
POINT NO.	1	2	3	4	5	6	7	8	9
W_A BED, pps	2.21	2.26	2.26	2.23	2.22	2.26	2.26	2.17	2.07
W_A COOL, pps	4.49	3.59	3.98	3.98	4.03	3.1	3.65	3.92	3.84
V_S, fps	2.54	2.61	2.62	2.64	2.62	2.66	2.70	2.65	2.56
EXCESS AIR, %	24	27	35	35	32	50	25	32	29
Ca/S	2.45	1.23	1.25	1.19	1.20	1.83	.67	.76	.99
AIR INLET TEMP. °F	499	510	505	499	510	505	511	495	505
BED GAS TEMP, °F	1687	1650	1644	1655	1651	1653	1650	1645	1646
BED PRESSURE, psia	97.8	95.3	95.0	95.1	94.8	93.8	91.7	89.1	91.0
HEAT EXCH. OUT TEMP, °F	1434	1470	1449	1458	1448	1493	1473	1451	1455
SO_2, PPM							182		137
NO_x, PPM							174		167
O_2, %							9.5		9.2
CO, PPM							4.96		8.2
CO_2, %							16.5		17.2
SULFUR RETENTION, %							90.0		92.8
COAL FLOW, PPH	619	619	582	572	586	522	618	563	544
DOLO FLOW, PPH	225	113	108	101	104	142	67	75	94
AERODYNE PRI/SEC.	1.65	1.68	1.59	1.52	1.48	1.44	1.49	1.51	1.48

Table 2.4

SGT/PFB RIG OPERATION CONDITIONS

2ND BUILD - TEST 10 & 11

COAL BURNING - HRS.	512	557	607	678	720	782	844	941	1016	1061	1103	1165	1207	1271
DATE	9/9	9/11	9/12	9/21	9/23	9/27	9/30	10/6	10/9	10/12	10/18	10/22	10/25	10/28
TIME	14:30	14:45	20:25	12:25	4:32	11:15	9:45	1:30	16:35	10:25	7:48	10:48	1:45	6:00
POINT NO.	10	11	12	13	14	15	16	17	18	19	20	21	22	23
W_A BED, pps	2.80	2.23	2.08	2.13	2.10	2.10	2.20	2.13	2.01	2.09	2.10	2.05	1.92	2.06
W_A COOL, pps	3.86	3.96	3.50	4.19	4.03	3.99	3.34	3.91	3.92	3.97	3.99	3.96	3.34	4.01
V_s, fps	-	2.74	2.62	2.68	2.58	2.64	2.59	2.66	2.54	2.61	2.62	2.67	2.65	2.65
EXCESS AIR, %	57	49	22	23	27	28	44	38	28	39	34	28	41	31
Ca/S	1.01	1.10	.90	.63	.94	1.16	1.14	1.11	.64	1.33	1.12	.68	1.07	1.06
AIR INLET TEMP, °F	504	497	494	494	499	501	506	503	499	512	505	499	515	503
BED GAS TEMP, °F	1650	1518	1650	1654	1641	1650	1649	1644	1658	1649	1653	1654	1666	1654
BED PRESSURE, psia	89.2	84.5	89.2	89.6	89.7	88.5	94.5	89.0	88.2	88.8	88.6	85.0	80.6	86.3
HEAT EXCH. OUT TEMP, °F	1497	1333	1446	1445	1437	1451	1473	1444	1453	1448	1450	1450	1489	1450
SO_2, PPM	138	72				191	130	127	51	36	23			
NO_x, PPM	125	156				96	76	76	19	10	6			
O_2, %	-	-								37	42			
CO, PPM	4.2	5.9				10				10	10			
CO_2, %	14.0	10.4				11	7	7	2	3	3			
SULFUR RETENTION, %	90.6	95.3				89.4	91.9	92.3	97.2	97.8	98.7			
COAL FLOW, PPH	576	482	549	561	541	531	493	541	552	528	550	556	475	550
DOLO FLOW, PPH	97	88	82	59	85	103	94	91	54	107	88	56	75	86
AERODYNE PRI/SEC FLOW	1.48	1.02	1.09	1.47	1.46	1.60	1.65	1.49	1.50	1.55	1.51	1.47	1.51	2.09

Table 2.5

SGT/PFB RIG OPERATION CONDITIONS

3RD BUILD - TEST 11

COAL BURNING - HRS.	1326	1387	1459	1517	1582	1628	1651	1696	1749
DATE	11/4	11/12	11/15	11/18	11/21	11/29	12/1	12/3	12/5
TIME	15:40	9:40	5:35	6:40	3:20	23:53	3:40	1:10	10:50
POINT NO.	24	25	26	27	28	29	30	31	32
W_A BED, pps	2.04	2.27	2.10	2.08	2.07	2.09	2.16	2.16	2.13
W_A COOL, pps	3.79	3.94	3.82	3.94	3.92	3.84	3.78	3.70	3.79
V_S, fps	2.64	2.68	2.63	2.60	2.59	2.64	2.70	2.68	2.65
EXCESS AIR, %	34	36	39	33	29	32	34	32	31
Ca/S	1.23	2.43	1.14	.81	.76	.91	1.28	.98	.80
AIR INLET TEMP, °F	517	524	501	510	506	494	512	504	516
BED GAS TEMP, °F	1657	1662	1655	1671	1677	1662	1650	1653	1652
BED PRESSURE, psia	85.0	84.0	88.8	89.3	89.9	89.0	89.4	90.2	89.5
HEAT EXCH. OUT TEMP, °F	1464	1463	1461	1468	1471	1457	1460	1453	1449
SO_2, PPM								96	108
NO_x, PPM								15	11
O_2, %								-	-
CO, PPM								13	6
CO_2, %								3	3
SULFUR RETENTION, %								94.9	94.1
COAL FLOW, PPH	529	565	513	531	544	535	547	553	550
DOLO FLOW, PPH	96	266	113	83	80	94	113	88	69
AERODYNE PRI/SEC FLOW	1.56	1.55	2.24	1.67	1.55	1.47	1.60	1.55	1.56

Table 2.6

COAL SAMPLE ANALYSES

SAMPLE	RAILROAD CAR #57086	RAILROAD CAR #85657	RAILROAD CAR #15650	RAILROAD CAR #153757	INJECTOR F-2	INJECTOR F-3	AVERAGE F-2 AND F-3	AVERAGE F-2 AND F-3
TEST	8	9	9	10-11	11	11	11	11
COAL BURNING HOURS	0-200	200-300	300-490	490-850	850-1100	1100-1325	1325-1700	1700-1750
HHV BTU/LBM	14185	14030	14080	13741	13648	13628	13208	13202
ASH	8.33	7.95	9.89	8.05	6.92	7.22	6.59	7.05
CARBON	73.27	73.58	73.07	73.18	73.62	73.35	75.59	74.96
HYDROGEN	6.00	5.95	6.05	5.98	5.64	5.90	5.70	5.94
NITROGEN	1.10	1.12	1.05	1.30	1.44	1.15	1.09	1.38
SULFUR	2.53	2.75	2.99	2.96	2.70	2.77	3.03	2.94
OXYGEN BY DIF	8.77	8.65	6.95	8.53	9.66	9.61	8.00	7.60

RESULTS IN % BY WEIGHT

PFB-III-291A

Table 2.7

DOLOMITE SAMPLES ANALYSES

COAL BURNING HOURS	0-450	450-1050	1050-1200	1200-1325	1325-1625	1625-1750
TEST	8-9	10-11	11	11	11	11
CALCIUM OXIDE	29.83	31.10	32.94	32.93	27.40	32.75
MAGNESIUM OXIDE	23.81	22.88	19.49	19.65	24.20	19.85
LOSS ON IGNITION	46.06	45.78	47.40	47.13	48.14	46.78
INERTS	0.30	0.24	0.17	0.19	0.26	0.5

RESULTS IN % BY WEIGHT

PFB-III-287A

Table 2.8

BED MATERIAL SAMPLE ANALYSES

TEST	8-9	11	11	11	11	11
DATE	6-18-79	10-15-79	10-29-79	11-19-79	11-26-79	12-10-79
CALCIUM OXIDE	26.94	22.56	21.70	23.27	23.26	26.34
MAGNESIUM OXIDE	23.98	13.95	17.27	20.16	19.29	14.97
CARBON DIOXIDE	1.35	2.28	2.97	.98	.92	4.27
SULFATE AS SO_3	41.48	60.44	56.23	53.47	54.3	50.99
SODIUM	.02	.008	< .01	< .01	.01	.02
POTASSIUM	.02	.006	< .01	< .01	.01	.01
IRON	4.69	.05	1.15	1.73	1.34	1.72
ALUMINUM	1.42	.61	.62	.35	.77	.79
NICKEL	< .02	.0007	< .01	< .01	.01	.09
CHROMIUM	< .02	.001	< .01	< .01	.01	.02
CHLORIDE	.08	.06	.05	.05	.06	.77

RESULTS IN % BY WEIGHT

Table 2.9a

SGT/PFB RIG OPERATING POINTS

ENERGY BALANCE

		Input Btu/Sec			Output Btu/Sec						Unaccounted	
Test	Pt #	Coal	Air	Total	Products	Ash	Sorbent	Tubes	Loss	Total	Btu/Sec	%
8	1	2533	207	2740	1068	6.6	23.5	1054	90	2242.2	497.8	18.2
8	2	2191	216	2407	1040	5.6	11.9	888	90	2035.5	371.5	15.4
8	3	2205	212	2417	1031	5.6	12.4	955	90	2094.0	323.	13.4
8	4	1957	207	2164	1021	5.0	11.7	983	90	2110.7	53.3	2.5
8	5	2206	210	2416	1017	5.6	12.7	1025	90	2150.3	265.7	11.1
9	6	1966	212	2178	1028	5.0	16.0	797	90	1936.0	242.0	11.1
9	7	2227	215	2442	1039	5.4	9.1	900	90	2043.5	398.5	16.4
9	8	2104	200	2304	999	6.4	10.8	971	90	2077.2	226.8	9.8
9	9	2107	198	2305	988	6.3	8.7	969	90	2062.	243.	10.6
10	10	2120	270	2390	1257	5.3	11.1	989	90	2352.4	37.6	1.6
10	11	1772	206	1978	916	4.1	9.3	844	90	1863.4	114.6	5.8
11	12	2021	188	2209	955	5.1	9.1	985	90	2044.2	164.8	7.5
11	13	2064	194	2258	988	5.2	6.9	1020	90	2110.1	147.9	6.5
11	14	1992	192	2184	962	5.0	9.7	976	90	2042.7	141.3	6.5
11	15	1962	194	2156	968	5.0	11.7	968	90	2042.7	113.3	5.3
11	16	1812	207	2019	996	4.6	10.8	838	90	1939.4	79.6	4.0
11	17	1932	198	2130	972	4.2	10.3	949	90	2025.5	104.5	4.9
11	18	2027	183	2210	933	4.4	6.2	962	90	1995.6	214.4	9.7
11	19	1952	202	2154	974	4.3	11.5	951	90	2030.8	123.2	5.7

Table 2.9b

SGT/PFB RIG OPERATING POINTS

ENERGY BALANCE

(Continued)

		Input Btu/Sec			Output Btu/Sec						Unaccounted	
Test	Pt #	Coal	Air	Total	Products	Ash	Sorbent	Tubes	Loss	Total	Btu/Sec	%
11	20	2005	195	2200	969	4.4	9.6	975	90	2048	152.	7.0
11	21	2036	188	2224	954	4.7	6.5	972	90	2027.2	196.8	8.9
11	22	1768	180	1948	892	4.1	8.1	842	90	1836.2	111.8	5.7
11	23	1980	190	2170	953	4.5	9.7	975	90	2032.2	137.8	6.4
11	24	1935	192	2127	937	4.4	10.9	932	90	1974.3	152.7	7.2
11	25	1970	223	2193	1057	4.3	30.9	959	90	2141.2	51.8	2.4
11	26	1812	193	2005	964	3.9	13.0	948	90	2018.9	- 13.9	- 0.7
11	27	1887	197	2084	972	4.1	9.6	970	90	2045.7	38.3	1.9
11	28	1926	194	2120	975	4.2	11.0	978	90	2058.2	61.8	3.0
11	29	1893	190	2083	972	4.1	11.0	957	90	2034.1	48.9	2.3
11	30	1902	204	2106	998	4.1	12.9	925	90	2030.	76.0	3.6
11	31	1922	204	2126	995	4.1	9.9	902	90	2001.	125.0	5.9
11	32	1927	203	2130	980	4.4	8.0	921	90	2003.4	126.6	6.0

2.4.2 Heat Exchanger Performance

The heat exchanger consisted of 1 bare tube (no external fins) and 8 tubes which had 38 outside fins. All the tubes had 38 inside fin convolutions. The heat transfer coefficients were based on measured air temperatures and the bed temperature. The outside coefficient based on metal skin temperature was calculated only for a short period at the beginning of the tests because metal thermocouples became inoperative later in the test.

The flow distribution among the tubes was estimated from the data obtained by the cold flow and pressure drop testing of individual heat exchanger tubes. Slight flow variations resulted from manufacturing tolerances and slight misalignment of the 18-inch long sections of fins brazed to the ID of the outer finned tube, see Figure 2.4.

A value of 84% fin attachment to the inner surface of the outer tube was used based on metallurgical inspection of other heat exchanger tubes. Furnace test of the insulation between the annular space and the return tube indicated that it contracted at temperature. The resultant air gaps reduced the insulation effectivensss to 85%. A small additional heat interchange through the insulation is assumed due to metal rings which support the insulation. The heat losses through the insulation, the air gaps, and the metal rings contribute to the heat interchange between the annular section and the return tube.

Outside heat transfer coefficients for the bare and the middle finned tube are shown in Figure 2.5. The high coefficient shown at 512 hours corresponds to the high space rate point (3.7 ft/sec). Although it is known that higher space rate has positive effect on heat transfer, it is believed that the effect indicated in the figure probably may be due to suspect thermocouple readings. Tube No. 5 which is located in the middle of the combustor had the highest coefficient. Tubes located near the combustor wall (No. 1, 3, 7, 9) had lower heat transfer coefficients because of wall effects. These coefficients varied with change in bed particle size and bed temperatures. The outside heat transfer coefficients calculated by using metal temperatures are higher than using air temperatures. The difference may be due to metal thermocouple readings or assumptions made in the calculation of internal heat transfer using air temperatures.

HEAT EXCHANGER TUBE ASSEMBLY

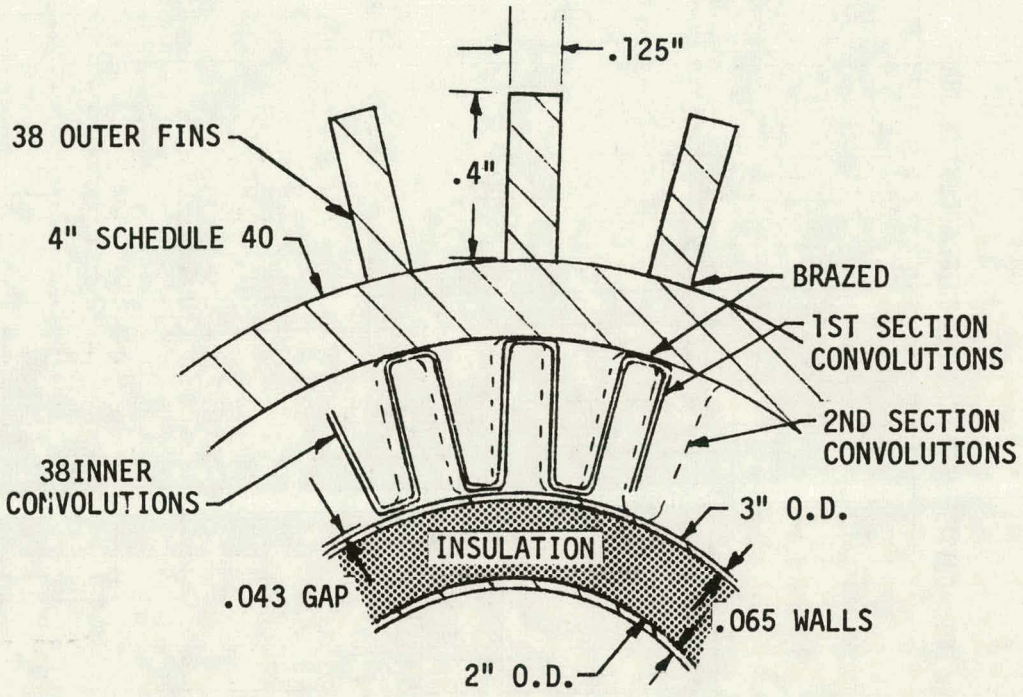

Figure 2.4

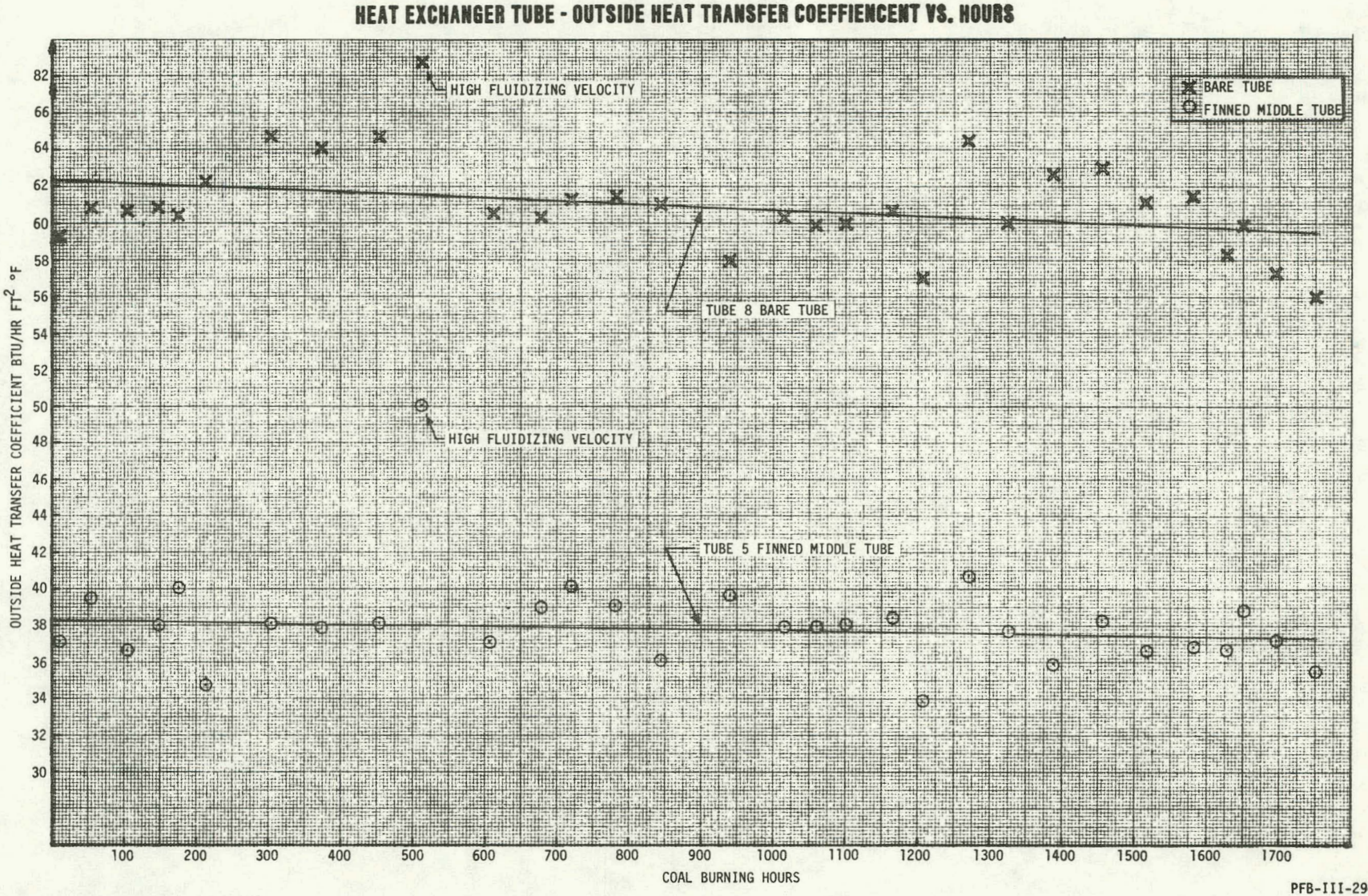
HEAT EXCHANGER TUBE - OUTSIDE HEAT TRANSFER COEFFIENCENT VS. HOURS
OUTSIDE HEAT TRANSFER COEFFICIENT BTU/HR FT² °F
COAL BURNING HOURS
BARE TUBE
FINNED MIDDLE TUBE
HIGH FLUIDIZING VELOCITY
TUBE 8 BARE TUBE
HIGH FLUIDIZING VELOCITY
TUBE 5 FINNED MIDDLE TUBE
82
66
64
62
60
58
56
54
52
50
48
46
44
42
40
38
36
34
32
30
100
200
300
400
500
600
700
800
900
1000
1100
1200
1300
1400
1500
1600
1700
PFB-III-294A

Figure 2.5

Figure 2.5 shows that heat transfer coefficients based on total surface area for the bare tube are higher than those for the finned tube. However, fins increase the total heat transfer area significantly, thus providing greater heat flow per tube. The maximum heat transfer from the bed to the coolant medium is obtained when the product of the outside heat transfer coefficient and the effective total outside area is largest. The finned tube shows higher total heat absorption, but not so high as to preclude consideration of bare tubes of larger diameter (equal to fin OD) with improved internal fin design.

A design study has shown that, there is a possibility that internal performance can be improved using channel fins to achieve overall heat exchange about equal to that of the current externally finned tubes. Figure 2.6 shows the test values of effectiveness obtained for bare tube and finned tube of the same pipe size plotted on the curve of effectiveness versus Number of Transfer Units (NTU) for a heat exchanger of this type. A dashed line on the curve indicates the estimated NTU value for a 5-inch pipe size bare tube based on the overall heat transfer coefficient, U of the bare tube diameter tested and shows an expected effectiveness equal to that of the finned tube.

Dependence of the outside heat transfer coefficients of the bare and the finned tube on the bed particle size is shown in Figure 2.7. This indicates that the coefficient reduction shown by the tubes was primarily caused by the bed particle size becoming coarser with time. A comparison of the outside coefficients between the bare and the finned tubes indicates that the bare tube was affected more than the finned tube by the particle size.

A temperature drop between the upstream and the downstream ends of the inner tubes indicated that a regenerative interchange of heat occurred between the inner tube and the annular space. This recirculation of heat as shown in Figure 2.8 lowered the tube outlet temperatures, thus reducing the overall effectiveness of the system. A better insulation of the inner tube will be used to maintain the higher outlet temperatures.

EFFECTIVENESS FOR HEAT EXCHANGER PERFORMANCE

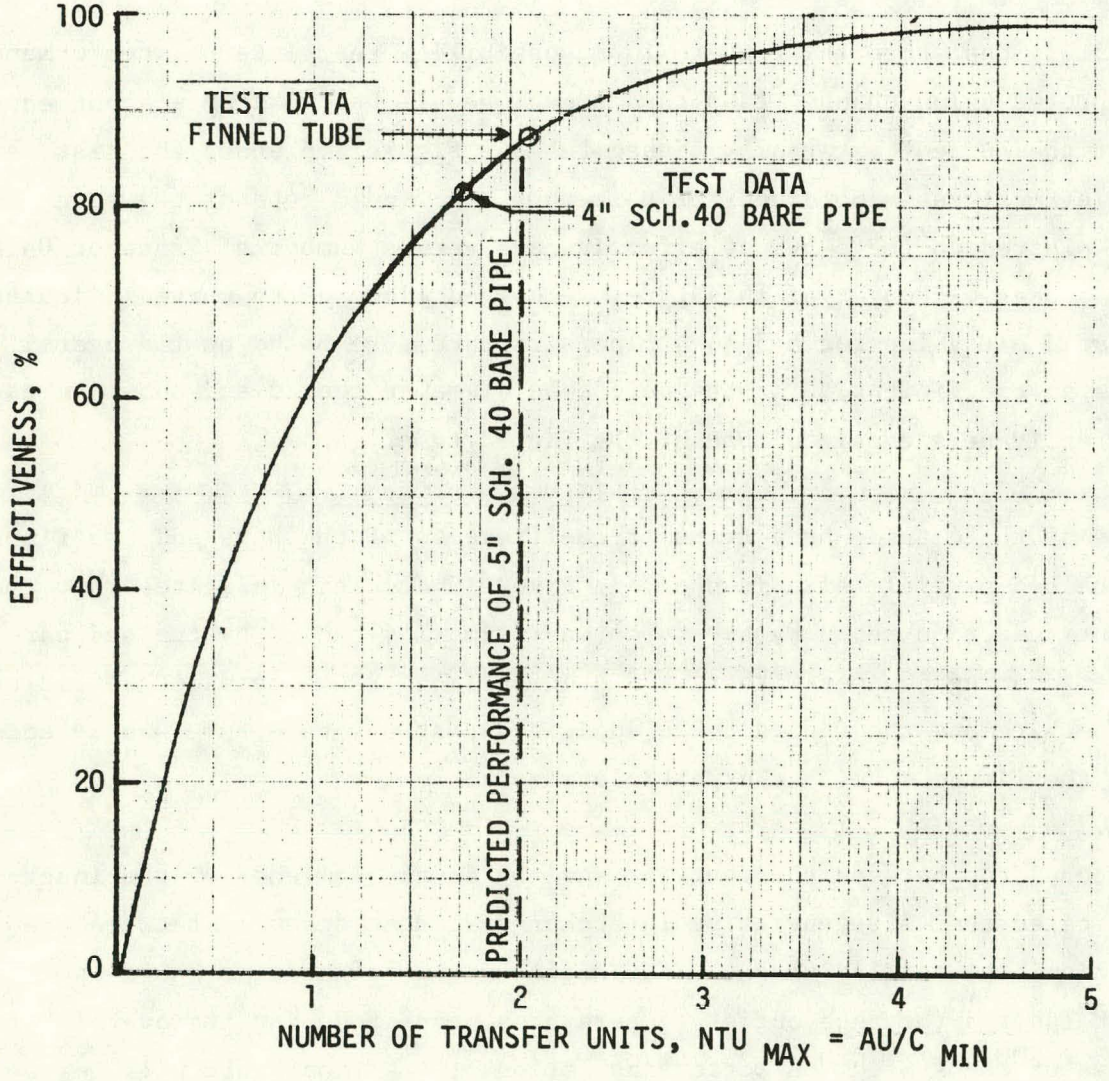

Figure 2.6

HEAT EXCHANGER TUBE - OUTSIDE HEAT TRANSFER COEFFICIENT
VS. BED PARTICLE SIZE

SGT/PFB 1979 TESTS

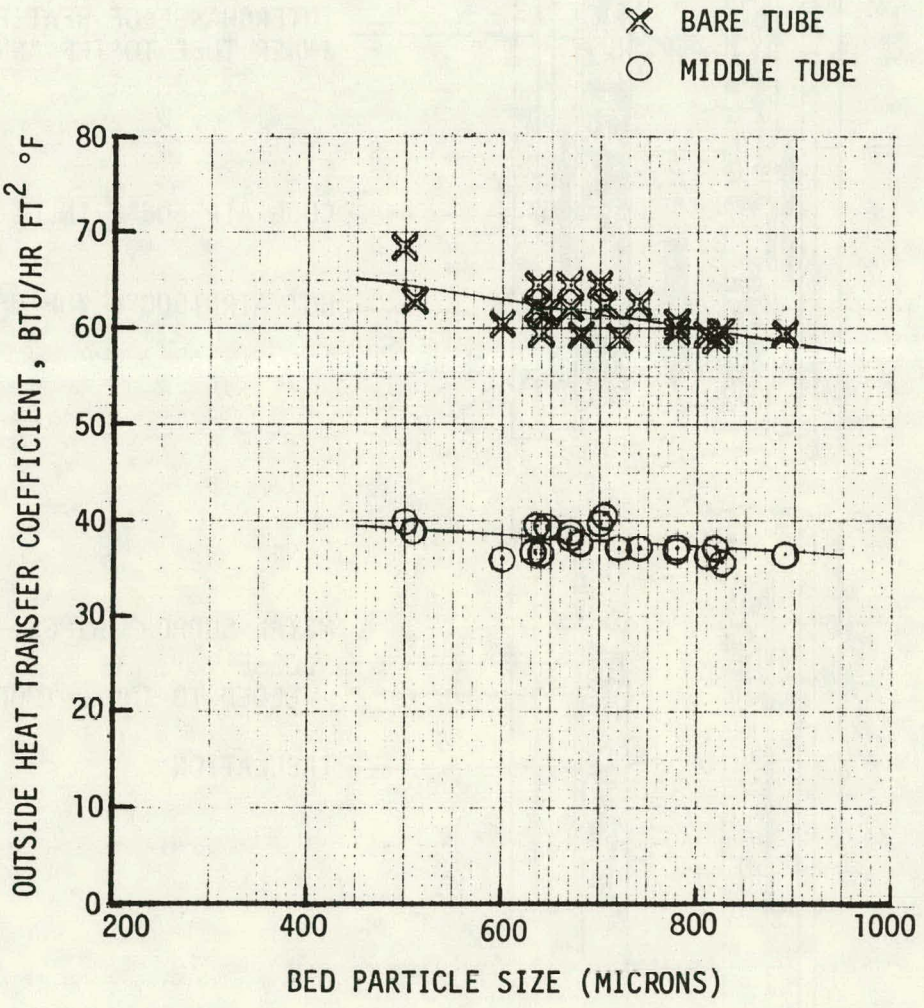

Figure 2.7 PFB-III-292A

HEAT INTERCHANGE IN THE COOLING TUBE

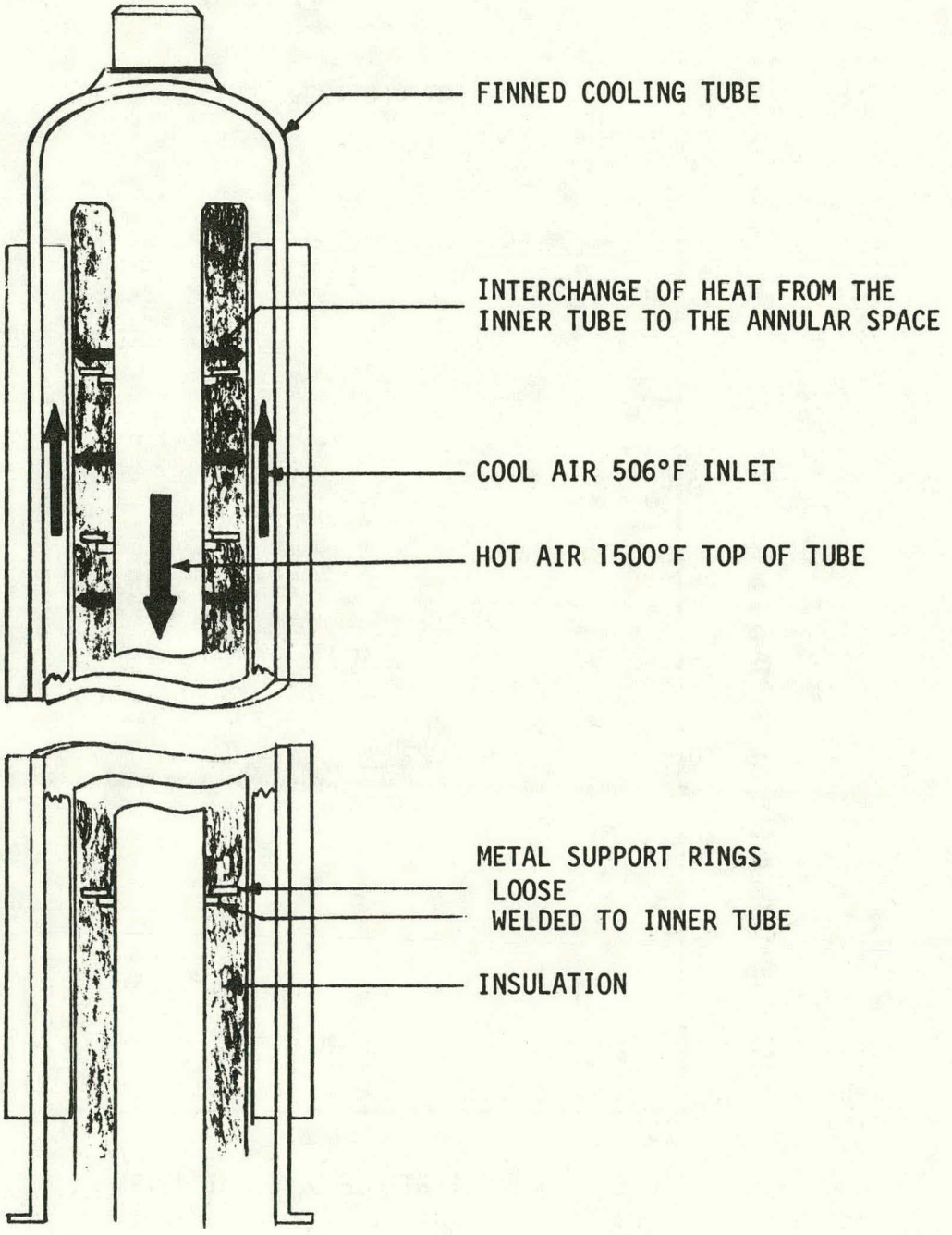

Figure 2.8

Tube No. 5 which is axisymmetrically located in the bundle is most representative of the finned tubes performance in larger beds. The design point heat exchanger effectiveness is 90.13%. Based on design flow of .411 lb/sec per tube, this tube had an effectiveness of 87.6%, Figure 2.9. A parametric analytical study showed that an additional 2.46% in tube effectiveness can be gained by using the proposed channel internal fins over the present corrugated fins. This change in internal fin configuration will increase the effectiveness to 90.06%. The effectiveness can further be increased with improved inner insulation to reduce the circulation effect and with better fin attachment from the new geometry. Thus, design point requirement for heat extraction will be met with the above improvements in heat exchanger internal conditions.

The overall performance of the heat exchanger is shown in Figure 2.10 as a function of the cooling airflow. At the design cooling airflow of 3.7 lb/sec, a heat output of 915 Btu/sec at an outlet temperature of 1466°F was achieved at an effectiveness of 83.5%. In comparison with Tube No. 5 whose effectiveness was 87.6%, it is quite apparent that the combination of radiation losses to the walls and poor circulation around the end tubes, materially decreased the effectiveness of the overall heat exchanger. In larger beds these effects will be greatly reduced because of the larger proportion of tubes not subject to wall effects.

2.4.3 Gas Analysis

Sulfur Retention - The sulfur retention shown in Figure 2.11 was based on the average value of exhaust gas sulfur dioxide content obtained at a specific Ca/S ratio of the coal and dolomite inputs. The stoichiometric line shown represents the theoretical maximum retention for a certain Ca/S ratio. The test points obtained to the left of the stoichiometric line imply sulfur retention greater than is theoretically possible. This may be attributed to the Ca/S ratio within the bed being greater than that in the inputs for some points.

EFFECTIVENESS VS COOLING AIR FLOW

SGT/PFB TUBE #5
(1979)

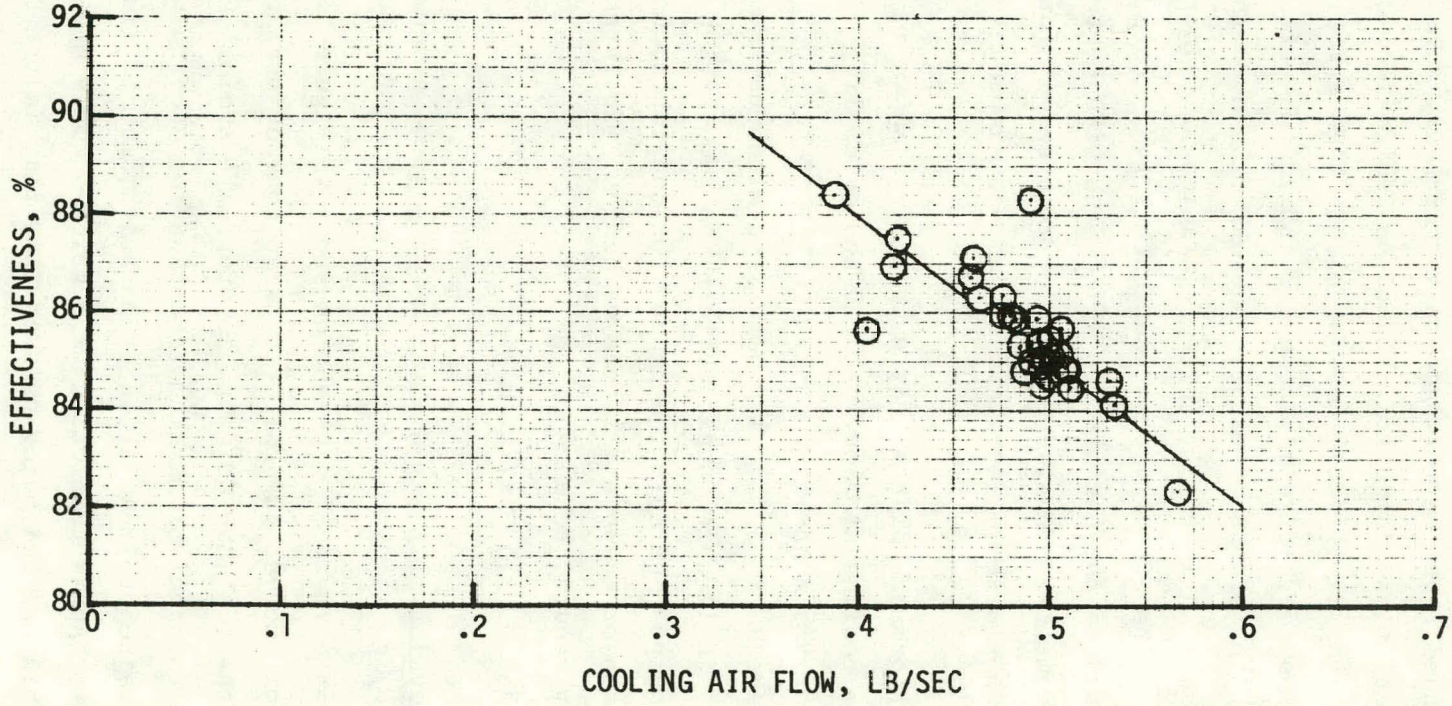

PFB-III-293B

Figure 2.9

OVERALL HEAT EXCHANGER PERFORMANCE

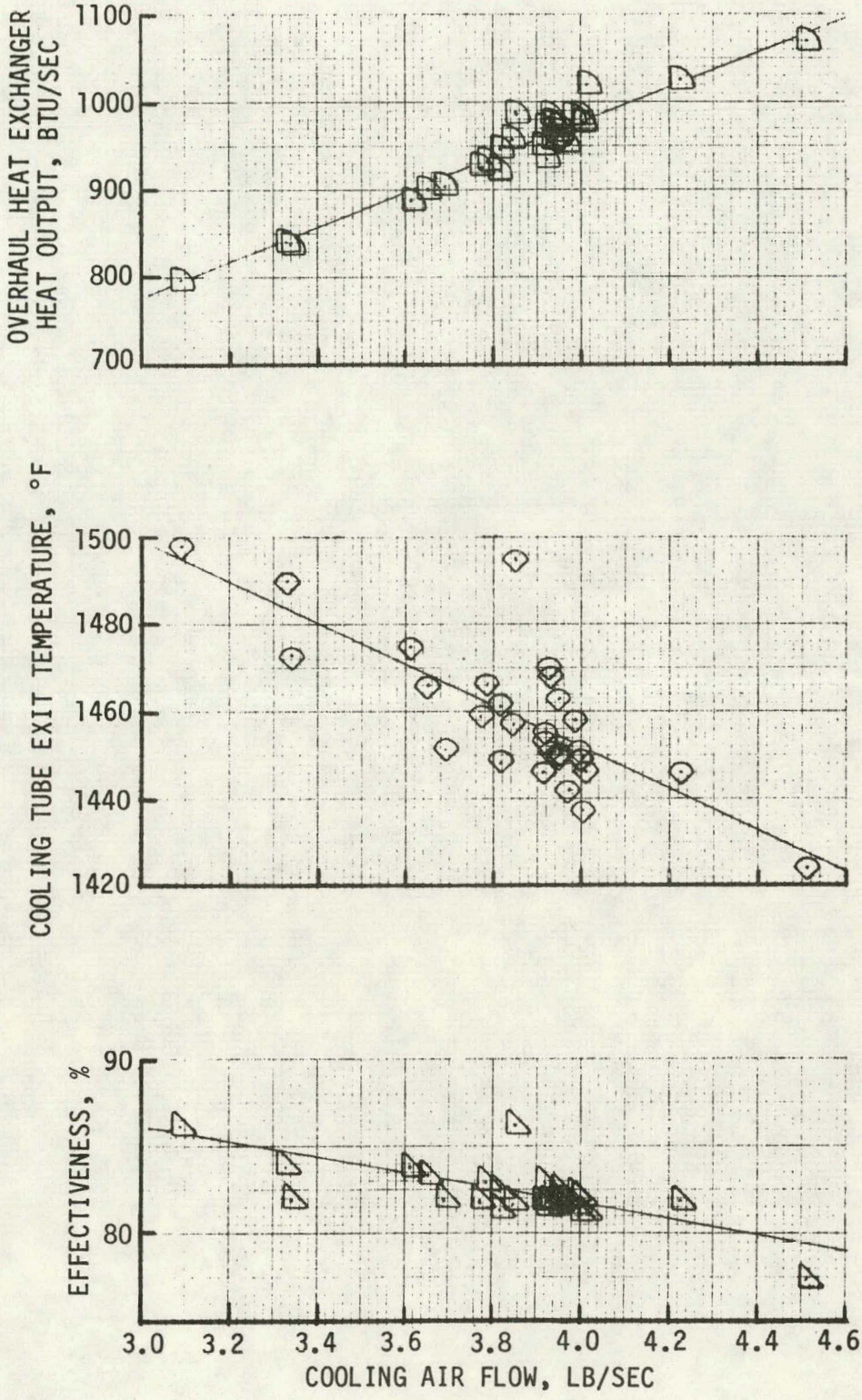

Figure 2.10

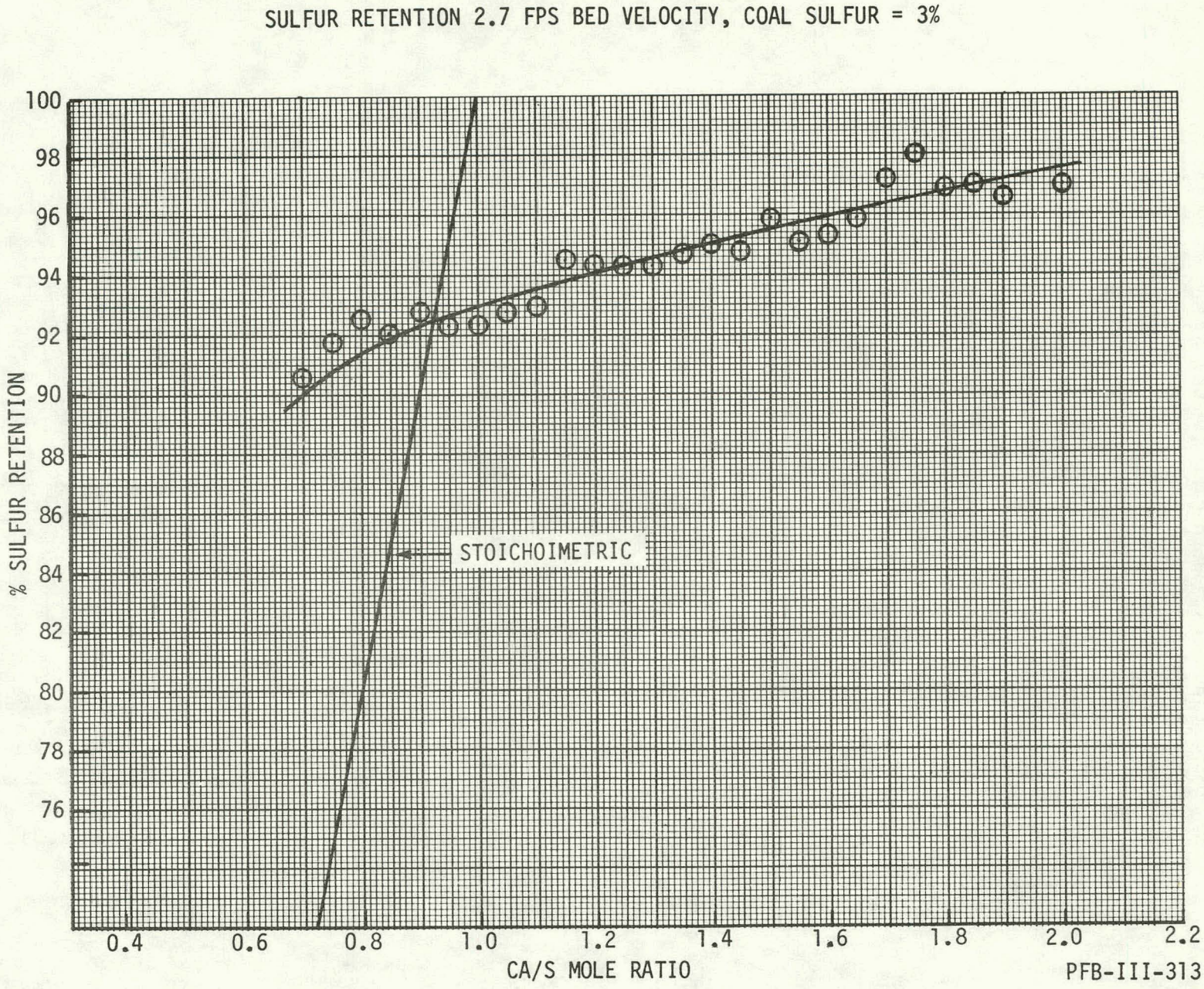
SULFUR RETENTION 2.7 FPS BED VELOCITY, COAL SULFUR = 3%
100
98
96
94
92
90
88
86
84
82
80
78
76
% SULFUR RETENTION
STOICHOIMETRIC
0.4
0.6
0.8
1.0
1.2
1.4
1.6
1.8
2.0
2.2
CA/S MOLE RATIO
PFB-III-313

Figure 2.11

This reason is the most probable in that most of the running in this test was done at a Ca/S ratio of between 1.1 and 1.2. For points below this range, the bed is less likely to be chemically stabilized. Other possible reasons for greater than theoretical sulfur capture are that (a) some of the magnesium in the dolomite may be sulfated, (b) sulfur content in the coal may vary, or (c) some of the sulfur in the coal may be present in the inorganic form which does not break down as readily as the organic sulfur to form SO_2. Post test analyses of coal samples indicated that about 25% of the sulfur in the coal is inorganic.

NO_x Emission - The NO_x emission as a function of the calculated percent oxygen by weight based on coal/air ratio is shown in Figure 2.12. At the design O_2 percent, NO_x averaged between 80 and 90 ppm which is approximately 0.15 lb per million Btu emission. This is much less than the Federal requirement of 0.7 lb per million Btu.

Gas analyses taken at various time intervals during the test are shown in Figure 2.13. The CO emission ranged between 2 and 15 ppm indicating excellent combustion efficiency. The CO_2 emission ranged between 6 and 20% by volume. The gas analysis measurements were taken before dilution with the heat exchanger airflow.

2.4.4 Mass Balance

A solids balance for two periods of continuous running is presented in Table 2.10. The starting and final bed weights are calculated based on the pressure differential across the bed, the weight of a bed particle being equal to the frictional drag required to support it in the gas. The input flows of coal and dolomite are determined from injector weight measurements. The solids from the coal ash and dolomite are based on eight coal and six dolomite samples as shown in Tables 2.6 and 2.7. The sulfur captured is assumed to be entirely in the form of calcium sulfate according to the following reaction:

$$CaO + SO_2 + 1/2\ O_2 = CaSO_4$$

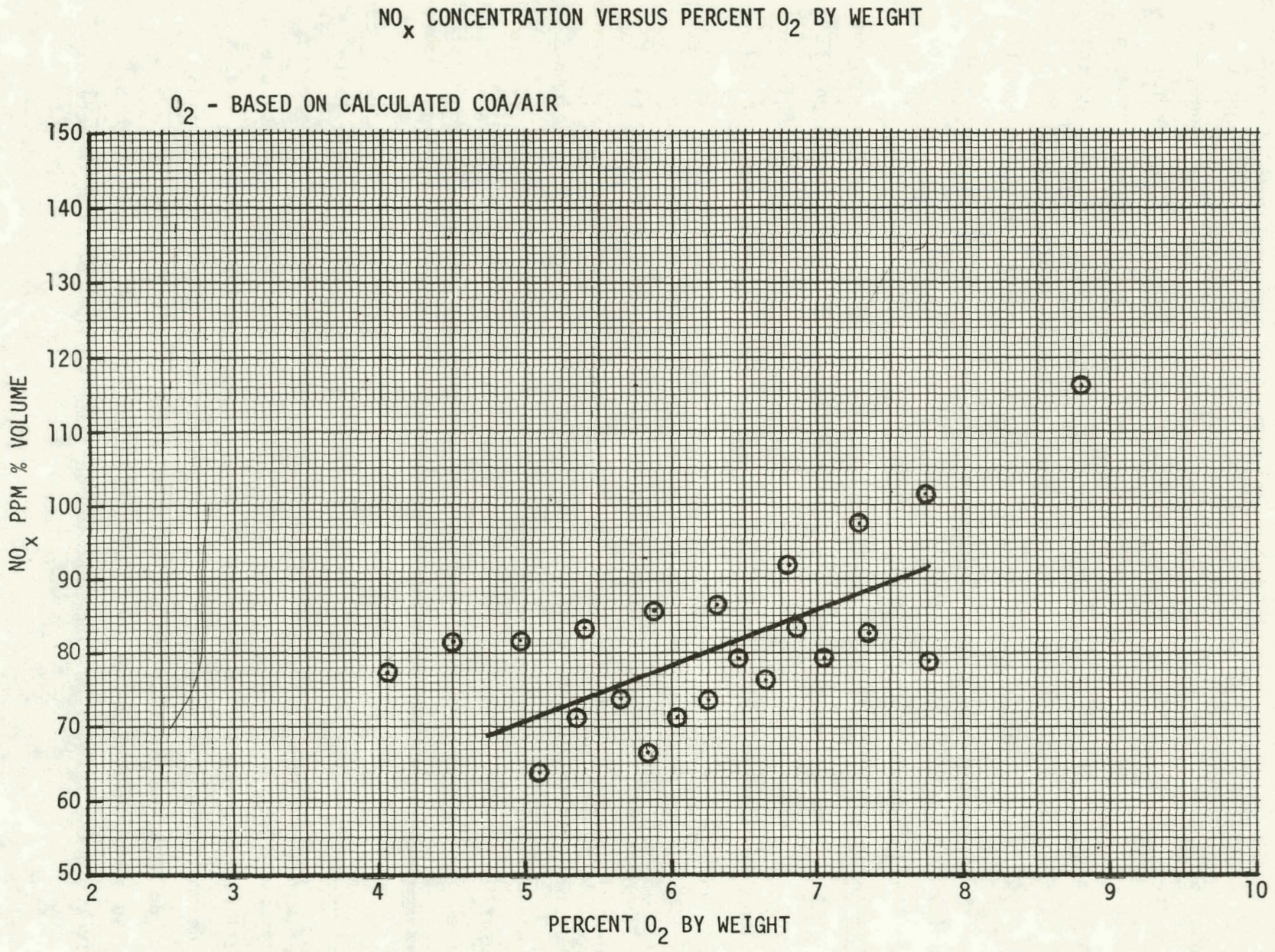
NO_x CONCENTRATION VERSUS PERCENT O_2 BY WEIGHT
O_2 - BASED ON CALCULATED COA/AIR
NO_x PPM % VOLUME
150
140
130
120
110
100
90
80
70
60
50
2
3
4
5
6
7
8
9
10
PERCENT O_2 BY WEIGHT

Figure 2.12

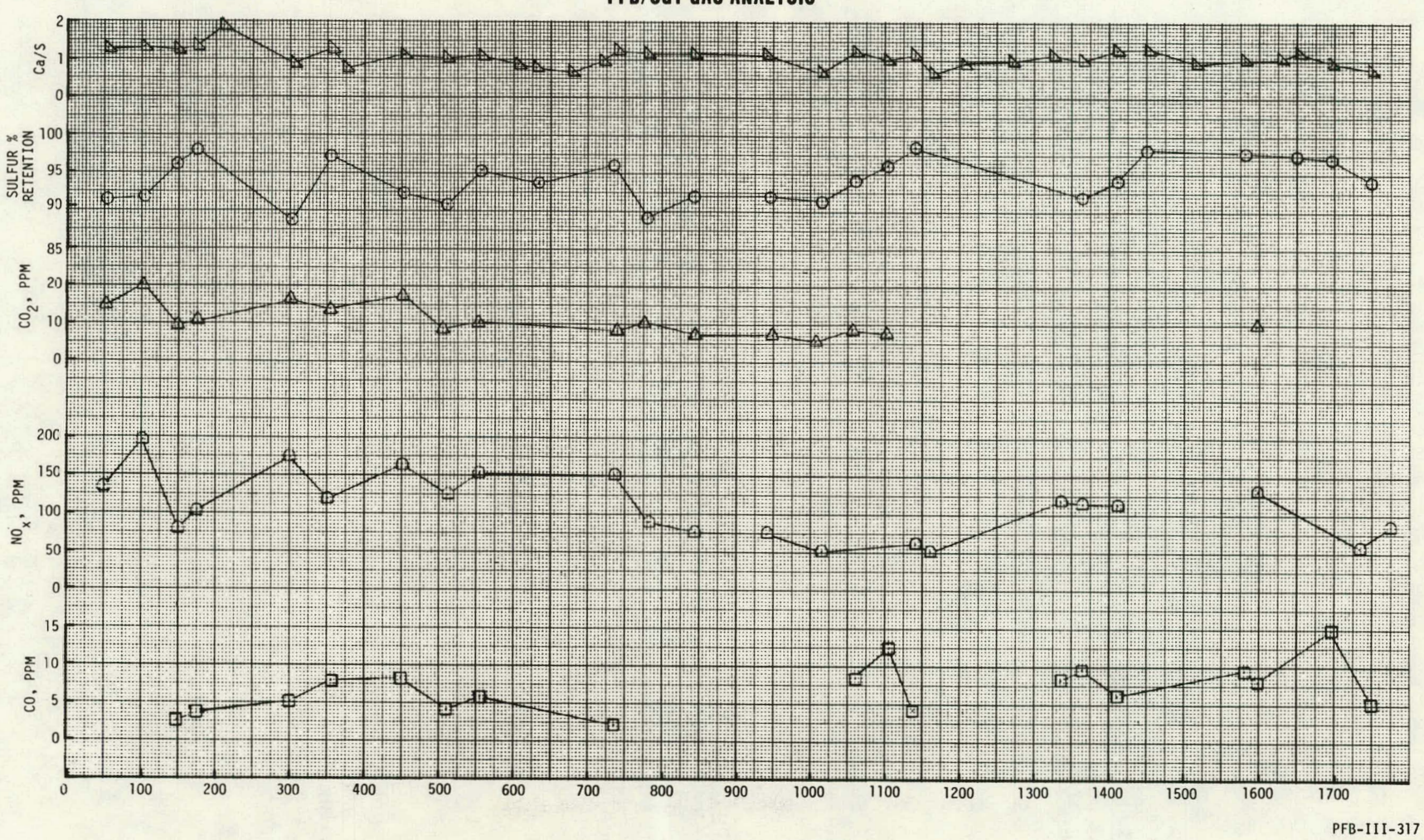
PFB/SGT GAS ANALYSIS
Ca/S
SULFUR % RETENTION
CO_2, PPM
NO_x, PPM
CO, PPM
PFB-III-317

Figure 2.13

TABLE 2.10

MASS (SOLIDS) BALANCE

Period	5-30-79 To 6-8-79	9-24-79 To 10-1-79
Input (Pounds)		
Starting Bed	6,193	7,679
Solids from Dolomite	9,982	7,260
Coal Ash	8,155	5,445
Sulfur As SO_3	6,176	4,650
Total	30,506	25,034
Output (Pounds)		
Final Bed	6,456	7,895
Main Ash Removal	9,892	6,728
Hot Gas Cleanup Catch	10,768	9,964
Solids to Stack	1,611	316
Total	28,727	24,909
Percent Balance	94.2	99.5
Running Time (Hours)	201	144

Material was removed from the bed through the ash cooler approximately twice a day to maintain bed height within ± 1/2 ft. This material was allowed to cool and was then removed from the hopper and weighed. The material removed from the gas stream in the three cleanup cyclones was monitored and representative data is shown in Table 2.11.

The solids going to the stack, part of which passed through the small gas turbine, are determined by isokinetic sampling of the outlet gas as well as by collecting samples of the scrubber inlet and outlet water and weighing the residue after evaporation or filtration.

TABLE 2.11

CYCLONE HOPPER CATCH RATE - POUNDS/HOUR

Test No.	Coal Burning Test Hours	1st Stage	2nd Stage	3rd Stage
8	100 - 200	31.2	10.8	9.8
9	350 - 450	30.8	10.9	9.4
11	650 - 850	44.1	20.0	1.2
11	950 - 1050	39.8	21.8	3.1
11	1200 - 1300	41.1	20.6	0.5
11	1450 - 1550	40.6	25.8	0.5
11	1650 - 1750	30.8	21.8	1.3

2.4.5 Gas Cleanup Performance

The performance of the hot gas cleanup system improved steadily throughout the test. A summary of the system's performance is presented in Table 2.12. Despite increasing bed carryover, each build substantially decreased the system's particulate effluent. In general the 2nd stage was the workhorse of the cleanup system, and the 3rd stage served as the back stop. Data typical of Tables 2.13 through 2.15 served as the basis for the cyclone performance. The performance of each cyclone during each build is discussed below.

1st Stage - The performance of the 1st stage cyclone for each of the three builds is shown in Table 2.13. The configuration of the different builds is shown in Figure 2.14.

The performance of the cyclone during the first build was seriously affected in part by two problems in the "top-hat" swirl element design. The original element was oversized and it deformed during operation at high temperature. Furthermore, the excessive particulate buildup on the outlet pipe centering supports may have disturbed the cyclone's vortex. Caking on the swirl vane element outer diameter was noted. This was eliminated in later tests by modifying the start-up procedure.

In the second build a reinforced, but grossly oversized, conical element was used. The decrease in pressure drop across this element demonstrates its larger flow capacity. Again, there was a large buildup on outlet pipe supports. At the end of the second build the outlet pipe was observed to have been off center. Then, despite the coarser inlet distribution, the performance of this element was worse than the original element.

The final build decreased the inlet area of the conical element. In this case there was no significant build up on the outlet pipe supports. However, by the end of the test the outlet pipe's eccentricity had increased. The test result for this configuration showed an increased collection efficiency with increased pressure drop.

TABLE 2.12

HOT GAS CLEANUP PERFORMANCE

	Build No. 1	Build No. 2	Build No. 3
System Inlet Loading, lb/hr	54.9	60.9	64.6
Overall System Efficiency, %	93	96	97
Outlet Loading, lb/hr	3.7	2.4	1.7
Particulate/Heat Input, $lb/10^6$ Btu	.47	.30	.21

TABLE 2.13

1st STAGE CYCLONE PERFORMANCE SUMMARY

	Build No. 1	Build No. 2	Build No. 3	Prediction Vendor Estimate
Inlet Loading, lb/hr	54.9	60.9	64.6	101
Inlet Mean Dia, Micron	6.7	13	21	5
Collection Efficiency, %	55	30	61	91
Pressure Drop, Inches H_2O	9.3	4.5	12.9*	6

* During initial testing of this build, the pressure drop was 11.0" H_2O.

TABLE 2.14

2nd STAGE CYCLONE PERFORMANCE SUMMARY

	Build No. 1	Build No. 2	Build No. 3	Based On Vendor Estimate
Inlet Loading, lb/hr	25.0	42.7	25.3	9.1
Inlet Mean Dia, Micron	4.6	10	5.1	3.1
Collection Efficiency, %	42	91	90	79
Pressure Drop, Inches H_2O	31	55	73	89

Build No. 1 Original Ducon with leak

Build No. 2 First repair of Ducon; still a small leak
Lengthened outlet pipe
Added refractory on bottom side of outlet pipe assembly

Build No. 3 Second repair/modification of Ducon
Repaired outlet pipe assembly refractory
Added refractory to topside of outlet pipe

TABLE 2.15

3rd STAGE CYCLONE PERFORMANCE SUMMARY

	Build No. 1	Build No. 2	Build No. 3	Based On Vendor Estimate
Inlet Loading, lb/hr	14.6	3.8	2.6	1.88
Inlet Mean Dia, Micron	4.4	1.5-20	2.6	2.5
Collection Efficiency, %	75	37	35	78
Dirty Side Pressure Drop, Inches H_2O	31	26	28	14
Clean Side Pressure Drop, Inches H_2O	32	32	30	28

DYNATHERM DESIGN CONFIGURATIONS

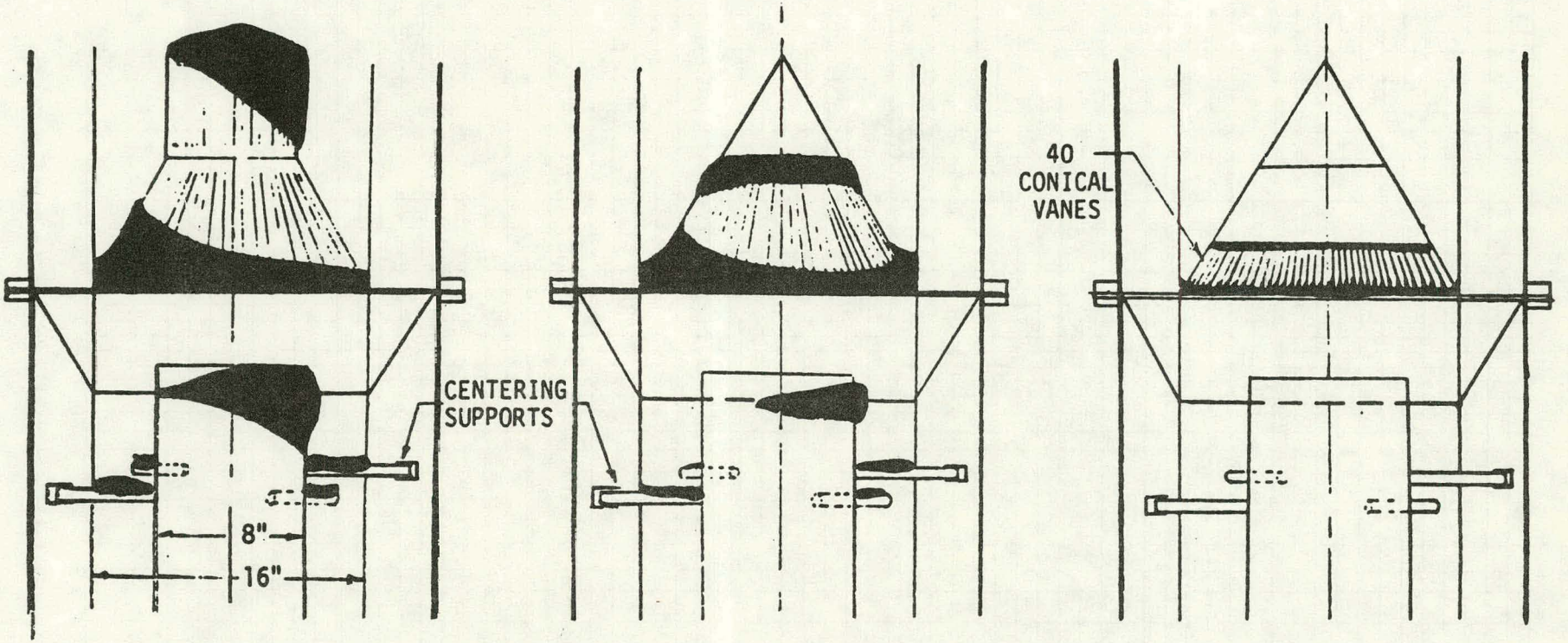

INITIAL DESIGN

REDESIGN #1

FINAL DESIGN

NOTE: SHADED REGIONS INDICATE AREAS OF HEAVY PARTICULATE ACCUMULATION.

PFB-III-547

Figure 2.14

DYNATHERM COLLECTION EFFICIENCY
SGT DATA

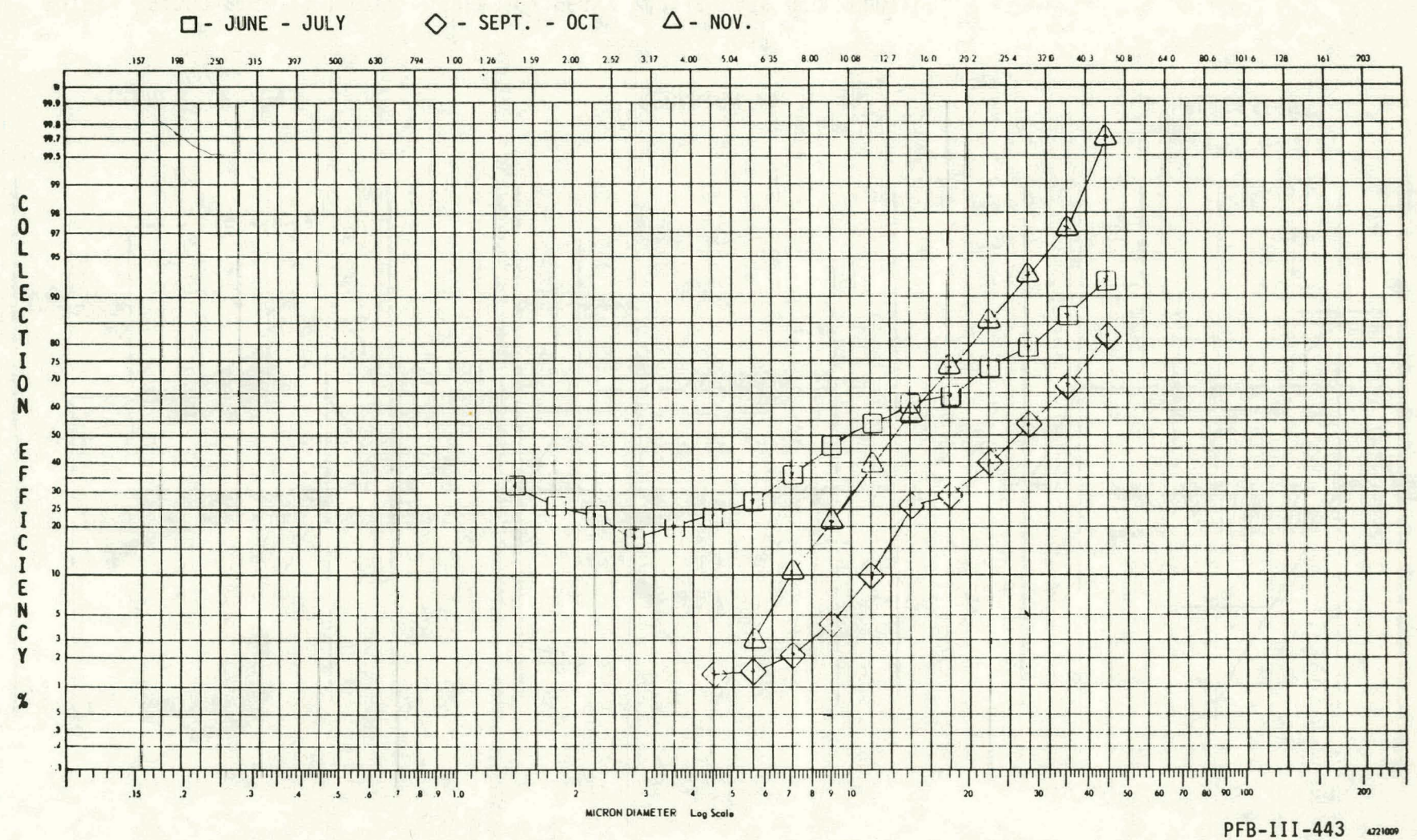

Figure 2.15

The fractional efficiency of the 1st stage unit for the three different builds is shown in Table 2.16 and Figure 2.15.

TABLE 2.16

1st STAGE CYCLONE COLLECTION EFFICIENCY (%)

Diameter Microns	Build No. 1	Build No. 2	Build No. 3
0.0 - 1.0	0.0	0.0	0.0
1.0 - 1.26	0.0	0.0	0.0
1.26 - 1.59	32.4	0.0	0.0
1.59 - 2.00	25.8	0.0	0.0
2.00 - 2.52	23.6	0.0	0.0
2.52 - 3.17	16.8	0.0	0.0
3.17 - 4.00	20.0	0.0	0.0
4.00 - 5.04	23.1	1.4	0.0
5.04 - 6.35	26.8	1.5	3.0
6.35 - 8.09	35.7	3.6	10.5
8.09 - 10.08	46.01	4.2	21.1
10.08 - 12.7	54.0	10.0	39.2
12.7 - 16.0	61.6	26.2	58.0
16.0 - 20.2	64.6	29.3	73.9
20.2 - 25.9	74.1	40.1	85.0
25.9 - 32	79.1	54.5	92.7
32 - 40.3	86.1	68.2	97.2
$\geq$ 40.3	92.3	81.7	99.9

DUCON DESIGN CONFIGURATION

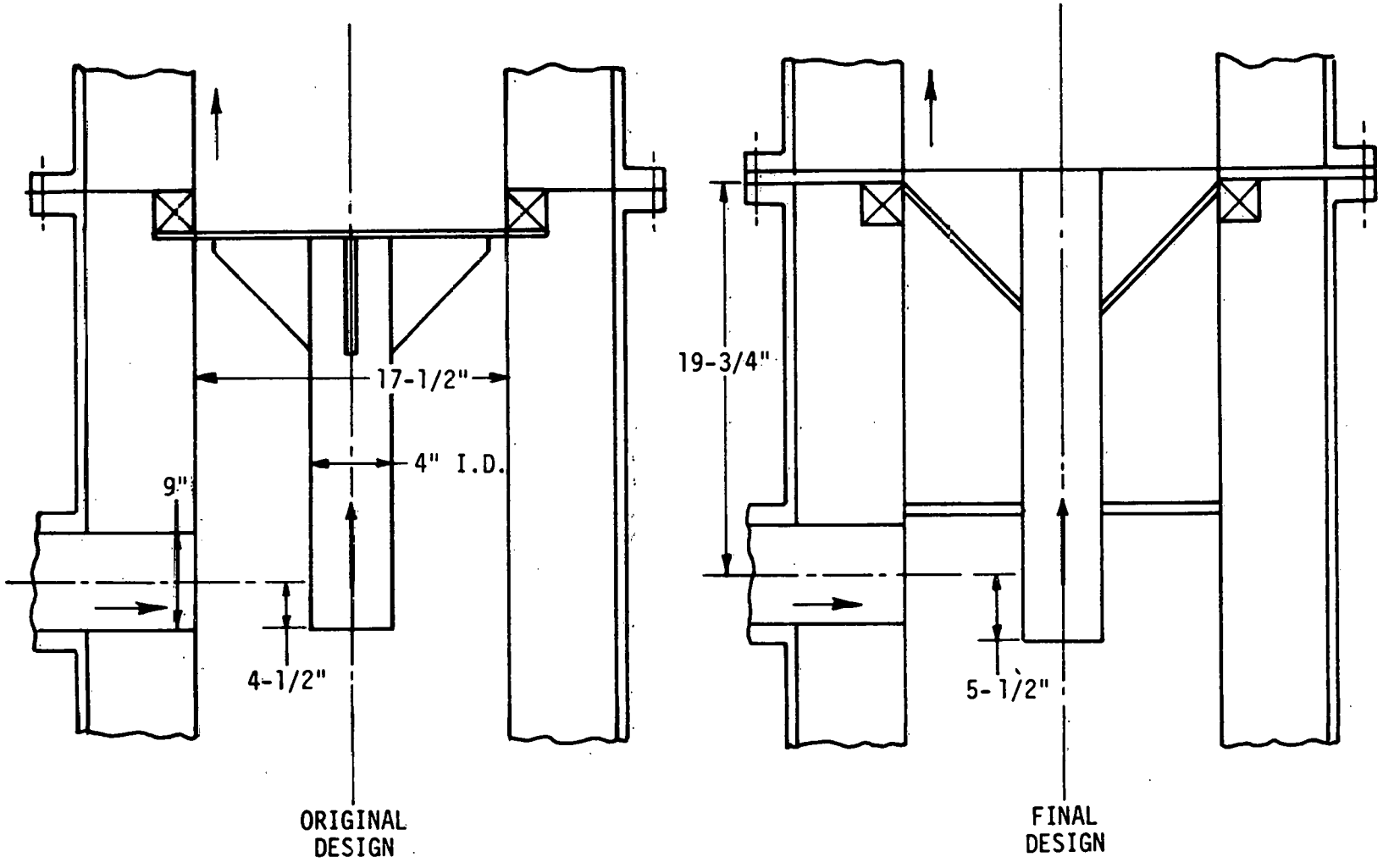

PFB-III-7C

Figure 2.16

2nd Stage - The original 2nd stage cyclone outlet pipe assembly developed a leak from inside the cyclone, around the outlet pipe assembly, to the cyclone outlet. Consequently the pressure drop and collection efficiency shown in Table 2.14 were low. In the second build a slug of refractory was added to the bottom of the outlet pipe assembly. The outlet pipe was also lowered to below the cyclone inlet. In this case the pressure drop and collection efficiency increased. The high collection efficiency is due in part to the unexpected inlet conditions of a large mean diameter and a high loading. Although the 2nd stage cyclone was collecting efficiently there was a significant number of large particles (> 50 micron) which were not collected. These particles may have bypassed the cyclone through one of the small leakage paths in the refractory. Also, the particles may have been thrown into the cyclone outlet gas stream or they may have been re-entrained by the deep vortex. In the third build the refractory around the outlet pipe was replaced. Furthermore, refractory was added to the outlet side of the outlet pipe assembly. The pressure drop increased but the carryover of large particles persisted. The original and final design of the cyclone internal element is shown in Figure 2.16.

The fractional efficiency of the Ducon unit for the three cleanup system builds is shown in Table 2.17 and Figure 2.17.

3rd Stage - During Build No. 1 the two upstream cyclones were not functioning well and the 3rd stage cyclone received a high inlet loading and large inlet particle sizes (Table 2.15). Even so, the 3rd stage collection was only that required by the specification. During Build No. 3 improvement in the 2nd stage reduced the 3rd stage inlet loading but its inlet mean particle size increased. However, the collection efficiency decreased. Further improvements in the 1st and 2nd stages in the third build decreased the 3rd stage's inlet mean particle diameter. However, in this case there was essentially no change in the 3rd stage collection efficiency.

The fractional efficiency of the 3rd stage unit for the three cleanup system builds is shown in Table 2.18 and Figure 2.18.

TABLE 2.17

2nd STAGE CYCLONE COLLECTION EFFICIENCY (%)

Diameter Microns	Build No. 1	Build No. 2	Build No. 3
0.0 - 1.0	31.0	0.0	0.0
1.0 - 1.26	13.6	0.0	0.0
1.26 - 1.59	15.3	29.4	51.6
1.59 - 2.00	19.7	67.6	70.6
2.00 - 2.52	33.7	86.2	86.2
2.52 - 3.17	49.9	93.6	93.9
3.17 - 4.00	58.9	96.6	97.6
4.00 - 5.04	61.3	98.3	98.8
5.04 - 6.35	60.2	98.8	99.1
6.35 - 8.09	57.2	98.6	98.8
8.09 - 10.08	50.3	98.1	97.6
10.08 - 12.7	41.7	97.1	94.6
12.7 - 16.0	34.3	96.1	89.4
16.0 - 20.2	28.8	94.7	81.7
20.2 - 25.4	13.4	92.7	73.0
25.4 - 32	4.5	89.0	61.4
32 - 40.3	9.5	83.2	53.8
$\geq$ 40.3	0.0	84.4	0.0

DUCON COLLECTION EFFICIENCY

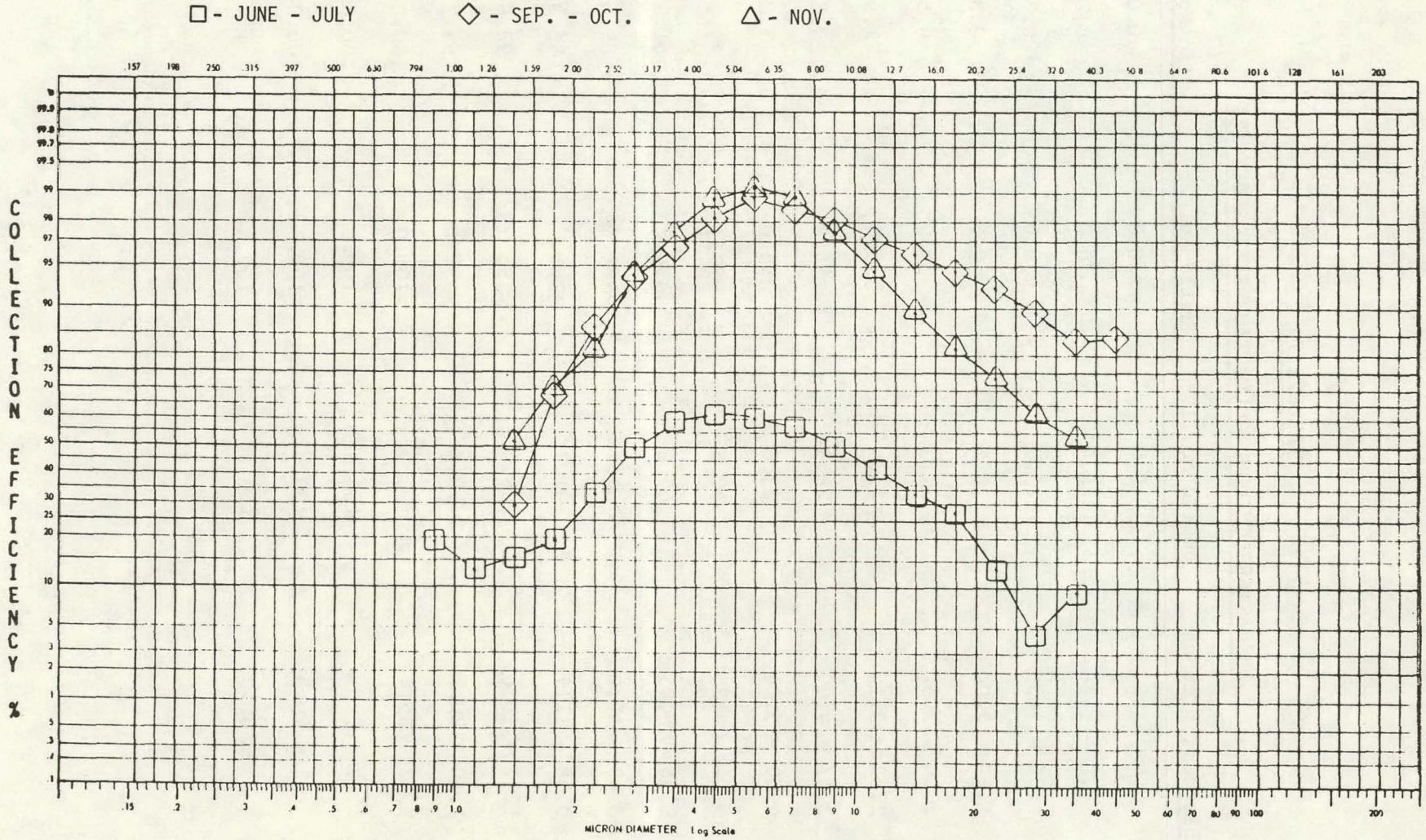

Figure 2.17

TABLE 2.18

3rd STAGE CYCLONE COLLECTION EFFICIENCY (%)

Diameter Microns	Build No. 1	Build No. 2	Build No. 3
0.0 - 1.0	0.0	0.0	0.0
1.0 - 1.26	0.0	0.0	0.0
1.26 - 1.59	23.3	0.0	0.3
1.59 - 2.00	19.2	0.6	0.3
2.00 - 2.52	21.3	0.9	0.5
2.52 - 3.17	22.4	2.4	1.9
3.17 - 4.00	28.9	6.3	3.8
4.00 - 5.04	33.0	14.0	13.3
5.04 - 6.35	42.6	27.5	29.2
6.35 - 8.09	65.6	54.2	61.1
8.09 - 10.08	84.2	80.0	89.6
10.08 - 12.7	91.7	89.7	96.3
12.7 - 16.0	95.3	95.9	98.6
16.0 - 20.2	99.4	99.1	99.2
20.2 - 25.4	98.9	100.0	100.0
25.4 - 32	100.0	100.0	100.0
32 - 40.3	100.0	100.0	100.0
$\geq$ 40.3	100.0	100.0	-

AERODYNE COLLECTION EFFICIENCY

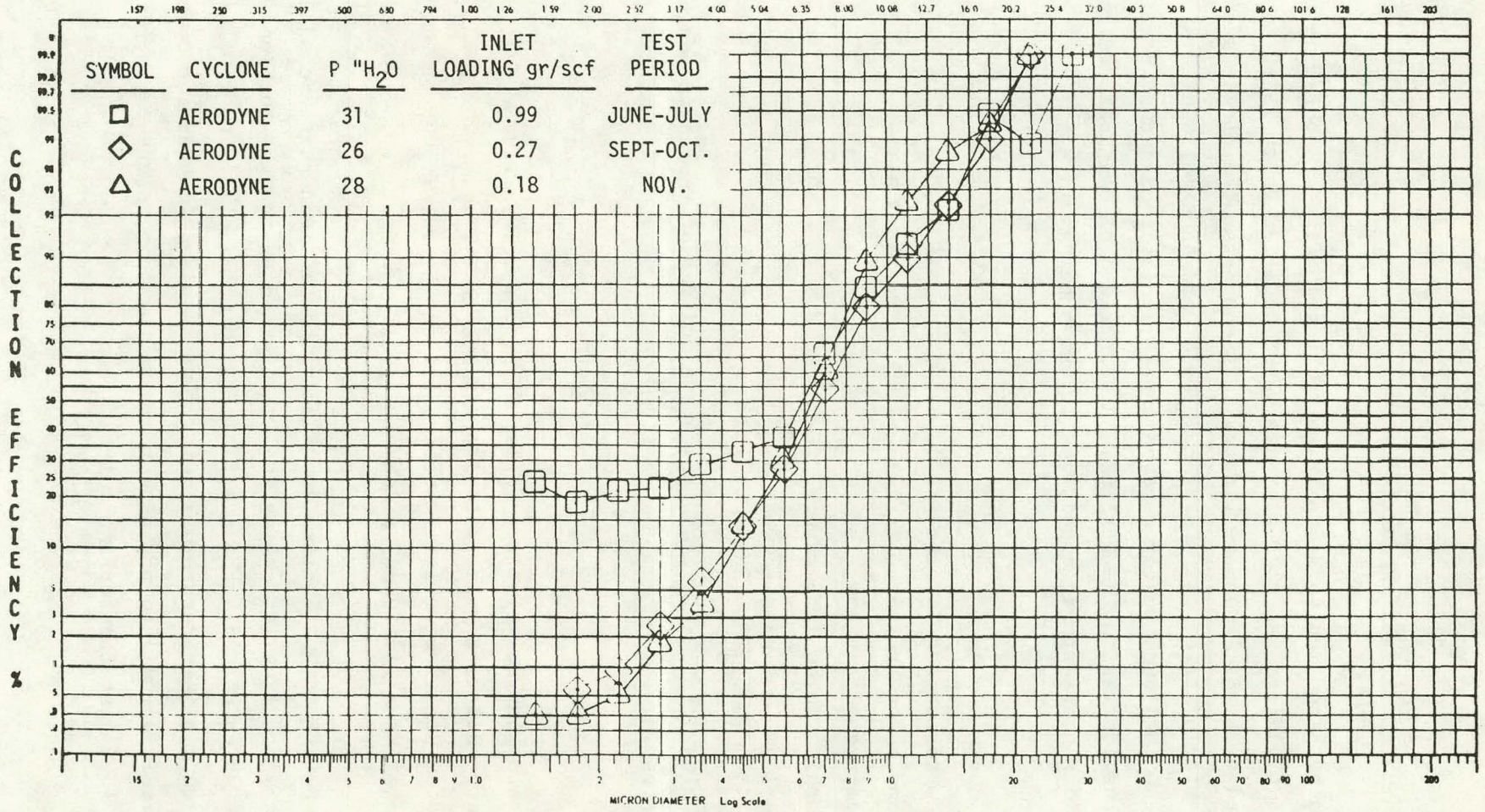

Figure 2.18

2.4.6 Gas Turbine Performance

The gas turbine used to demonstrate the feasibility of operating on pressurized fluidized bed combustor gas was a modified Rover 1S/60 engine manufactured by Lucas Aerospace Limited. It consists of a single shaft machine with a single stage centrifugal compressor and an axial single stage reaction turbine with its combustor removed and the inlet modified to permit the flow of combustion gas to the turbine. A comparison of original design operating conditions and test rig conditions is shown below.

	Original Design	Test
Compressor and Turbine Speed, rpm	46,000	38,000
Compressor Pressure, Ratio	3.0:1	1.87:1
Compressor Airflow, lb/sec	1.3	1.0
Turbine Inlet Temperature, °F	1350	1550
Maximum Continuous Power, HP	60	20

Shown below are the blade and stator velocities of the engine as operated during test.

	Test
Stator Outlet Velocity, ft/sec	1362
Rotor Relative Inlet Velocity, ft/sec	476
Rotor Relative Outlet Velocity, ft/sec	1288
Rotor Mean Tip Speed, ft/sec	1098

After the PFB combustion gas is mixed with the clean heat exchange air, part of this mixed flow is isokinetically diverted to the gas turbine through an orifice which controls the gas flow at approximately .9 to 1.0 lb/sec. Since the mixed gas temperature was lower than required for turbine operation, kerosene was injected into the pipe to raise the temperature to approximately 1550 - 1600°F at the turbine inlet.

The turbine performance is shown in Figure 2.19 as a function of turbine endurance time. During testing, the alternator load was varied between 0 to 20 horsepower. The turbine horsepower is a function of the inlet airflow, turbine inlet temperature, speed and ambient pressure. The airflow is dependent on the back pressure and temperature of the PFB. The turbine or compressor speed is a function of the variation in alternator load, turbine horsepower and ambient pressure and temperature.

The turbine performance as shown on Figure 2.19 indicated a variation of horsepower between 75 and 85, turbine pressure ratio from 1.68 to 1.79, corrected speed range between 830 to 870 and an efficiency between 80 to 85% with the exception of two points. The average change in speed of 2.4%, pressure ratio of 3%, horsepower of 7% and efficiency of 3% indicated that no deterioration of turbine performance occurred due to the turbine gas particulate loading as shown in Figure 2.20.

2.5 MATERIALS EVALUATION

2.5.1 Heat Exchanger Materials

At the conclusion of Test No. 6 (Table 2.1), the PFB heat exchanger was removed and the nine tubes were replaced as planned with the tube material configuration for Test No. 7. The tube, fin and coating material data for the installed heat exchanger are shown in Table 2.19 and a plan view of the tube locations is shown in Figure 2.21. Also installed at this time were the 17 ft high coupon trees to enable evaluation of many candidate alloys and coatings throughout the full bed and in the freeboard environment. Figure 2.22 shows a closeup of the "limb" assembly prior to welding to the "tree".

Sample coupons were exposed in the following locations (Figures 2.21 and 2.23):

1. Near the Coal Feed Gun
2. Remote from the Coal Feed
3. Lower Portion of the Bed
4. Upper Portion of the Bed
5. Freeboard Above the Bed

Table 2.19

SGT/PFB MATERIALS EVALUATION

HEAT EXCHANGER TUBES

TUBE NO. (LOC. IN BED)	TUBE MATERIAL	O.D. FIN MATERIAL	I.D. FIN MATERIAL	REMARKS
4	310	30-310 8-188	INCO 600	ALONIZED (NEW)
7	HAYNES 188	30-310 8-188	HASTELLOY S	SPRAY COATED WITH HOSKINS 750 (Fe-Cr-Al-Si)
3	310	30-310 8-188	INCO 600	
1	HAYNES 188	26-310 8-188 4-(16-5-Y)	TOP HALF 3 - HAST. S 2 - INCO 600 BOTTOM HALF 5 - INCO 600	
5	310	30-310 8-188	INCO 600	
6	HAYNES 188	30-310 8-188	INCO 600	
2	310	26-310 8-188 4-(16-5-Y)	INCO 600	
8	310	NONE	INCO 600	HEAT TRANSFER EVALUATION OF SMOOTH O.D. TUBE
9	310	30-310 8-188	TOP HALF 3 - HAST. S 2 - INCO 600 BOTTOM HALF 5 - INCO 600	

PFB-III-276 A

ESTIMATED GAS TURBINE PERFORMANCE
ROVER ENGINE

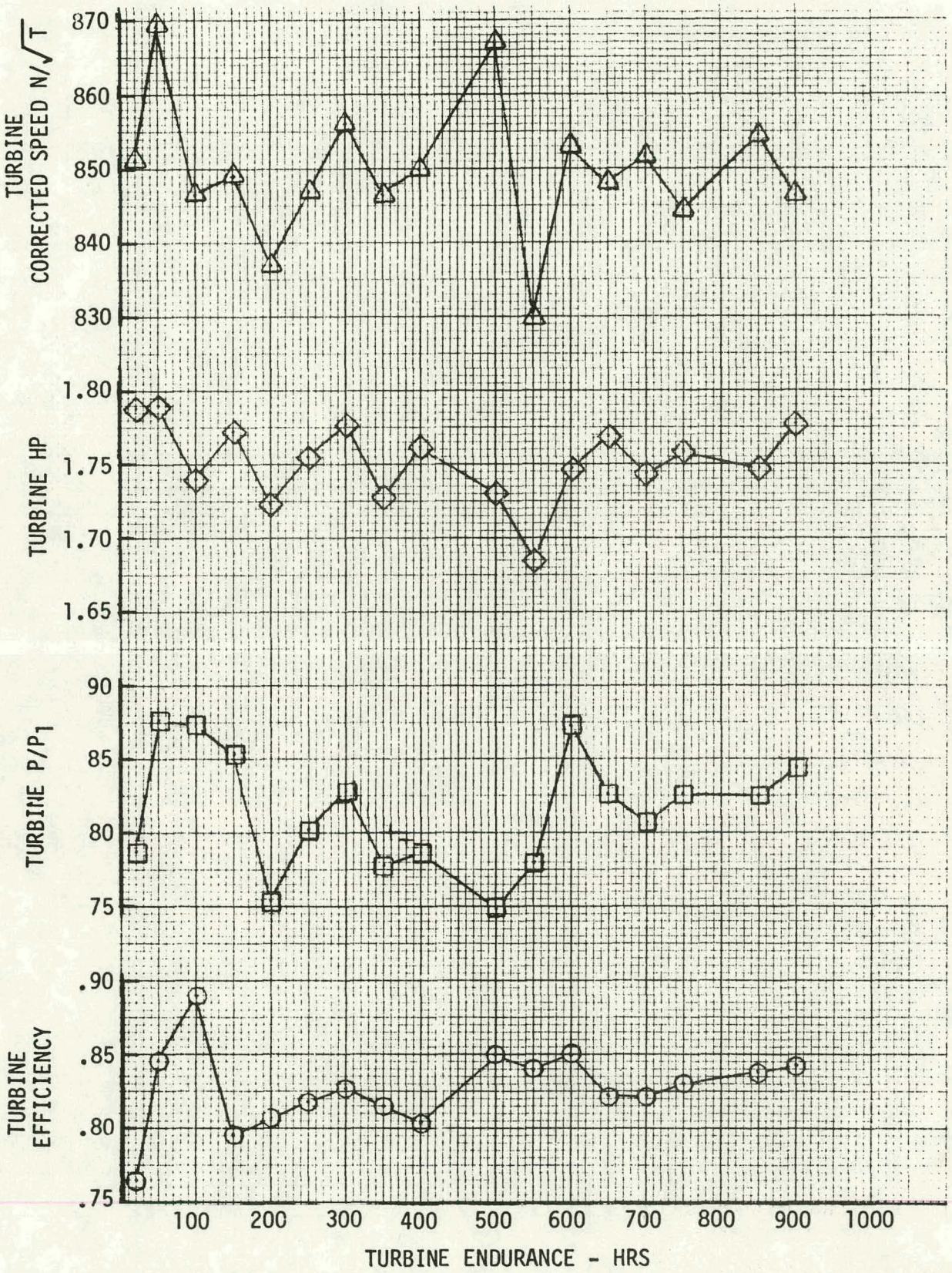

Figure 2.19

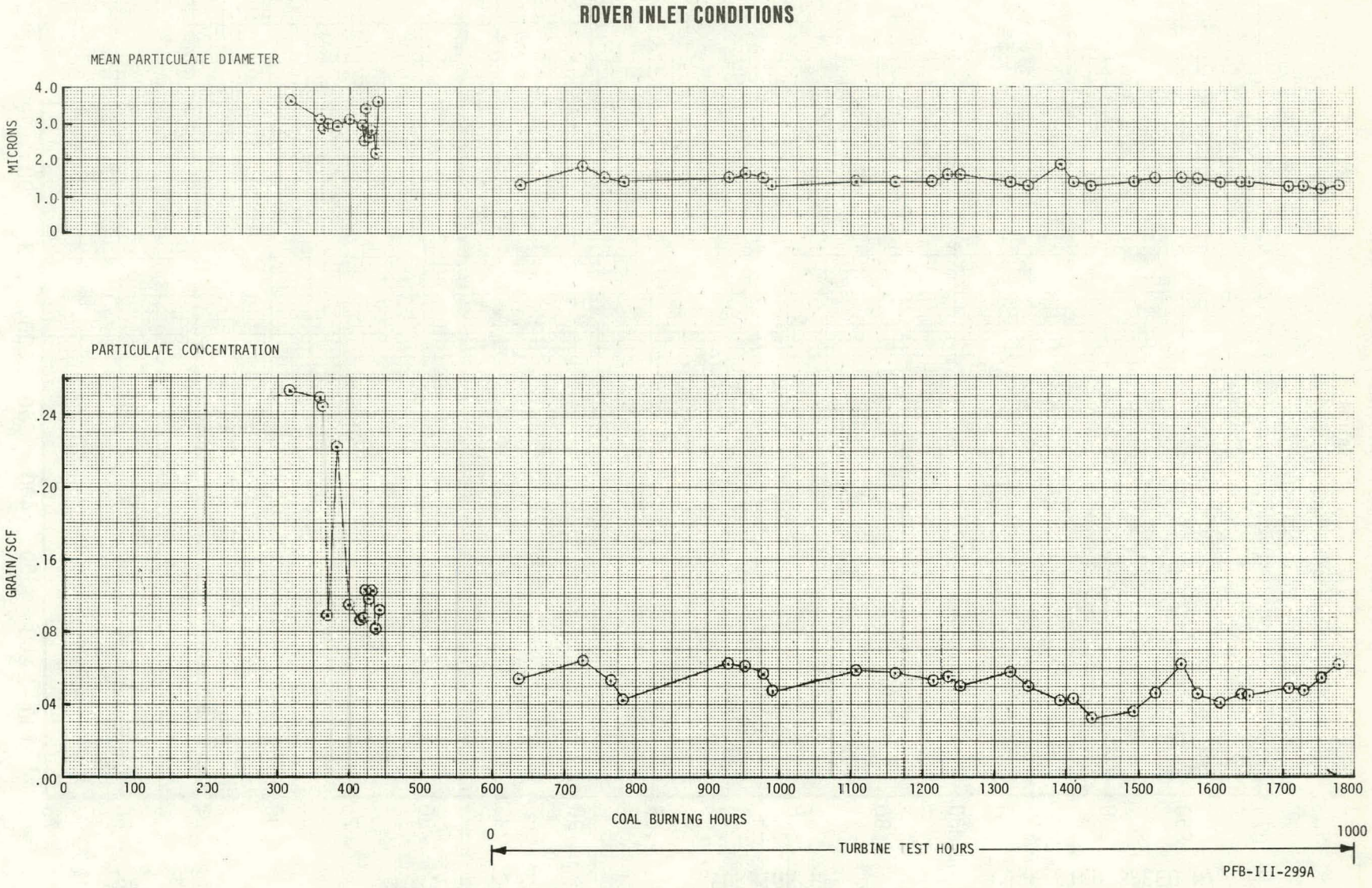
ROVER INLET CONDITIONS
MEAN PARTICULATE DIAMETER
MICRONS
4.0
3.0
2.0
1.0
0
PARTICULATE CONCENTRATION
GRAIN/SCF
.24
.20
.16
.08
.04
.00
0
100
200
300
400
500
600
700
800
900
1000
1100
1200
1300
1400
1500
1600
1700
1800
COAL BURNING HOURS
0
TURBINE TEST HOJRS
1000
PFB-III-299A

Figure 2.20

PFB/SGT TECHNOLOGY UNIT
HEAT EXCHANGER TUBE AND SAMPLE COUPON
TREE AND LIMB CONFIGURATION

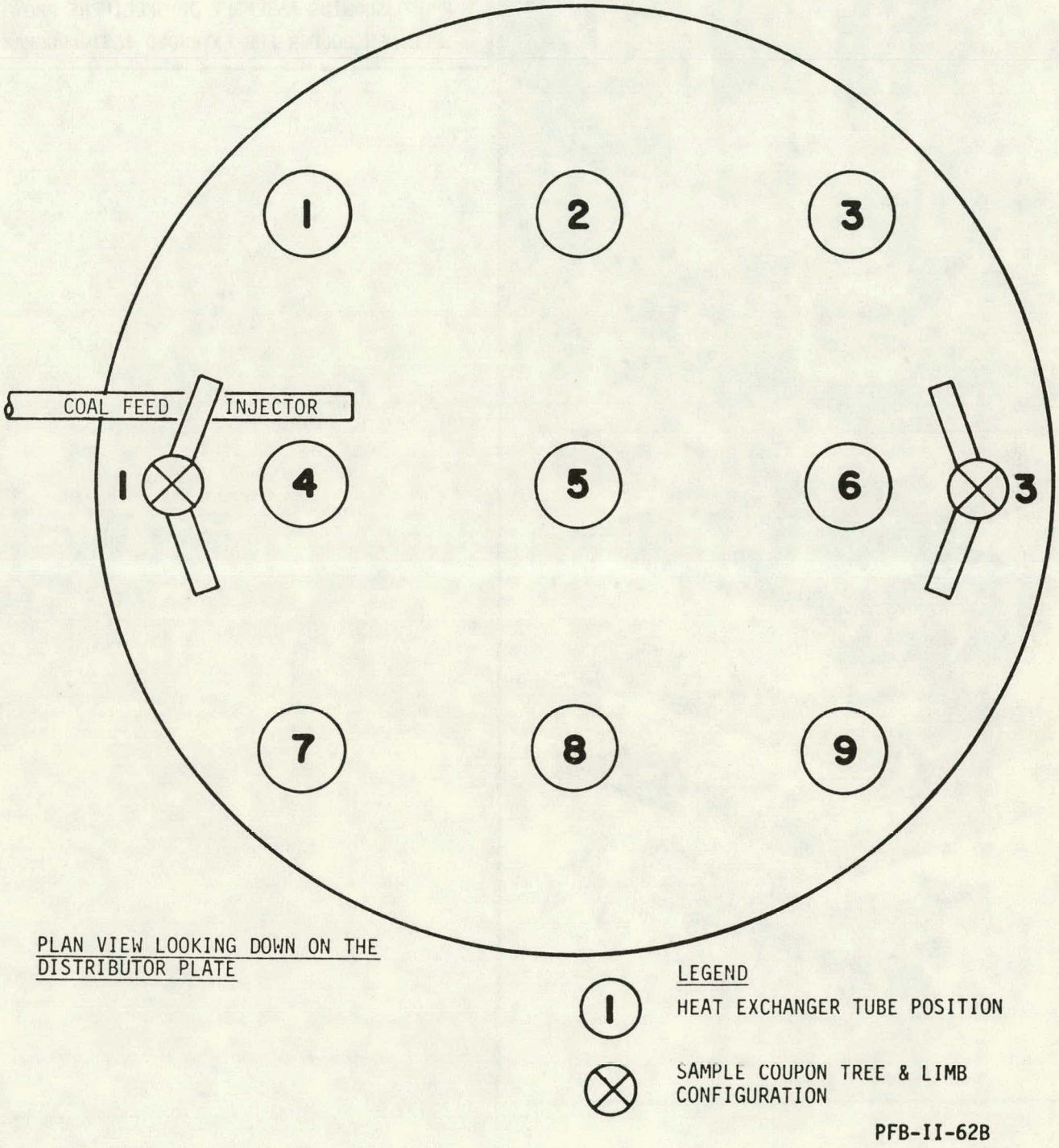

Figure 2.21

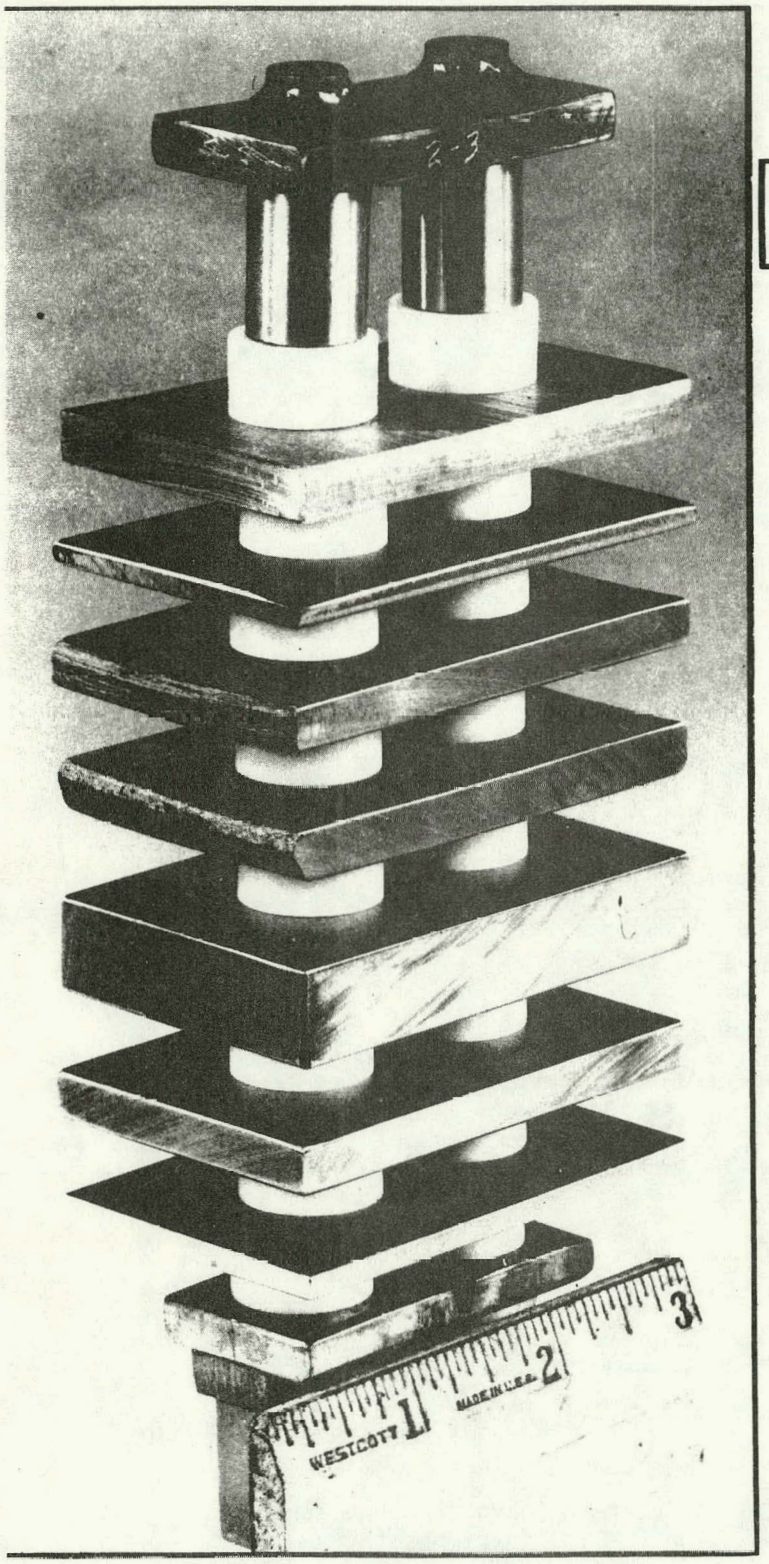

PHOTO SHOWING ASSEMBLY OF SPECIMENS AND SPECIMEN HOLDER FOR EXTENDED TEST PROGRAM

PFB-II-124A

Figure 2.22

COUPON SPECIMENS INSTALLED ON VERTICAL POST

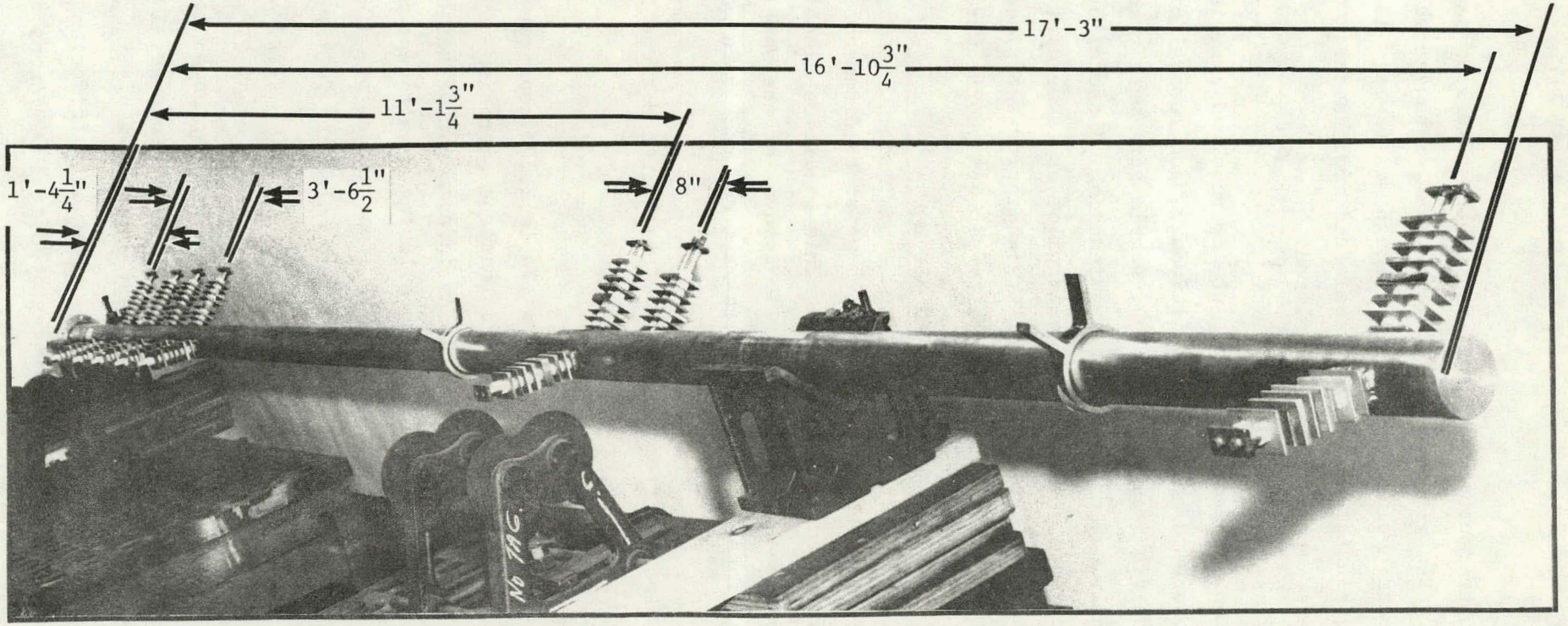

Figure 2.23

Photograph of one of the Assembled "Christmas Trees" Ready for Installation.
Note That Materials are Being Evaluated at Various Bed Heights.

PFB-II-126B

In addition to the coupon specimens, one of three sets of small tab specimens welded to the tips of fins on the original heat exchanger tubes and exposed for some 800 hours during Tests No. 1 through No. 6 were reattached to fins of the new tubes in the vicinity of coal feed impingement. The remaining two sets of tabs were metallurgically analyzed.

At the conclusion of the test period, the coupons had experienced a total of 2000 hours exposure to operating conditions. Upon removal of the heat exchanger from the rig (see Figure 2.24), sample sets were removed from the heat exchanger assembly and prepared for examination. Those alloys and coatings having the greatest likelihood of use in pilot or commercial plant equipment from the standpoint of cost, availability and prior experience are reported upon. Some alloys which were expected to perform poorly were included in this group as controls.

A rack of samples is shown in Figure 2.25 prior to disassembly. There is refractory debris wedged into the racks. This condition closely approximates the condition of the tube O.D. fins. During removal of the sample from the racks, no metallurgical interaction of samples with the rack bars was noted.

Specimens were also cut from O.D. fins of each of the three fin alloys, in several random locations throughout the bed.

Metallographic analysis of the coupons (Table 2.20) confirmed the findings of the visual examination which concluded that the corrosion conditions within the bed and in the freeboard are essentially independent of height or proximity to the coal feed location. Further, the following results appear to favor the use of lower cost and commonly available iron-base alloys (Figure 2.26). Metallurgical examination of the coupons revealed the following:

1. Alloys 310S (Fe-25 Cr-20 Ni) shown in Figure 2.27 and 800H (Fe-22Cr-35 Ni) shown in Figure 2.28 experienced relatively little corrosion, averaging about 20 and 40 microns per 1000 hours, respectively. The Fe-Cr-Al-Y alloys (Figure 2.29) suffered substantially more corrosion, of an oxidation/sulfidation type, than expected. Attack was uniform and averaged 75 to 100 microns per 1000 hours.

SGT/PFB AIR COOLED HEAT EXCHANGER - 2000 HRS ENDURANCE TIME

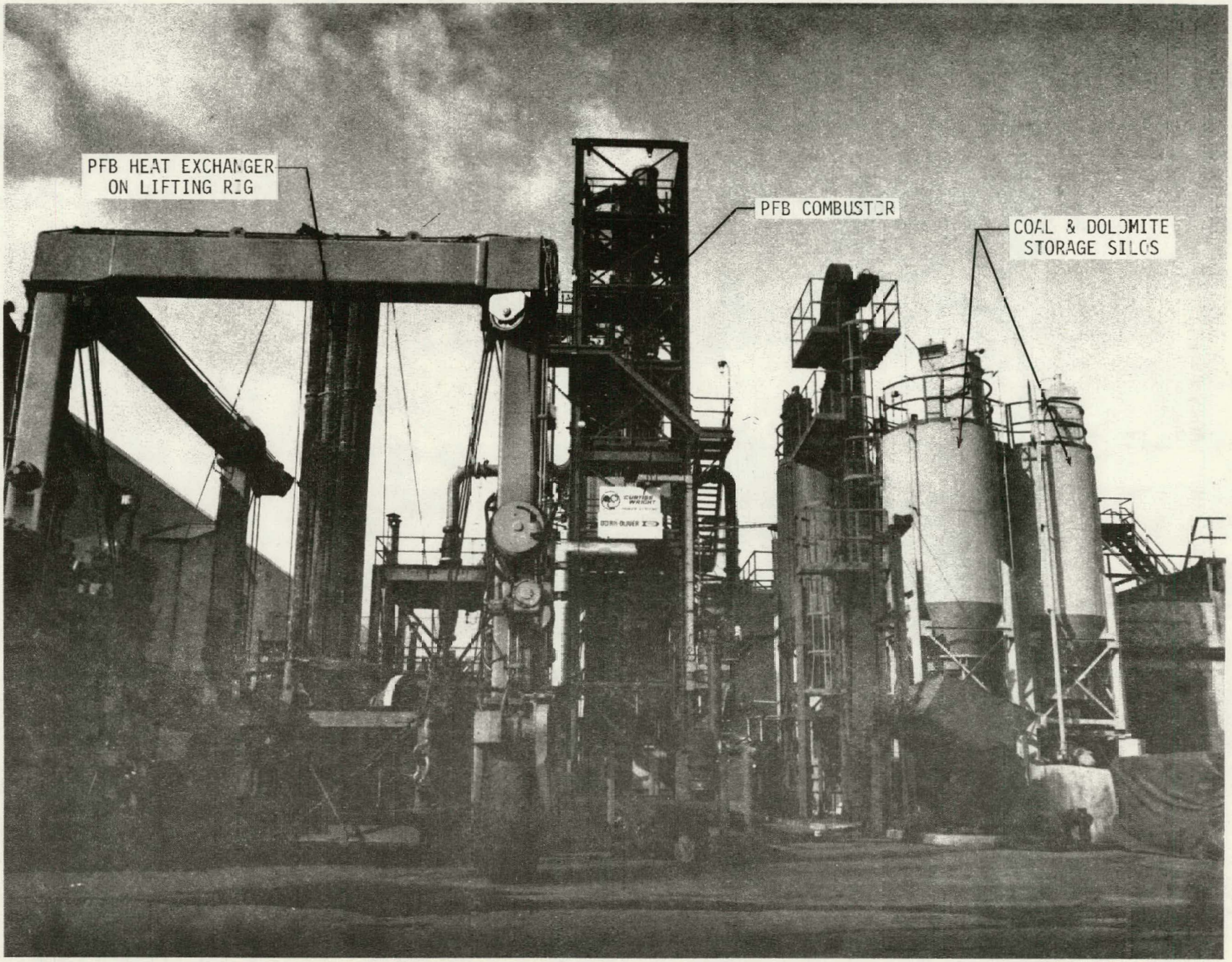

Figure 2.24

COUPON SPECIMEN RACKS AFTER REMOVAL

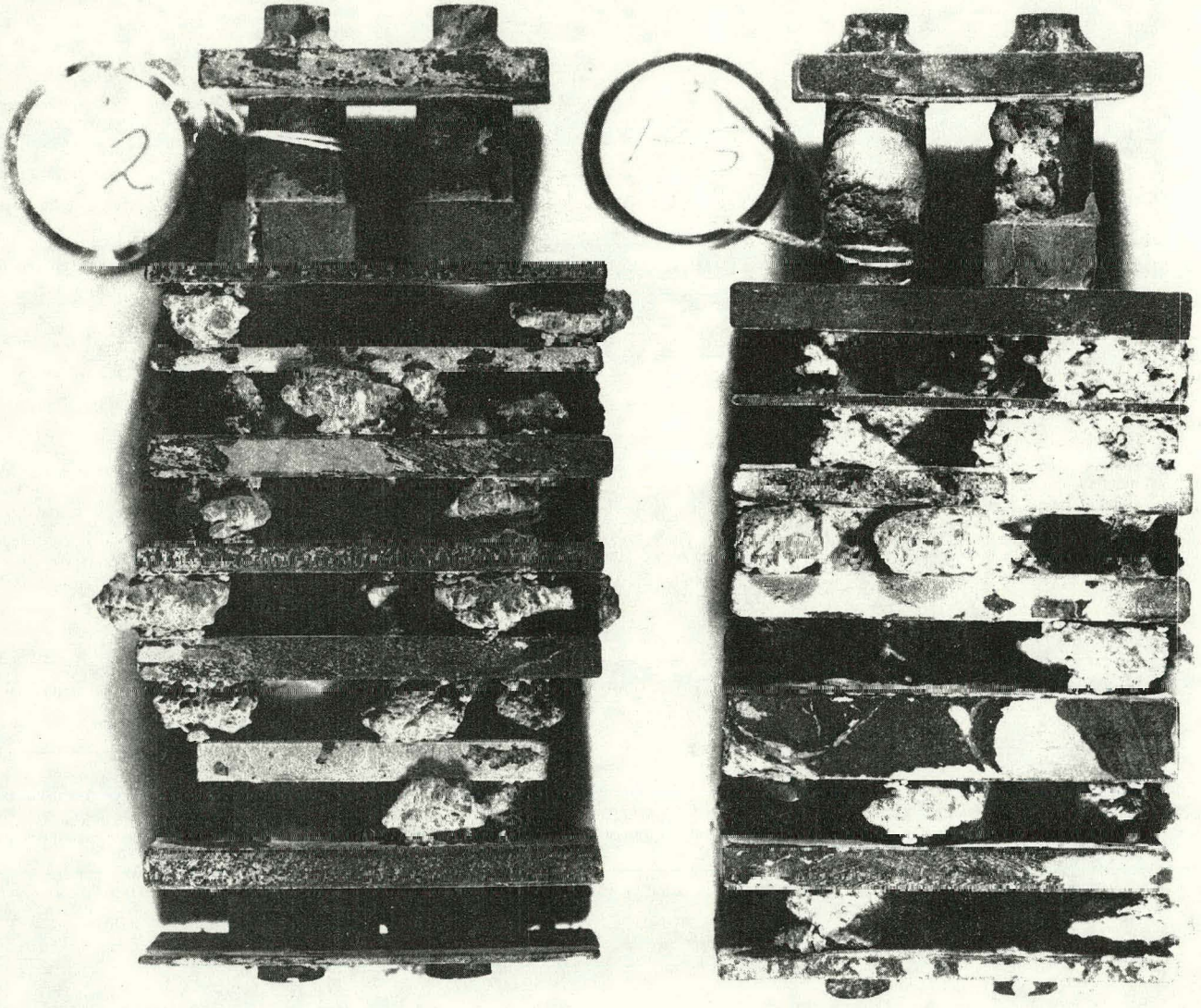

Actual Size - Photo of two specimen racks as removed from the posts. Note refractory debris wedged between samples.

80-099

Figure 2.25

Table 2.20

METALLURGICAL EVALUATION OF HEAT EXCHANGER ALLOY COUPONS AND TUBE OD FIN SAMPLES

WORK PERFORMED	LOCATION			MICROS & PHOTO-MICRO	EDXA (NO. OF AREAS) SCANNED	ELEMENTAL DISTRIBUTION MAPS							
COUPON ALLOY	LOW	HIGH	FREEBOARD			Cr	S	O	Fe	Al	Ni	Co	Ta
AL 16-5-Y	2	2	1	5	4	X	X	X	X	X			
800H	1	2	1	4	5 & 1	X	X	X	X		X		
INCO 601	1	-	-	1			•						
INCO 600	1	1	-	2	-	X	X	X			X		
MA 956	2	2	-	4	3	X	X	X	X	X			
INCO 671	2	-	-	2									
Fe-Cr-Al-Y/800H	1	1	-	2	1	X	X	X	X		X		
ALONIZED 800H	1	-	1	2									
HAYNES 188	1	1	-	2									
310 S.S.	1	1	1	3	5 & 3	X	X	X	X		X	(2 SAMPLES)	
INCO 811	1	-	-	1									
Fe-Cr-Al-Mo-Hf	1	-	1	2	5	X	X	X	X	X			
Co-Cr-Al-Ni-Ta-Y/800H	1	1	1	3	2	X	X	X		X		X	X
N-155	1	-	-	1	-	X	X	X	X		X	X	
				34	11								
FIN ALLOY													
310 S.S.	4	-	N/A	4	-								
HAYNES 188	2	-	N/A	2	-								
A.L. 16-5-Y	1	-	N/A	1	-								
				7	-								

PFB-III-308

SUMMARY OF RESULTS

2000 HOUR EXPOSURE OF COUPONS IN SGT/PFB COMBUSTOR

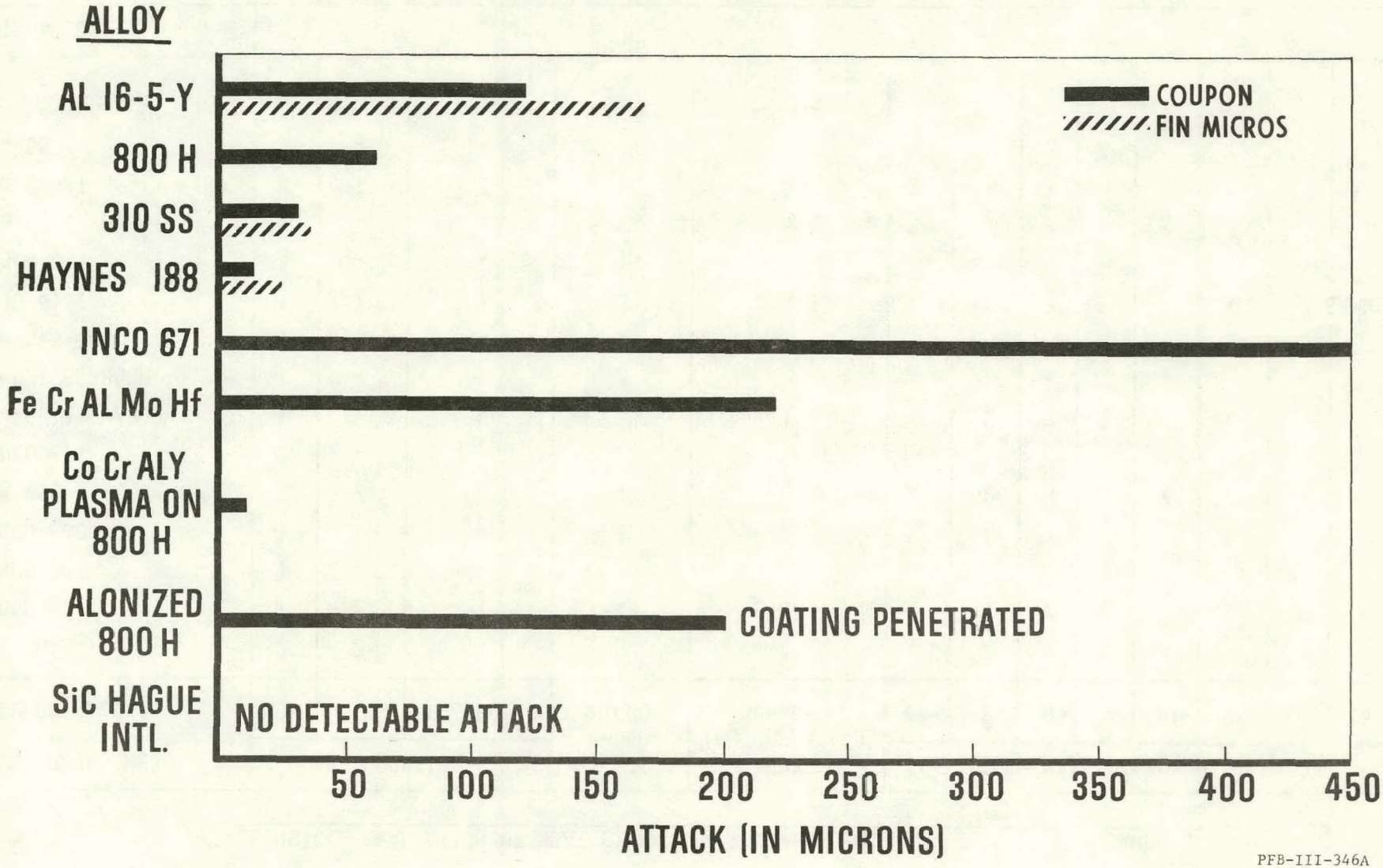

Figure 2.26

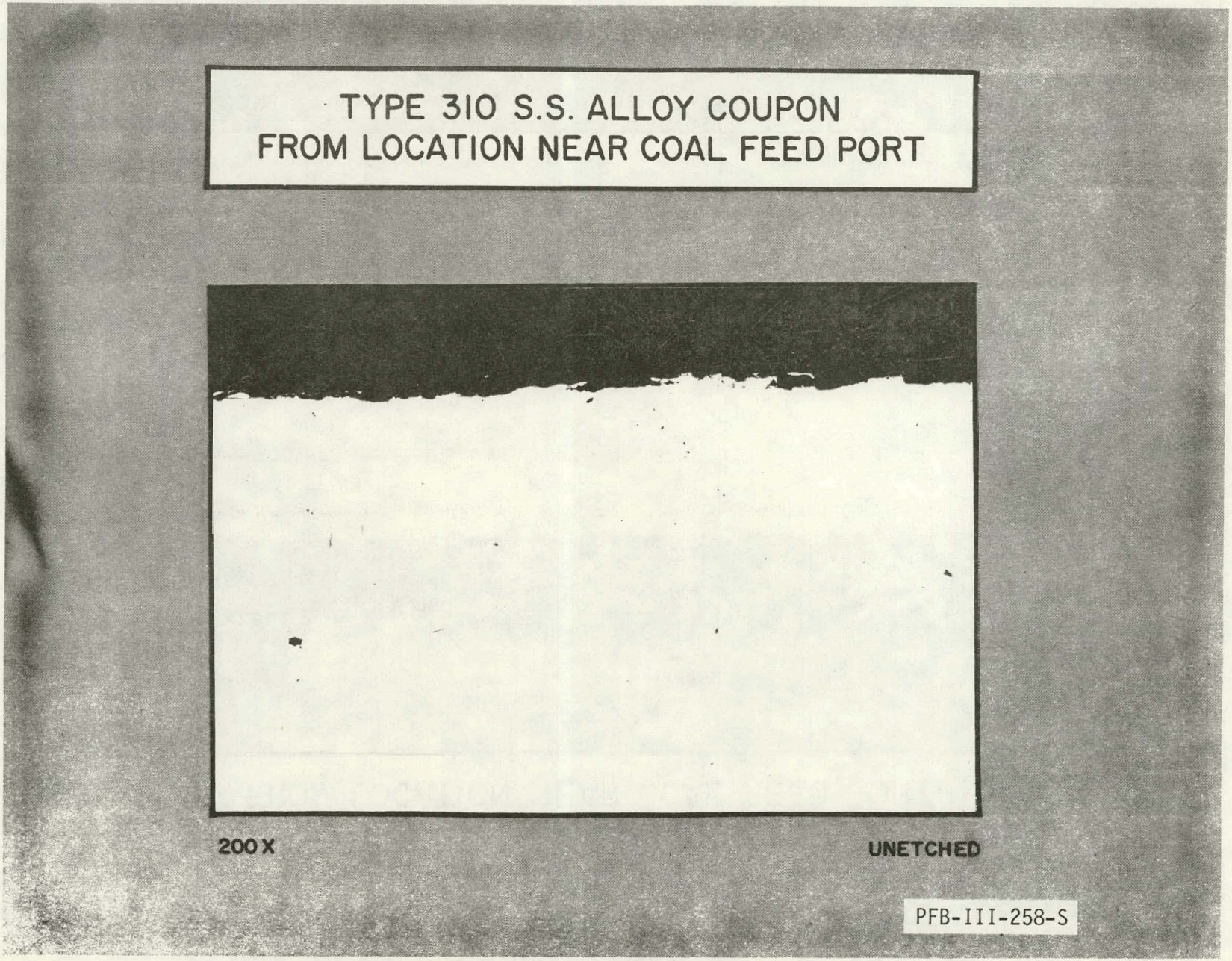
TYPE 310 S.S. ALLOY COUPON
FROM LOCATION NEAR COAL FEED PORT
200 X
UNETCHED
PFB-III-258-S

Figure 2.27

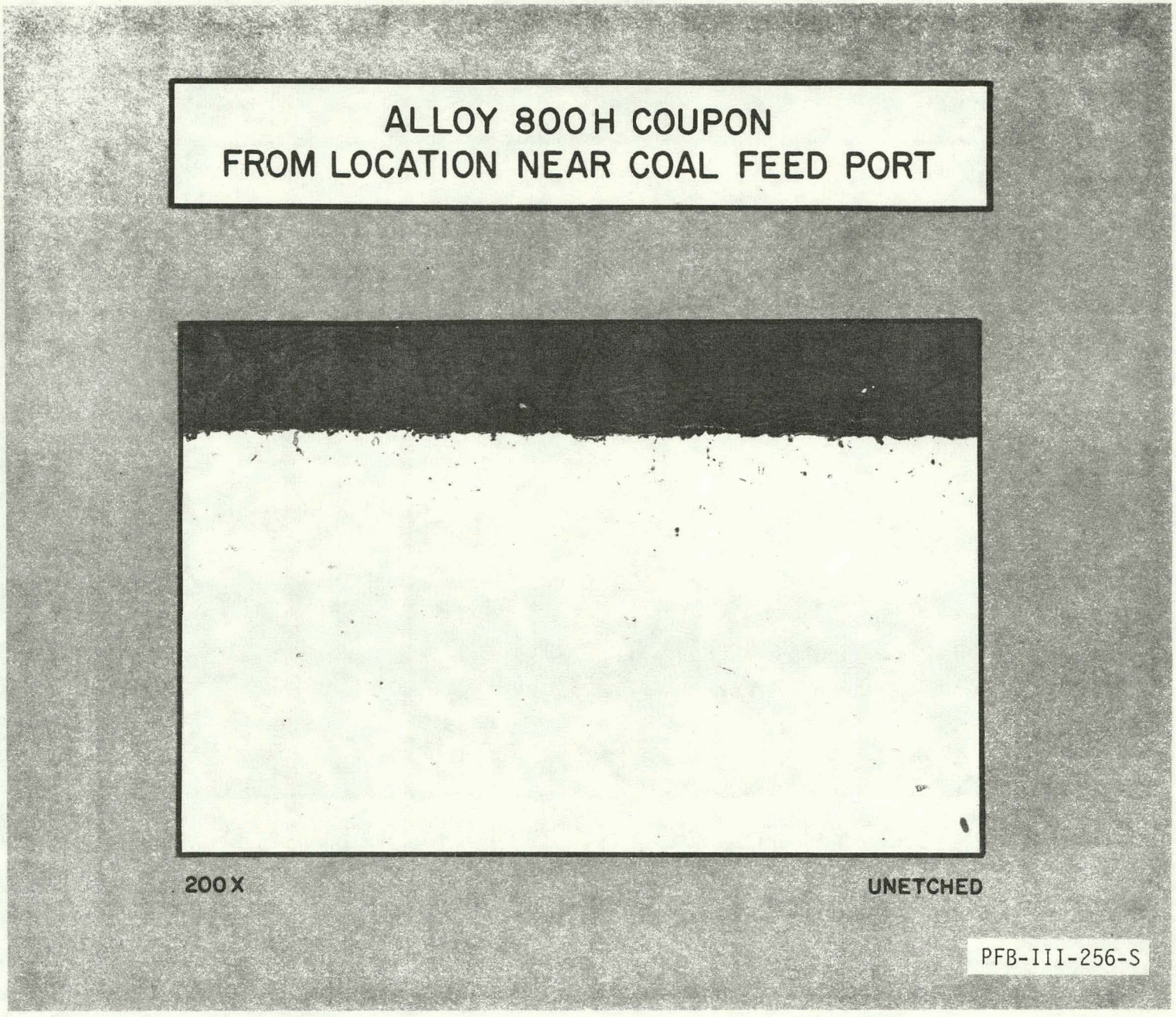
ALLOY 800H COUPON
FROM LOCATION NEAR COAL FEED PORT
200X
UNETCHED
PFB-III-256-S

Figure 2.28

2. The nickel-based alloys (Alloy 600, 671) shown in Figure 2.30 behaved as expected for this atmosphere, experiencing severe sulfidation attack up to 1000 microns per 1000 hours.

3. The cobalt alloy, Haynes 188, (Figure 2.31) behaved quite well except where subject to crevice conditions. Pits to 100 microns in depth were measured (50 microns per 1000 hours).

4. The SiC material experienced no detectable attack. The material is, however, brittle and would require further work to be considered for large heat exchanger tubes.

5. The low pressure chamber plasma arc spray coatings of Co-Cr-Al-Y type (Figure 2.32) and Fe-Cr-Al-Y had mixed results. The Co-Cr-Al-Y type was generally better, protecting the substrate where it was applied although, suffering heavy oxidation in some samples in crevice conditions.

6. The behavior of the Fe-Cr-Al-Y type alloy provided the only unexpected result in the testing. Corrosion of this type alloy in previous tests had indicated good resistance. In this test tab specimens from all locations, i.e., freeboard, low bed position near coal feed, and high bed position remote from the coal feed experienced heavy oxidation of the surface and considerable sulfur penetration. Fin sections taken from two, five and eight foot heights exhibited oxidation attack. In many cases, an iron-yttrium phase was noted in the matrix below the corrosion layer, perhaps indicating a depletion of yttrium which led to oxide spalling. Other investigators have evaluated a 25% chromium version of this alloy in a PFB environment with excellent results. The higher chromium containing alloy should be evaluated in future tests.

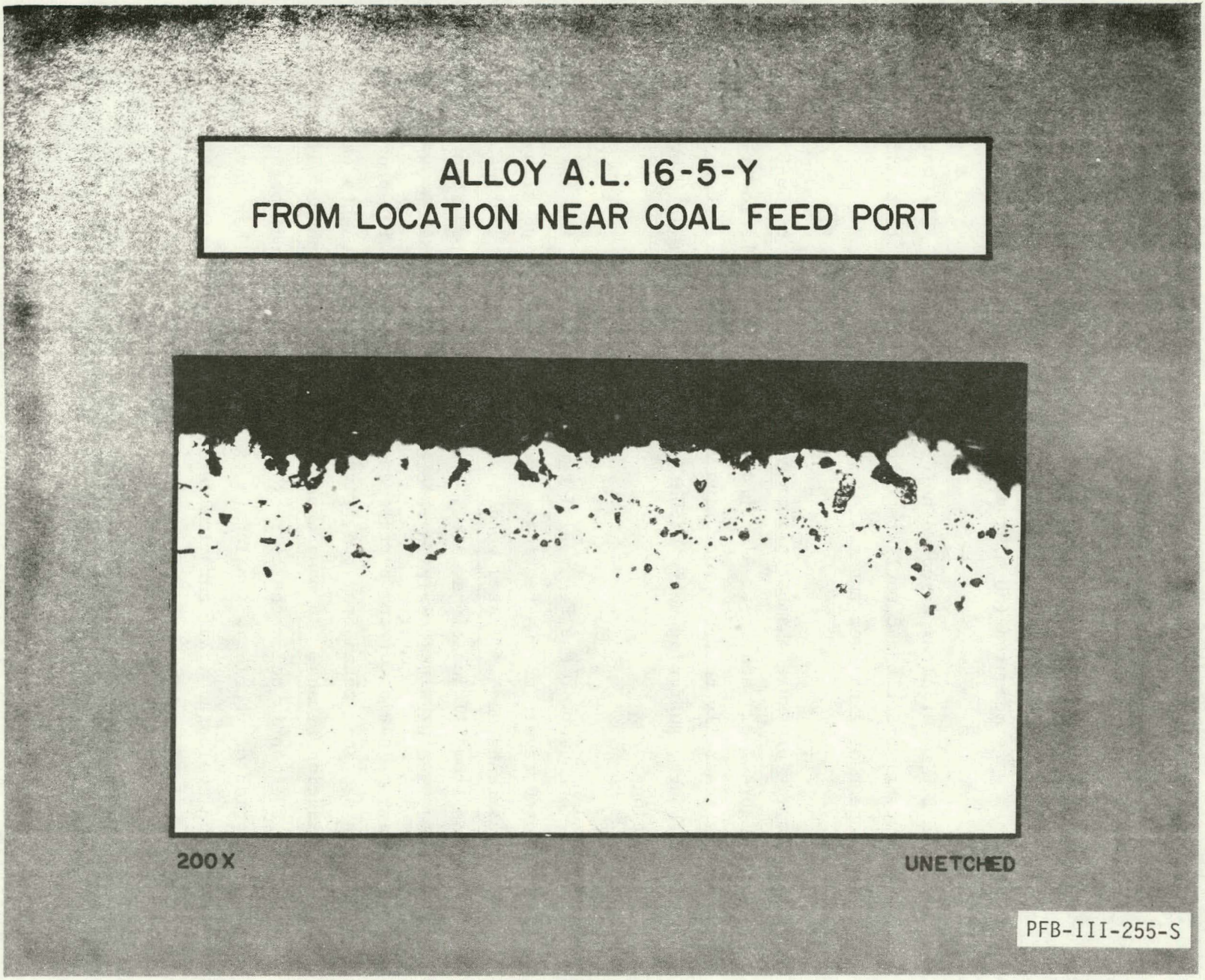
ALLOY A.L. 16-5-Y
FROM LOCATION NEAR COAL FEED PORT
200X
UNETCHED
PFB-III-255-S

Figure 2.29

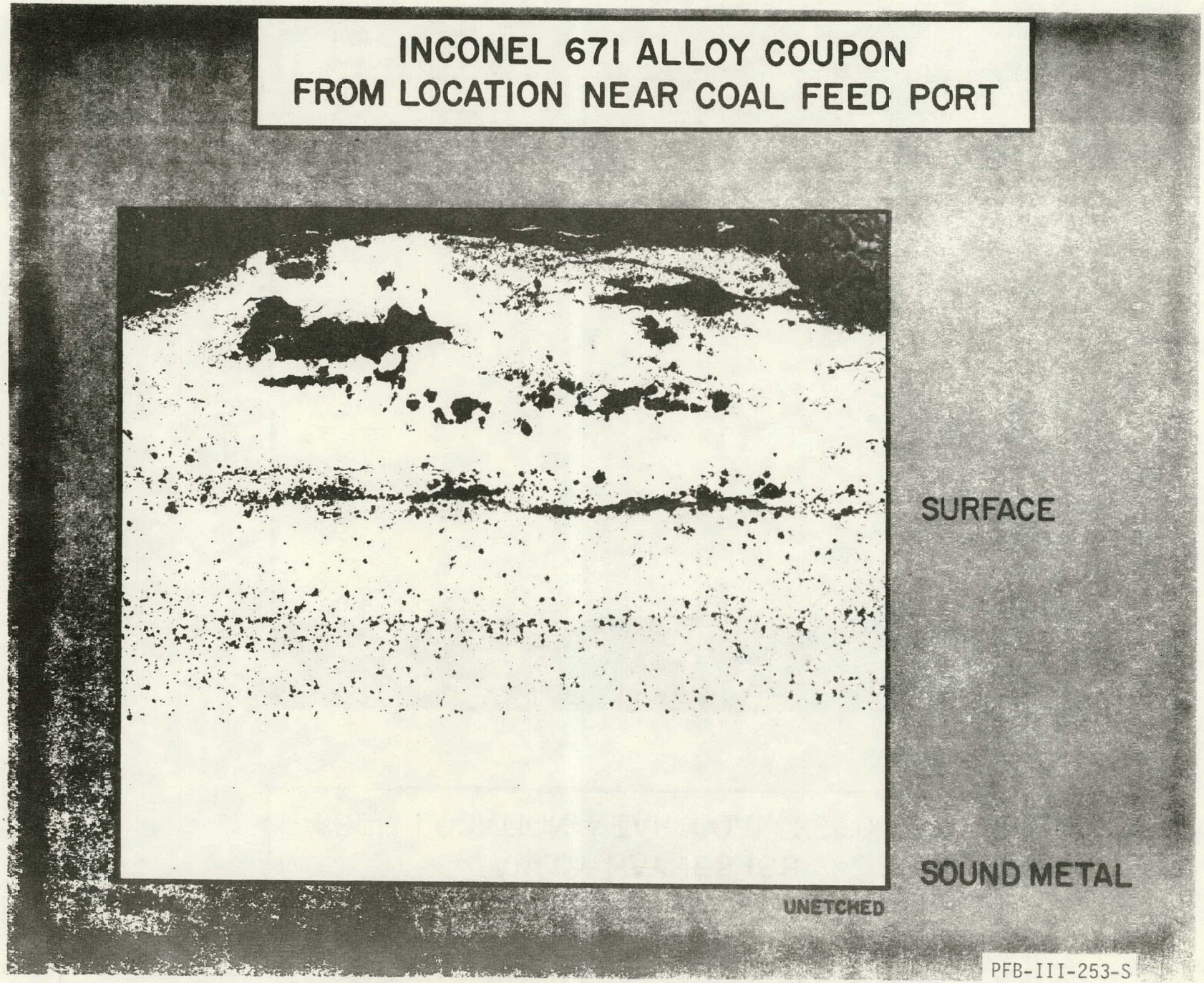
INCONEL 671 ALLOY COUPON
FROM LOCATION NEAR COAL FEED PORT
SURFACE
SOUND METAL
UNETCHED
PFB-III-253-S

Figure 2.30

ALLOY HAYNES 188
FROM LOCATION NEAR COAL FEED PORT
200 X
UNETCHED
PFB-III-257-S

Figure 2.31

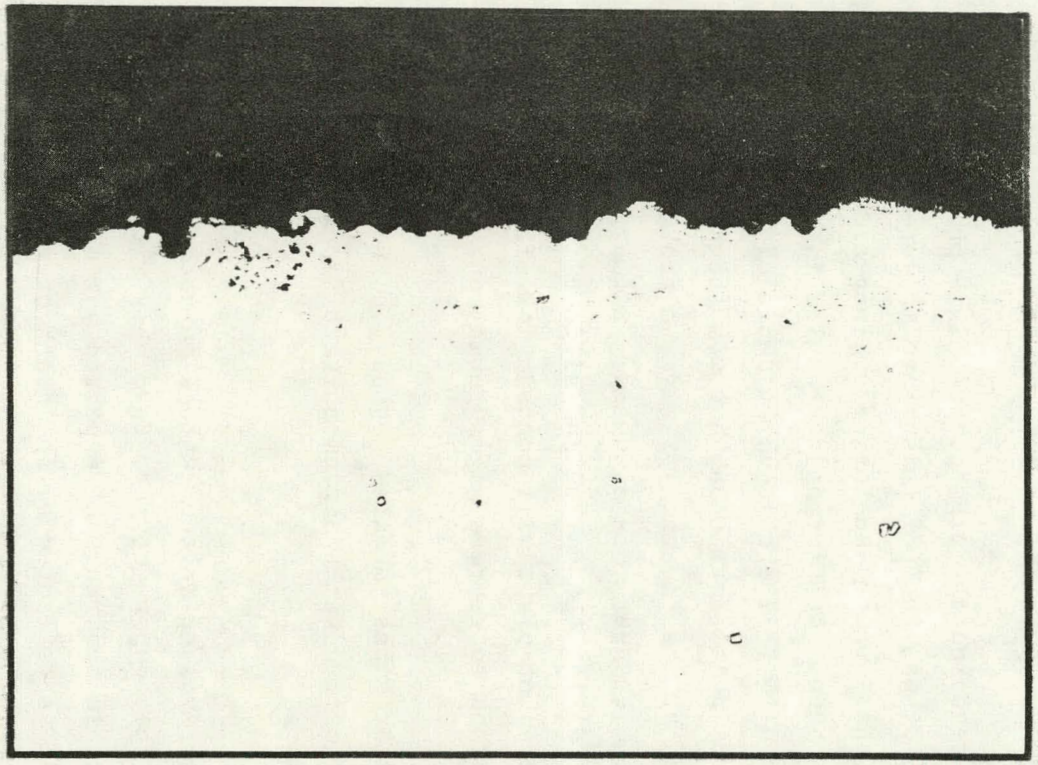

Low Pressure Chamber Plasma Arc Spray Coating (Co-Cr-Al-Ni-Ta-Y) Onto Alloy 800 H Substrate. Location Remote From Coal Feed Port.

PFB-III-254-S

Figure 2.32

Metallurgical examination of samples cut from heat exchanger tube O.D. fins in a number of random locations revealed:

1. Corrosion rates for the fin alloys Al-16-5-Y (Figure 2.33), Fe-Cr-Al-Y type, 310S (Figure 2.34), and Haynes 188 were similar to the results for coupons.

2. The fin analysis confirms the corrosion conditions in the bed to be similar irrespective of location.

3. Examination of fins revealed the presence of sigma phase (Figure 2.35). Unexposed alloy was free of this phase (Figure 2.36). Sigma is an iron-chromium phase which can form from long time exposure in the PFB temperature range. Its formation results in a lowering of the ductility of the alloy. There is no evidence of an effect upon corrosion rate of this phase formation, nor was the room temperature embrittlement induced by the presence of sigma a problem in the handling of the heat exchanger tube assembly. Sigma formation can be repressed by controlling the carbon and silicon. The 310 SS tubing selected for the pilot plant will contain low silicon and intermediate levels of carbon to repress sigma formation.

Examination of the heat exchanger tubes revealed no heavy corrosion, rather, the materials appeared lightly coated with calcium sulfate deposit and otherwise similar to the coupon samples.

Figure 2.26 is a summary of the average rate of attack on each alloy considered for Pilot Plant use. The coupons compare favorably with the fin results for the tested alloys within the range of expected variation. The corrosion conditions within the bed, as reflected by the depth of attack on both coupons and fins, were very uniform. No pattern of attack rate with location with respect to coal feed or to height in the bed, (including freeboard), was discernible.

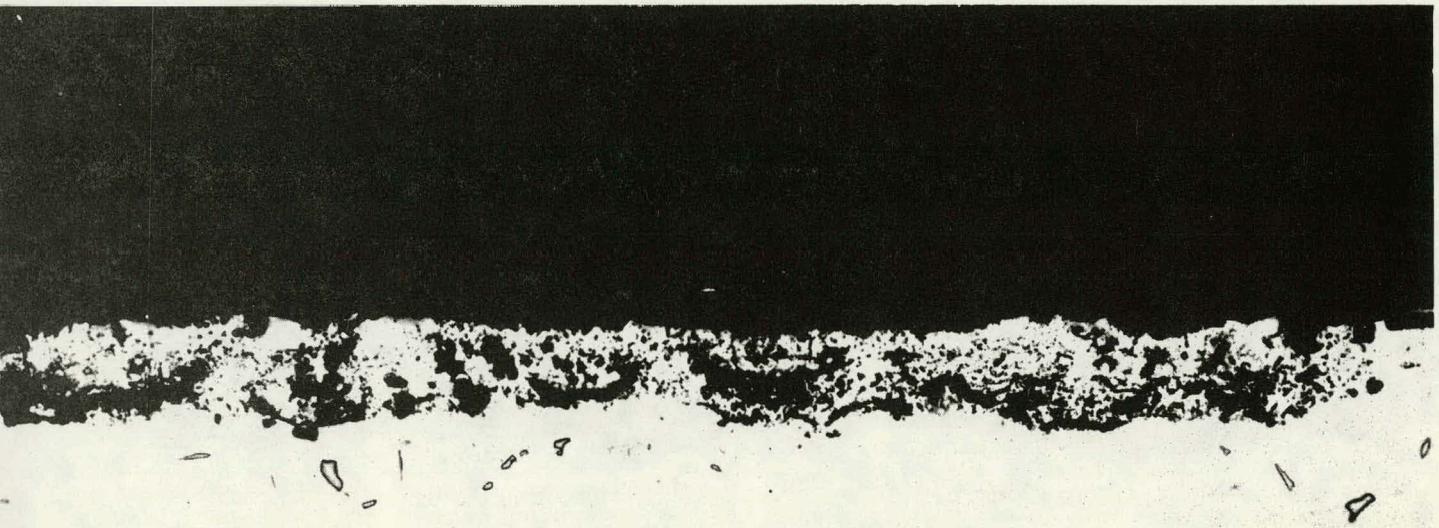

Allegheny Ludlum 16-5-Y Fin, Tube #2, 8' Up
Typical Wastage in the Cross-Section

200X

Figure 2.33

80-100

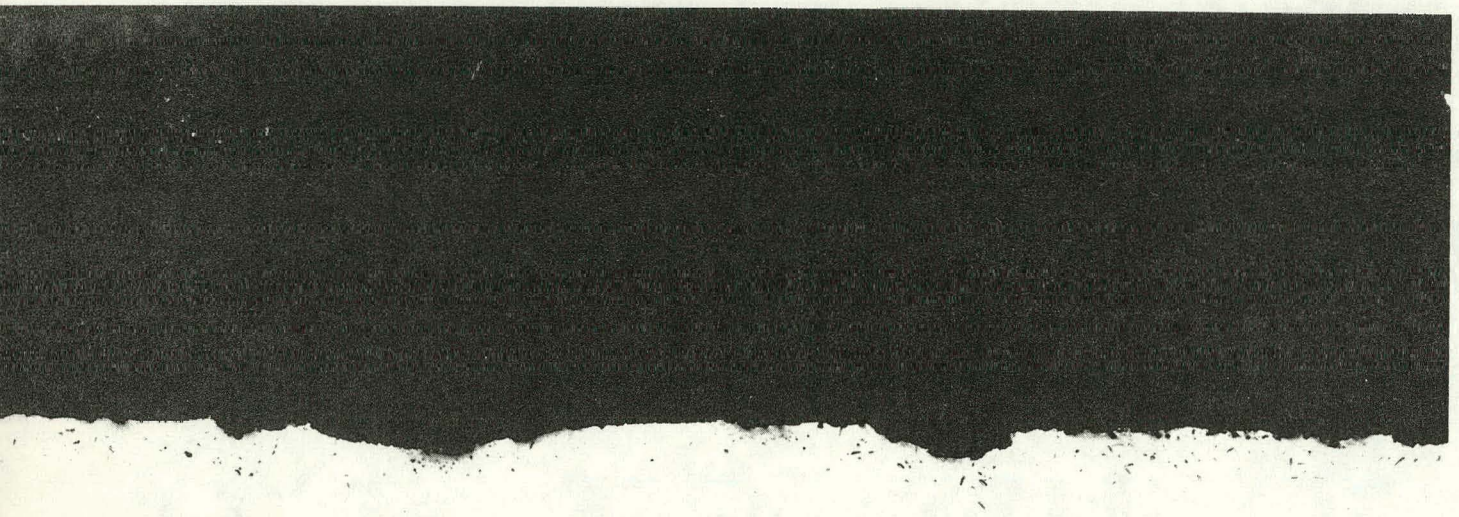

AISI Type 310 Fin, Tube #2, 8' Up
Typical Pitting in the Cross-Section

200X

Figure 2.34

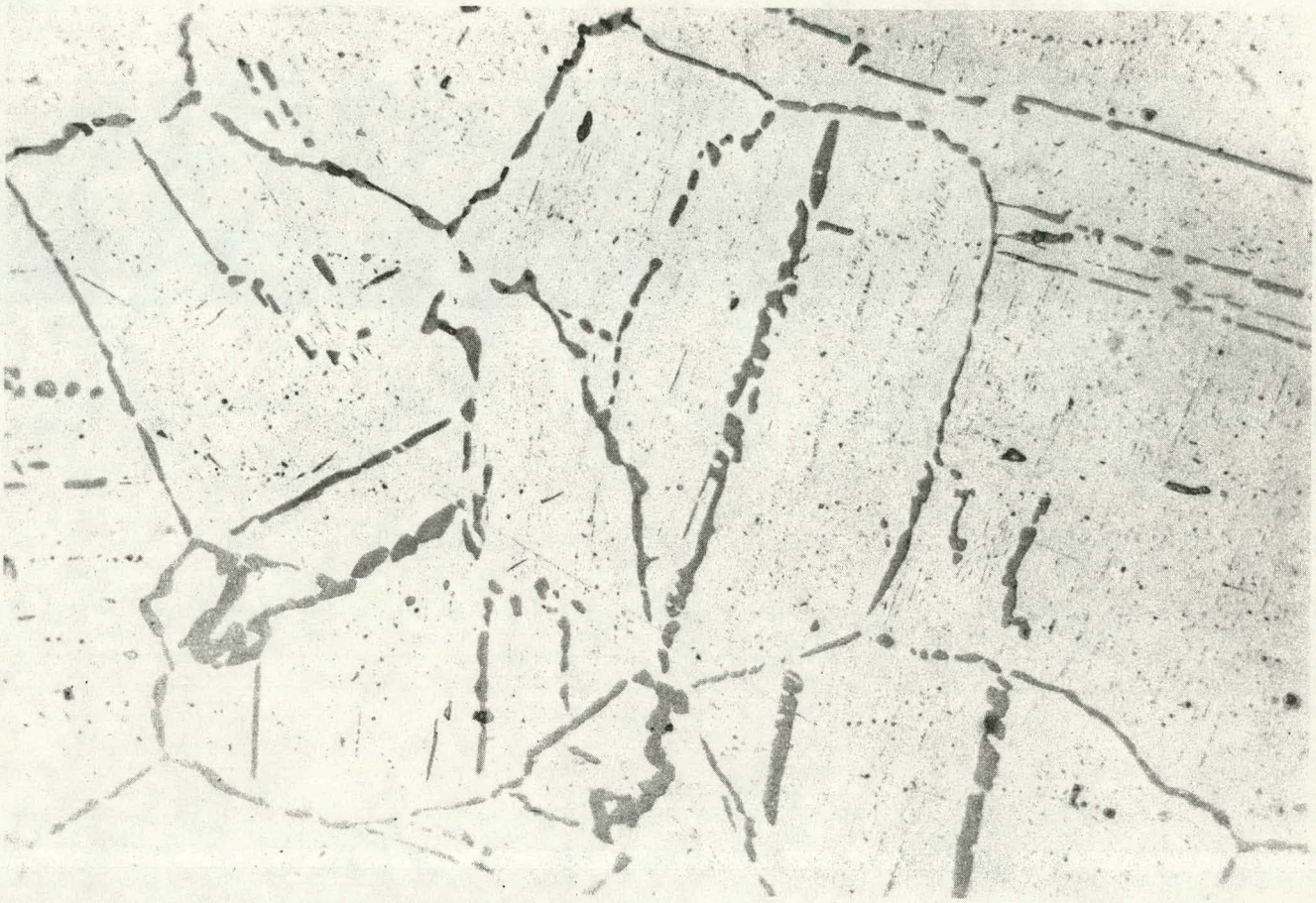

AISI Type 310 Fin, Tube #3, 5' Up

Sigma Phase

Murikami's Etch 500X

Figure 2.35

80-102

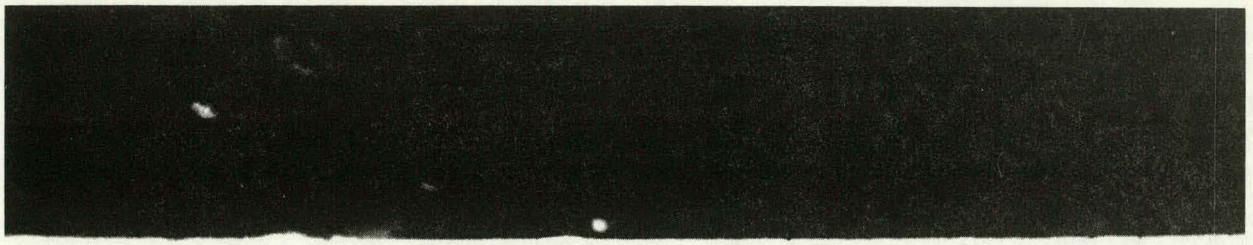

AISI Type 310 Fin, Unused
No Sigma Phase

Murikami's Etch 500X

Figure 2.36

The rate of attack for the various alloy types investigated falls within the range of results experienced previously by both Curtiss-Wright and other investigators.

2.5.2 Turbine Materials and Coatings

Initial shakedown testing of the turbine used a standard turbine rotor and stator supplied with the engine, modified to include several different coatings. The rotor was made from Nimonic 90 material, and the stator from Nimonic 80. Both are nickel-base superalloys. During this initial 150-hour test run (Test No. 9), the cyclone separators as received from the manufacturer did not perform in the hot gas cleanup train (Build No. 1) as expected. The particulate concentration, measured by isokinetic probes at stations located before the turbine inlet, was 0.15 grains/scf. The mean particle size in the stream was 3.7 microns and the maximum size was 27 microns.

Inspection of the turbine after 150 hours of operation at these conditions showed erosion at the trailing edge tip of the rotor blades, as shown in Figure 2.37. The trailing edges of four adjacent stator vanes also showed localized erosion. The eroded vanes were located 180 degrees away from the gas inlet into the scroll supplying the stator, as shown in Figure 2.38. The remaining vanes did not exhibit any erosion.

From this test it was evident that an improvement in particulate removal would be required to insure a reasonable turbine life. For this reason no further analysis was performed on the turbine. Inspection of the separators indicated several different reasons for their failure to perform as expected. Modifications were made to both the 1st and 2nd stage separators (Build No. 2) before initiating the 1000-hour turbine test. At approximately midway through the 1000-hour test, further modifications were made to the 1st stage and 2nd stage separators (Build No. 3). These final modifications resulted in a reduction of the grain loading from 0.056 to 0.046 gr/scf to the turbine. The mean particle and maximum particle diameter of the particulate entering the turbine was not significantly affected by the change, remaining essentially at a mean size of 1.3 microns and a maximum size under 10 microns through the entire 1000-hour test.

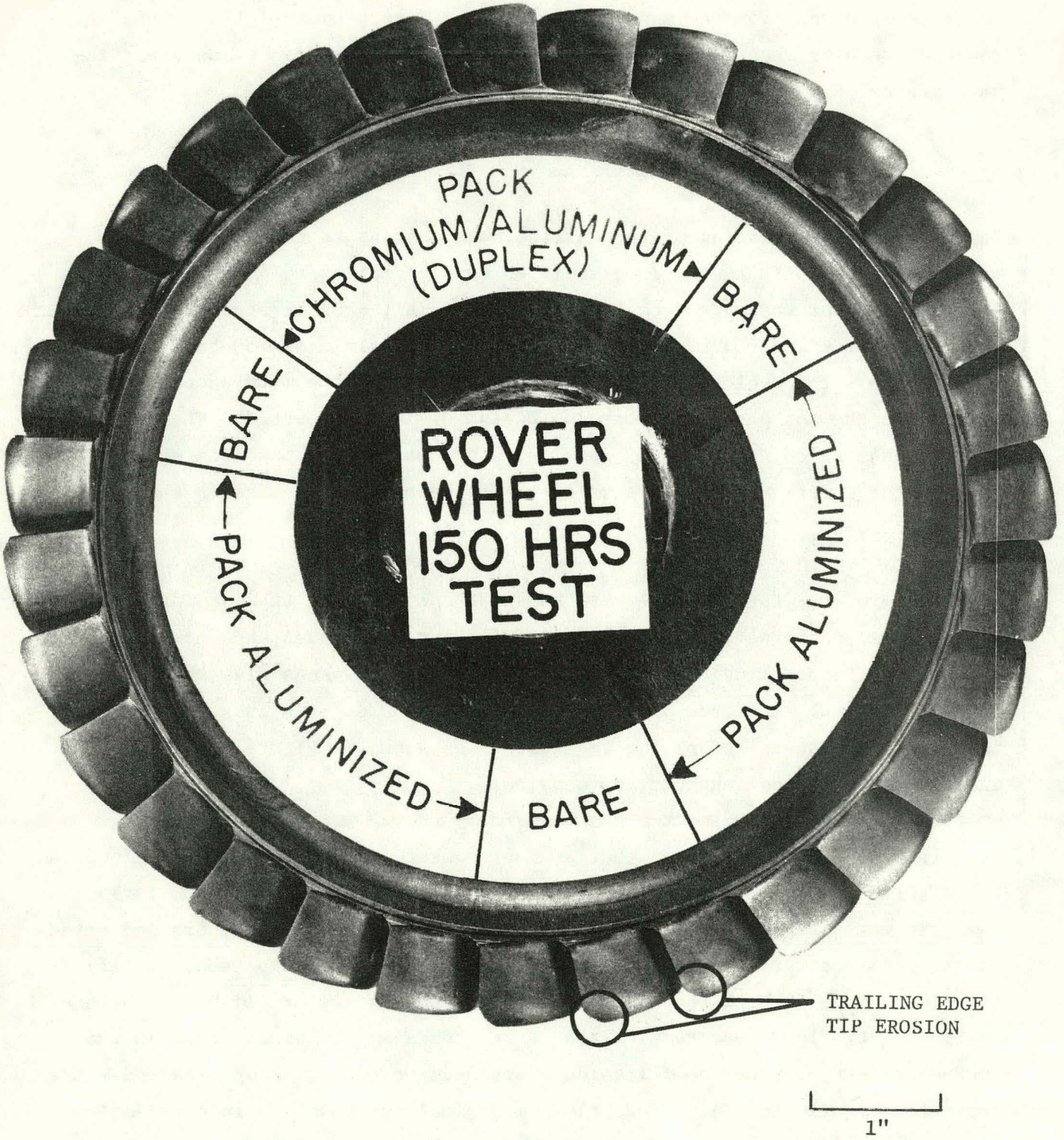

A trailing edge view of the Nimonic 90, Rover turbine rotor after the 150 hour "shakedown" test. Note the erosion of the trailing edge blade tips.

Figure 2.37

80-207

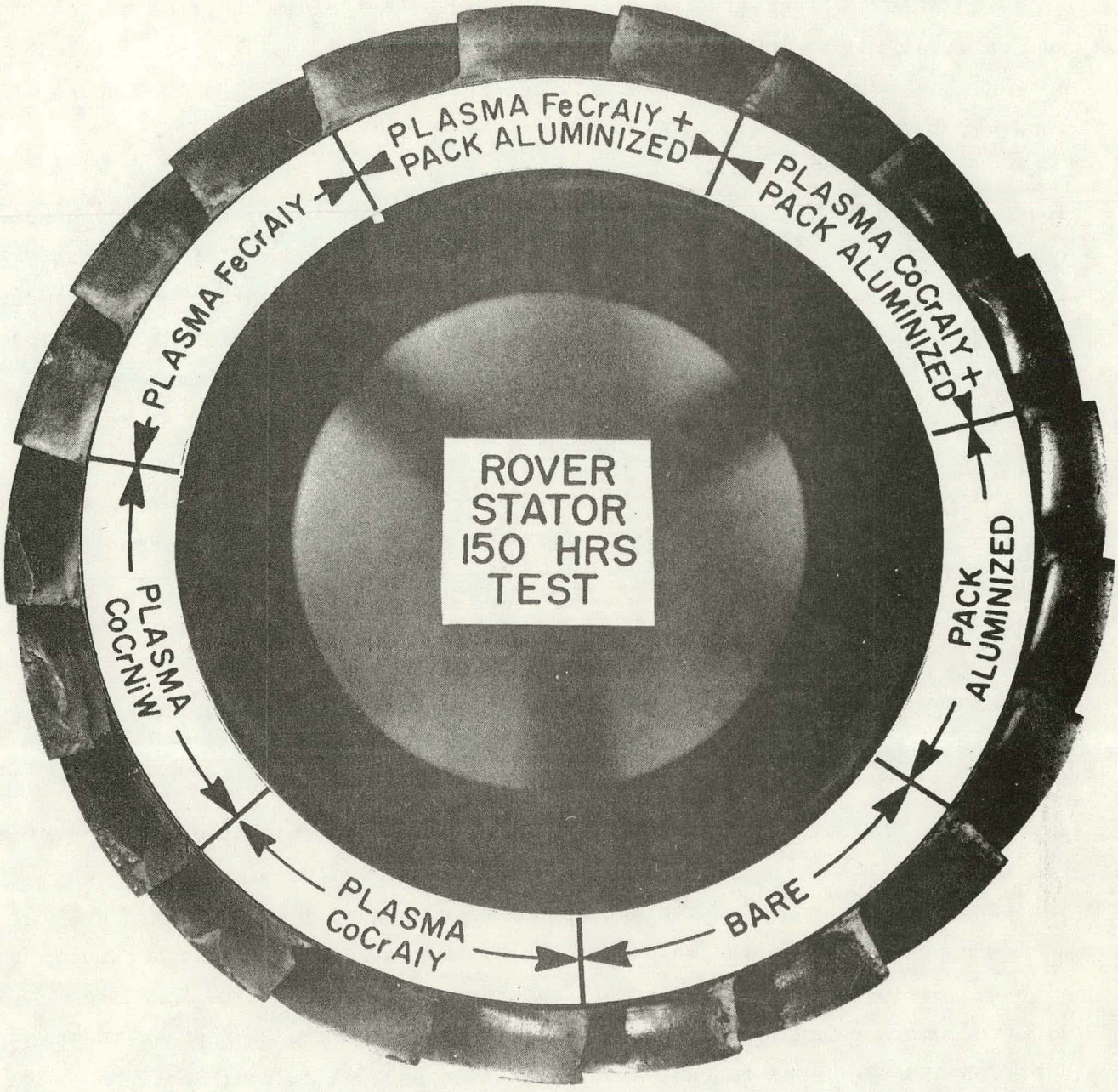

A trailing edge view of the Nimonic 80, Rover turbine stator after the 150 hour "shakedown" test. Note the localized erosion of the vane trailing edges in the lower left hand corner, which is 180° from the scroll inlet.

Figure 2.38

80-105

A new turbine was installed so that a variety of materials and coatings could be evaluated in the 1000-hour test and a metallurgical analysis was carried out on the turbine stator and rotor after the completion of the 1000 hours of running.

The turbine is a single stage axial reaction type turbine with a stator assembly containing 21 individual replaceable vanes and an integral forged rotor with 31 blades. The stator assembly contained ten alloy-coating combinations. The rotor was coated with two different coatings. A description of the alloy-coating combinations in both the stator and rotor is listed in Table 2.21.

Several times during the course of the 1000-hour run, the PFB Technology Rig was shut down and the turbine stator and rotor inspected. Figure 2.39 shows the concave surface of the rotor after 160 hours and Figure 2.40 after 1000 hours of running. Figure 2.41 shows the turbine stator and rotor after 1000 hours.

The results of the turbine metallurgical examinations are summarized in Table 2.22.

In order to characterize the corrosion/erosion/deposition that occurred during the 1000-hour test, representative stator vanes and rotor blades were subjected to both non-destructive and destructive examination. Metallographic analysis provided information on the following: ash deposit thickness, remaining coating thickness, and depth of erosion/corrosion. The Scanning Electron Microscope along with the microprobe was utilized for phase identification and elemental concentration traces on several airfoil sections. Table 2.22 lists the tests carried out in this analysis. The ash deposits were submitted for (a) quantitative elemental analysis and (b) X-ray diffraction analysis for phase identification.

A rouge colored deposit was found in the hub rim of the turbine wheel, It was compacted but not difficult to dislodge. It easily broke up into a fine powder. The chemical analysis of this powder deposit is as follows:

TABLE 2.21

TURBINE ALLOY-COATING COMBINATIONS AND PRELIMINARY CORROSION/EROSION MEASUREMENTS

Vane Alloy/Coating	Thickness, Mils	Maximum Corrosion Penetration in Coating, Mils	Coating Composition	Remarks
IN-738/MDC-1	3	2	Aluminide Diffusion Coating	Light coating attack. Maximum on suction surface around point of maximum camber.
IN-738/ATD-17	8-10	< 1	Fe-Cr-Al-Y Vapor Deposited Coating	Very light coating attack. Maximum on suction surface around point of maximum camber.
IN-738/RT-22	4-5	2	Platinum-Aluminide Diffusion Coating	Light coating attack. Maximum on suction surface around point of maximum camber.
IN-738/ATD-1	4-8	3	Ni-Cr-Al-Y Vapor Deposited Coating	Light coating attack. Maximum on suction surface around point of maximum camber.
IN-738/ATD-12	5-8	3	Co-Cr-Al-Y Vapor Deposited Coating	Light coating attack. Maximum on suction surface around point of maximum camber.
FSX-414/ATD-17	6-14	< 1	Fe-Cr-Al-Y Vapor Deposited Coating	Very light coating attack. Maximum on suction surface around point of maximum camber.
FSX-414/RT-44	3-4	2	Rhodium-Aluminide Diffusion Coating	Light coating attack. Maximum on suction surface around point of maximum camber.

TABLE 2.21 (Continued)

TURBINE ALLOY-COATING COMBINATIONS AND PRELIMINARY CORROSION/EROSION MEASUREMENTS

Vane Alloy/Coating	Thickness, Mils	Maximum Corrosion Penetration in Coating, Mils	Coating Composition	Remarks
FSX-414/ATD-1	5-7	2	Ni-Cr-Al-Y Vapor Deposited Coating	Light coating attack. Maximum on suction surface around point of maximum camber.
FSX-414/ATD-12	6-7	5	Co-Cr-Al-Y Vapor Deposited Coating	Light coating attack. Maximum on suction surface around point of maximum camber.
FSX-414/RT-19	1-2	2*	Aluminide Diffusion Coating	Coating penetrated on suction surface around point of maximum camber.
Blade Alloy/Coating				
U-720/RT-21	3	2	Aluminide Diffusion Coating	Light coating attack. Some coating erosion on blade suction surface near leading edge, and pressure surface at trailing edge tip.
U-720/RT-22	3	1	Platinum-Aluminide Diffusion Coating	No coating attack. Some coating erosion on blade suction surface near leading edge and pressure surface at trailing edge tip.

* Penetration in Base Alloy

SGT/PFB ROVER TURBINE WHEEL - 160 HOURS OPERATION

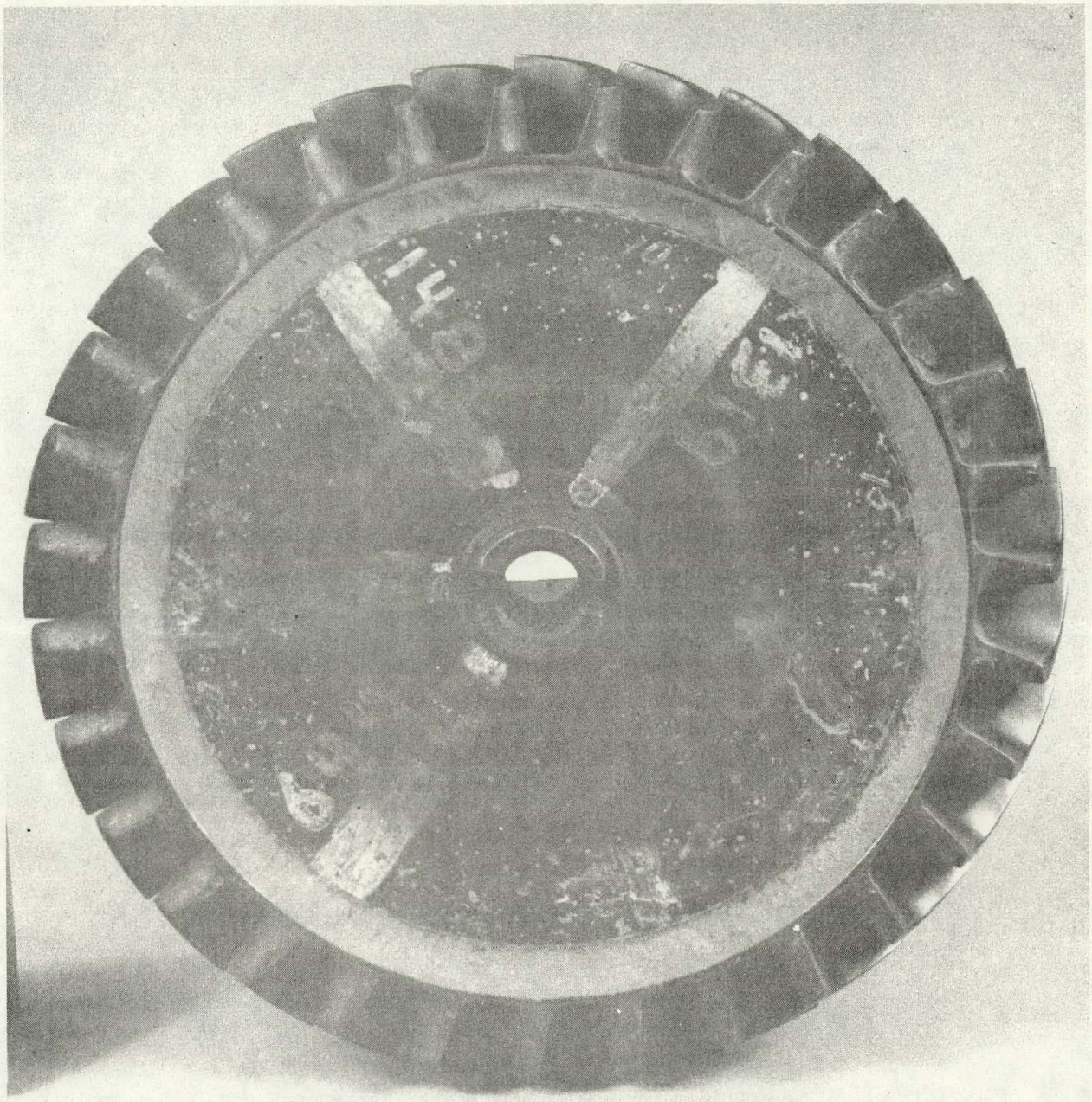

PFB-III-117

Figure 2.39

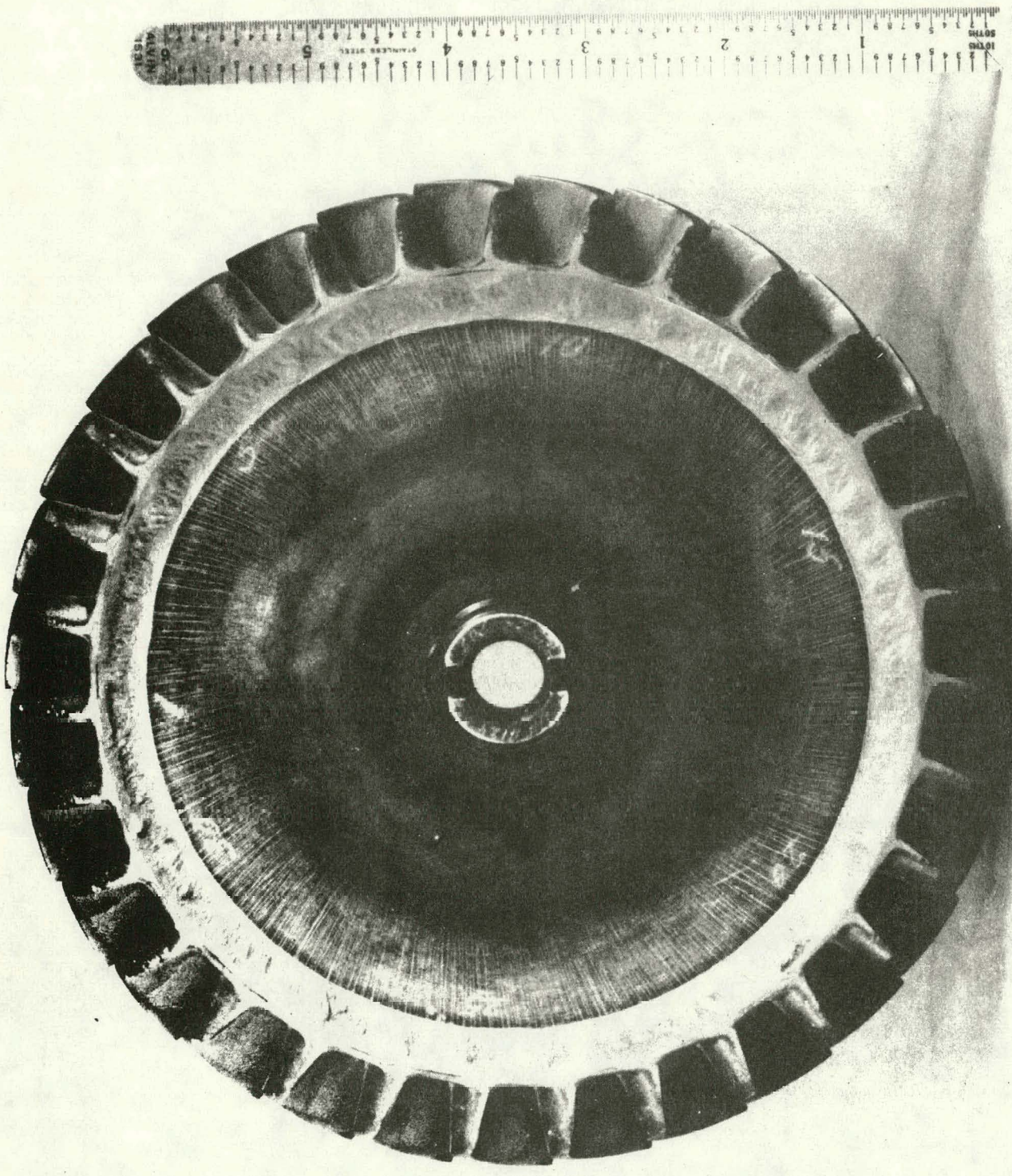
PFB-III-273
SGT PFB ROVER TURBINE WHEEL - 1000 HRS RUNNING TIME

Figure 2.40

ROVER STATOR AND ROTOR AFTER COMPLETION OF THE 1000 HOUR TEST

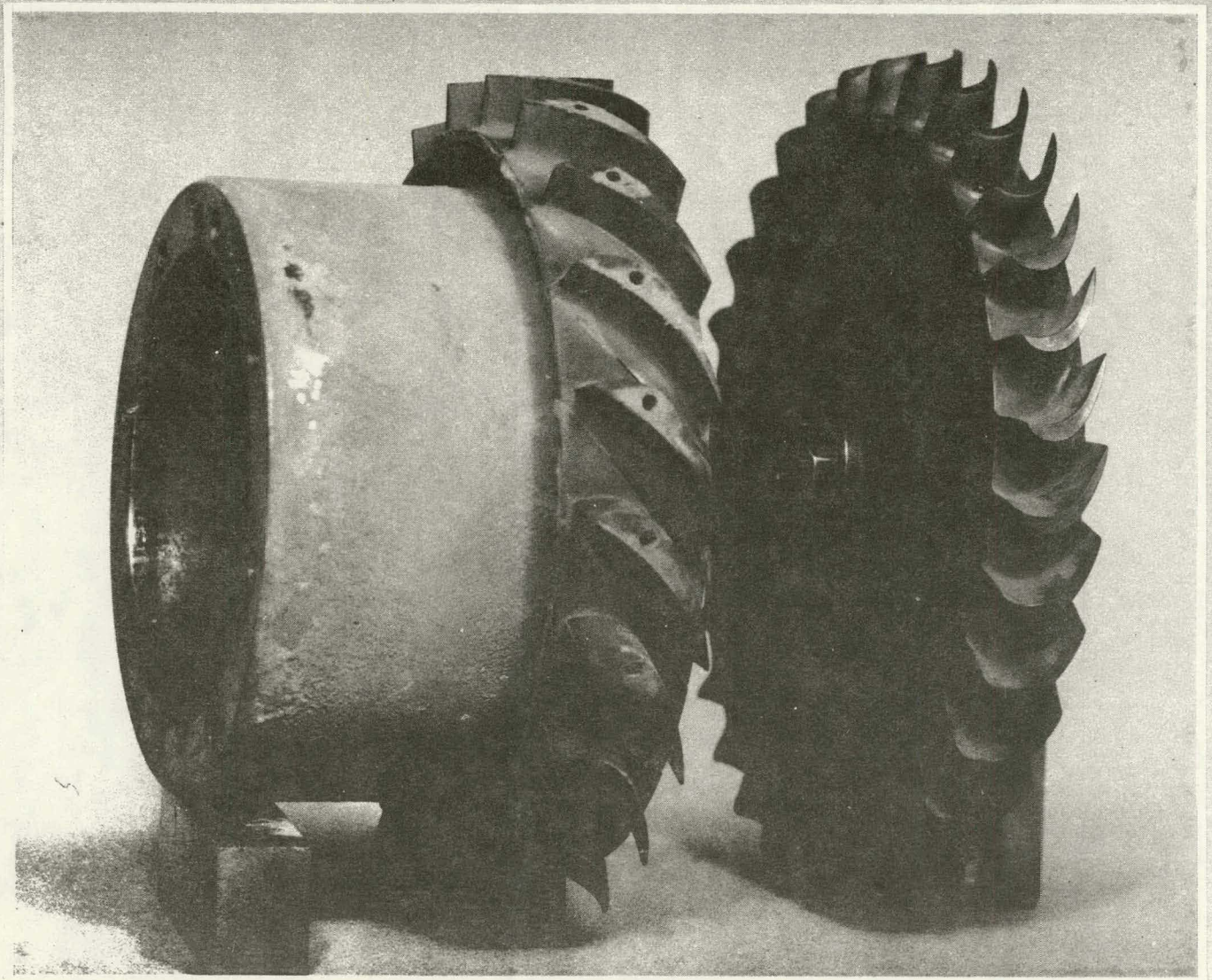

PFB-III-265-S

Figure 2.41

Table 2.22

METALLURGICAL ANALYSIS OF ROVER TURBINE BLADES AND VANES

COMPONENT	NO.	MICROS	EDXA	SEM PHOTOS	ELEMENTAL MAPPING																ELEMENTAL TRACES						
					Na	K	Mg	Ca	Fe	Si	C	Ti	P	Cr	S	O	Ni	Al	Pt	Co	Y	Co	Al	Cr	Ni	S	Pt	O
BARE BLADES	2	8	YES	YES	-	-	-	-	-	-	-	-	-	X	X	X	X	X	-	-	-	-	X	X	X	X	-	-
RT-21 COATED BLADES	2	8	NO	NO	-	-	-	-	-	-	-	-	-	-	-	-	-	-	-	-	-	-	-	-	-	-	-	-
RT-22 COATED BLADES	2	8	YES	YES	-	-	-	-	-	-	-	-	-	X	X	X	X	X	X	-	-	-	X	X	X	-	X	-
ATD-17 COATED IN-738 VANE	1	1	YES	YES	-	-	-	-	-	-	-	-	-	-	-	-	-	-	-	-	-	-	-	-	-	-	-	-
RT-19 COATED FSX-414 VANE	1	1	YES	YES	-	-	-	-	-	-	-	-	-	X	X	X	-	X	-	X	-	X	-	X	-	X	-	X
RT-22 COATED IN-738 VANE	1	1	NO	NO	-	-	-	-	-	-	-	-	-	-	-	-	-	-	-	-	-	-	-	-	-	-	-	-
ATD-1 COATED FSX-414 VANE	1	1	NO	NO	-	-	-	-	-	-	-	-	-	-	-	-	-	-	-	-	-	-	-	-	-	-	-	-
ATD-12 COATED FSX 414-VANE	1	1	NO	NO	-	-	-	-	-	-	-	-	-	-	-	-	-	-	-	-	-	-	-	-	-	-	-	-
ATD-17 COATED FSX-414 VANE	1	1	YES	YES	-	-	-	-	X	-	-	-	-	X	X	X	-	X	-	-	X	-	-	-	-	-	-	-
ATD-1 COATED IN-738 VANE	1	1	NO	NO	-	-	-	-	-	-	-	-	-	-	-	-	-	-	-	-	-	-	-	-	-	-	-	-
ATD-12 COATED IN-738 VANE	1	1	NO	NO	-	-	-	-	-	-	-	-	-	-	-	-	-	-	-	-	-	-	-	-	-	-	-	-
MDC-1 COATED IN-738 VANE	1	1	NO	NO	-	-	-	-	-	-	-	-	-	-	-	-	-	-	-	-	-	-	-	-	-	-	-	-
RT-44 COATED FSX-414 VANE	1	1	YES	YES	X	X	X	X	X	X	X	X	X	-	X	X	-	X	-	-	-	-	-	-	-	-	-	-

PFB-III-309

Sodium	0.3%
Potassium	0.7
Sulfur	6.
Calcium	15.6
Magnesium	4.6
Aluminum	6.5
Silicon	1.0
Iron	7.5
Acid Insoluble	32.
Oxygen	Difference

There was an insufficient sample to analyze for oxygen, carbon, chlorine or other minor elements such as titanium and phosphorous. The sample, as received, was a light, reddish homogenous powder of fine particles. A portion of the powder was dissolved in nitric and hydrochloric acids, the undissolved residue being the acid insoluble portion.

Energy dispersive X-ray analysis (EDXA) (Figure 2.42) showed Al, Si, Fe and Ca as major constituents plus minor concentrations of magnesium, sodium and less-than-minor concentrations of potassium, sulfur and titanium.

There appears to be a discrepancy between the quantitative analysis and the EDXA analysis relative to the sulfur and silicon contents. The EDXA analysis is qualitative in nature and was the analysis obtained, taken from a 3 micron diameter area of the fly ash. Since the fly ash is not a homogenous material, variations in chemistry exist on a microscopic level and these variations are reflected by this analysis.

X-ray diffraction analysis showed $CaSO_4$ (Anhydrite) as the major crystalline component plus minor Fe_2O_3 and less-than-minor Al_2SiO_5. Other possible candidates in less-than-minor category are $FeAl_2SiO_5(OH)_2$, $CaAl_2Si_2O_8$, SiO_2 and $K_2CaMg(SO_4)_3$. The form the sodium is present in is undetermined since the concentrations are too low to give a meaningful diffraction pattern.

DISPERSIVE X-RAY ANALYSIS RESULTS
FLY ASH
SPOT BEAM
UFS-8192
18.240
0.000
200
Fe
Ni
Zn
Cu
Sn
S
K
Ca
Ti
Mn
Fe

Figure 2.42

At the 368-hour inspection, a foreign refractory type material was found lodged in three turbine stator passages. Experiments carried out in the laboratory at the completion of the 1000-hour test produced a similar material by heating fly ash from the 3rd stage cyclone catch to between 2000°F and 2200°F. It appears likely that the material found lodged in the stator was fused fly ash, formed during an overheating condition in the kerosene burner installed in the hot gas piping, downstream of the 3rd stage cyclone to raise the gas temperature to between 1550-1600°F prior to entering the turbine. The chemical spectra, determined by EDAX, of the foreign material was found to be identical to fused fly ash spectra; supporting the theory that a localized overheat condition existed at the kerosene nozzle sometime between 160 and 368 hours of turbine operation.

Rotor Blades

Two rotor blades of each configuration (uncoated, RT-21 coated and RT-22 coated) were subjected to metallurgical examination. One blade of each configuration was sectioned in the chordwise direction in three radial planes (Figure 2.43) for examination. The second blade of each configuration was sectioned in the radial direction in five axial planes (Figures 2.44) for examination. All sections were examined at 400X.

All the rotor blades exhibited slight erosion on the convex surface near the leading edge, and on the concave surface at the trailing edge tip (Figures 2.45 and 2.46). In addition, all rotor blades showed a small area of wear at the leading edge close to the airfoil tip (Figure 2.45). (This wear was observed at the 368-hour inspection and did not significantly increase during subsequent running.) This leading edge tip wear was caused by a rub between the rotor and the fused fly ash lodged in the three stator passages which occurred between the 160 and 368-hour inspection. This was made evident by the presence of fused fly ash in all the rotor blades subjected to metallurgical examination. Fragments like the one shown in Figure 2.47 were found imbedded in the leading edge tip of all the rotor blades examined at high magnification. Elemental chemical spectra of this material was identical to the spectra of the material lodged in the stator passages, and to the spectra of the fused fly ash from the laboratory experiments.

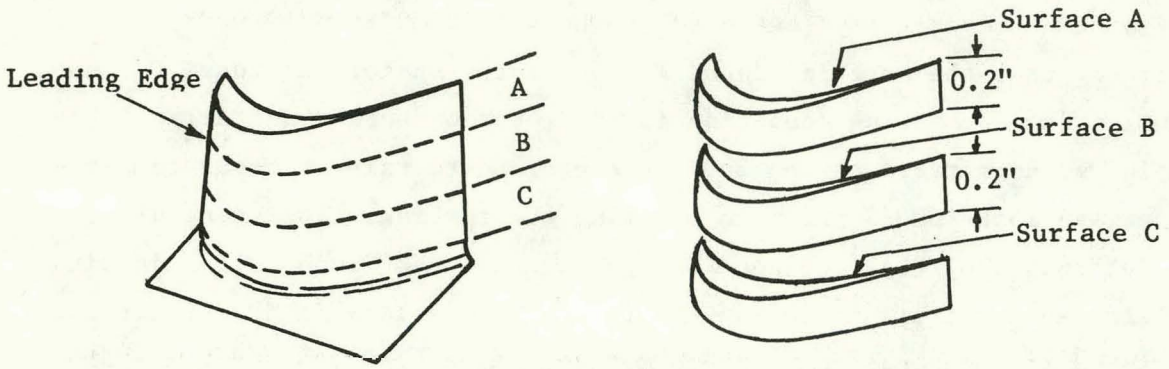

Figure 2.43 Rotor Blade, Convex Surface. Dash Lines Indicate Where Chordwise Sections Were Made For Metallographic Examination. Surfaces A, B, and C Were Examined At High Magnification

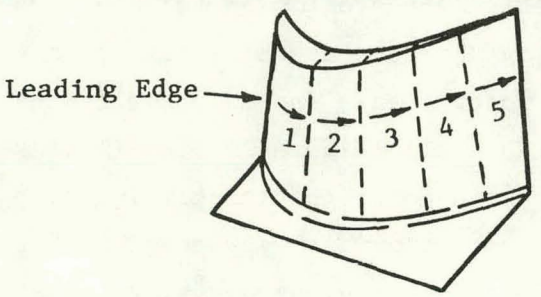

Figure 2.44 Rotor Blade, Convex Surface. Dash Lines Indicate Where Radial Sections Were Made For Metallographic Examination. Arrows Indicate Surfaces Examined At High Magnification

PLATINUM ALUMINIDE COATED ROVER BLADE ILLUSTRATING EROSION ON SUCTION SURFACE

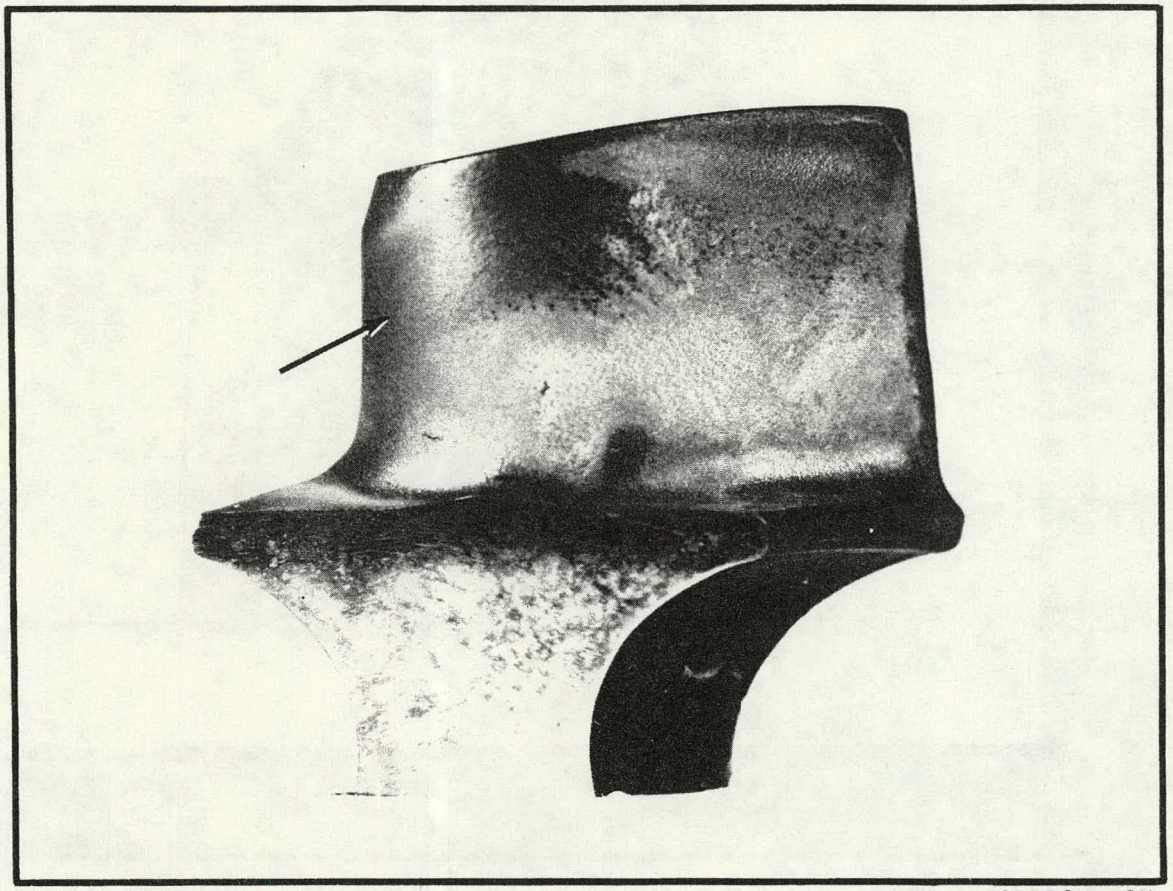

APPROX. 3X

PFB-III-305

Figure 2.45

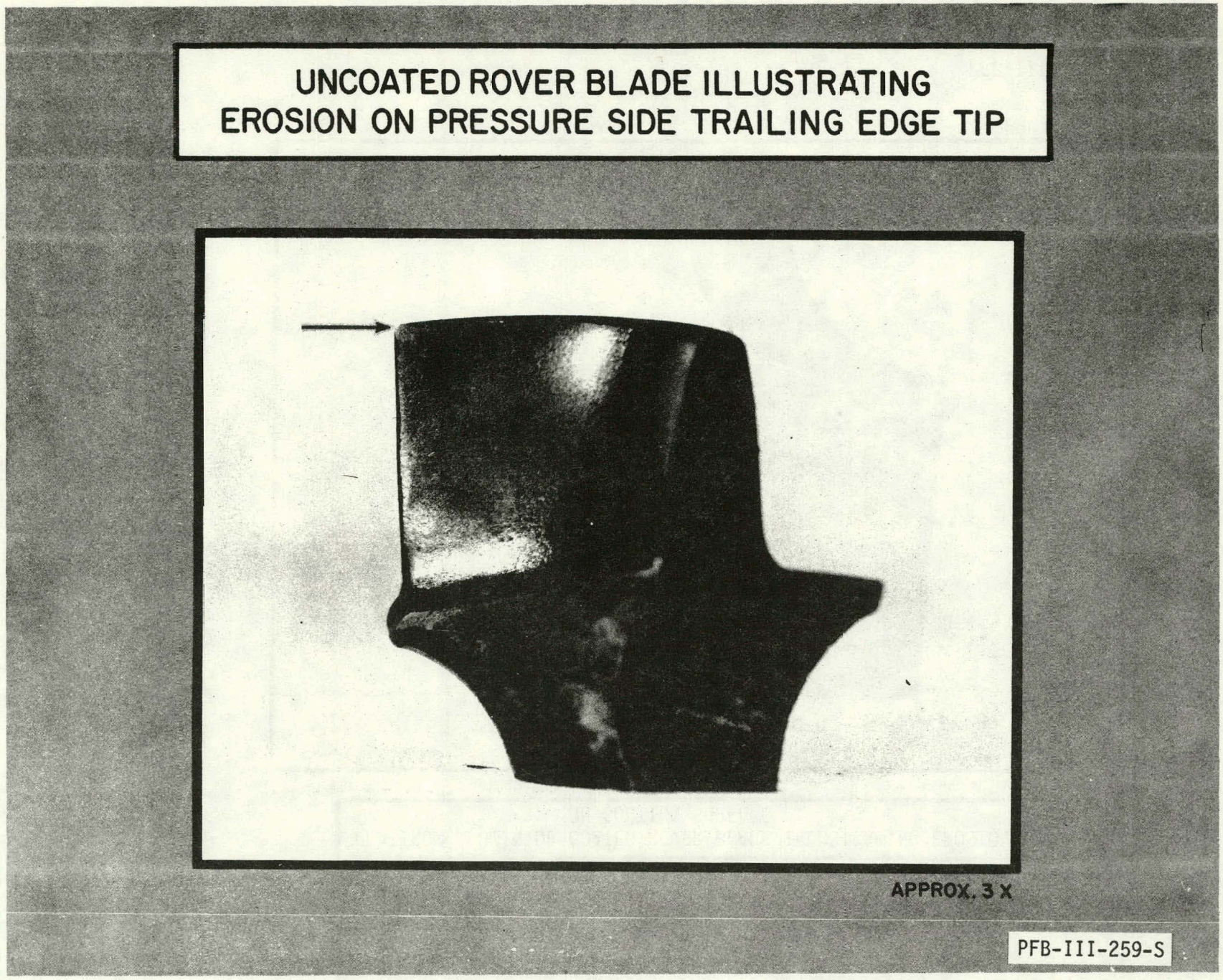
UNCOATED ROVER BLADE ILLUSTRATING
EROSION ON PRESSURE SIDE TRAILING EDGE TIP
APPROX. 3 X
PFB-III-259-S

Figure 2.46

PFB-III-262-S
1000 X
FOREIGN MATERIAL IMBEDDED IN ROVER BLADE
ON SUCTION SURFACE NEAR LEADING EDGE TIP

Figure 2.47

Examination of the nominal 3.2 mil platinum aluminide (RT-22) coated blades revealed that very little corrosion/erosion occurred during the 1000-hour test. Minor corrosion (to 1 mil) occurred on the convex surface. Total coating loss due to corrosion and/or erosion, was up to 1 mil except for the leading edge wear reported above. A thin adherent moderately hard fly ash deposit was present on the airfoil on the concave surface from the leading edge for 1/3 the distance to the trailing edge and on the convex surface covering the back half of the airfoil. Maximum deposit thickness of 3.6 mils was on the concave surface behind the leading edge. Figure 2.48 shows the microstructural characteristics of the RT-22 coating after 1000 hours of testing. Figure 2.49 shows the fly ash deposit on the concave surface of the RT-22 coated blade. Figure 2.50 shows the corrosion scale on some areas of the airfoil.

Figure 2.51 is a photomicrograph of the nominal 2.5 mil straight aluminide (RT-21) coating. This coating exhibited 2 mils of corrosion on both the convex and concave airfoil surfaces, but the corrosion did not penetrate into the base metal (Figure 2.52). Coating loss was up to 2 mils due to corrosion/erosion in some areas.

Examination of the uncoated blades at 400X revealed that a 0.5 mil corrosion scale was present. Since there was no coating present to act as a marker of the original blade surface, metal loss due to erosion could not be determined.

The blade sections were etched to reveal the microstructure at the metal surface. This etching revealed the presence of a 0.6 mil light etching zone along the outer metal surface (Figure 2.53). This zone was present over most of the airfoil surface except in those areas where erosion was evident on all rotor blades (Figure 2.54). This light etching zone is an alloy depleted zone caused by a loss of aluminum and chromium. It indicates that the blade was subject to high temperature oxidation during exposure. The presence of this zone indicates that oxidation would be the life limiting mechanism on most of the airfoil. In those areas where this zone does not exist, erosion would be the life limiting mechanism.

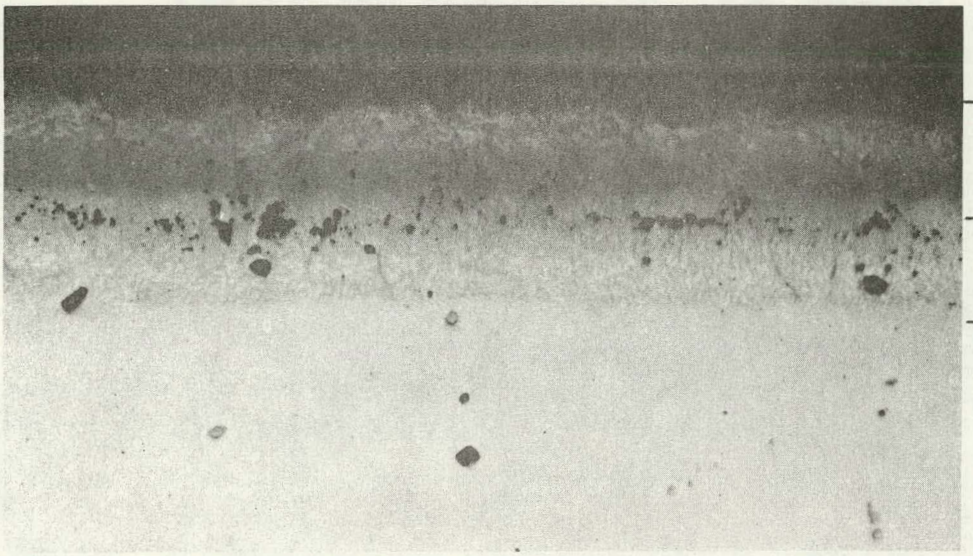

400X

Figure 2-48 Photomicrograph Of The Platinum-Aluminide Coating On Concave Surface Of Rover Rotor Blade After 1000 Hour Test Illustrating No Corrosion Scale

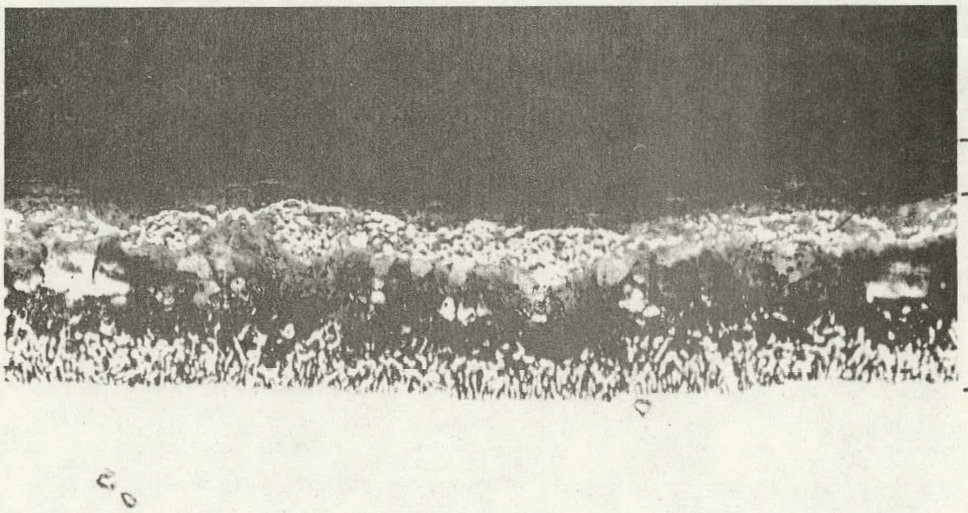

ETCH: $HCI-HC_2H_3O_2-HNO_3$

400X

Figure 2-49 Photograph Showing the Fly Ash Deposit on a RT-22 Coated Rover Turbine Blade.

80 309

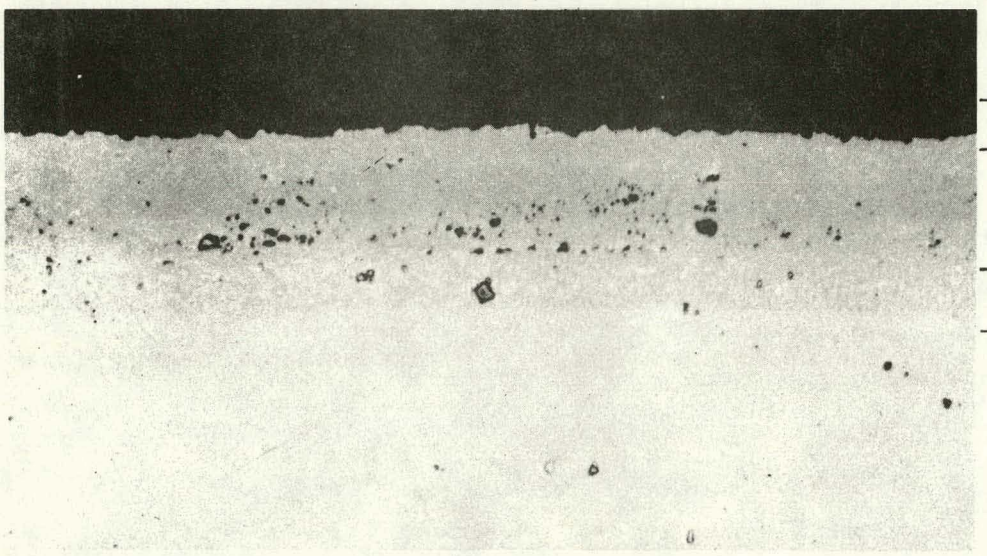

Figure 2.50 Photomicrograph Of Platinum-Aluminide Coating On Convex Surface Of Rover Rotor Blade After 1000 Hour Test Illustrating Corrosion Scale

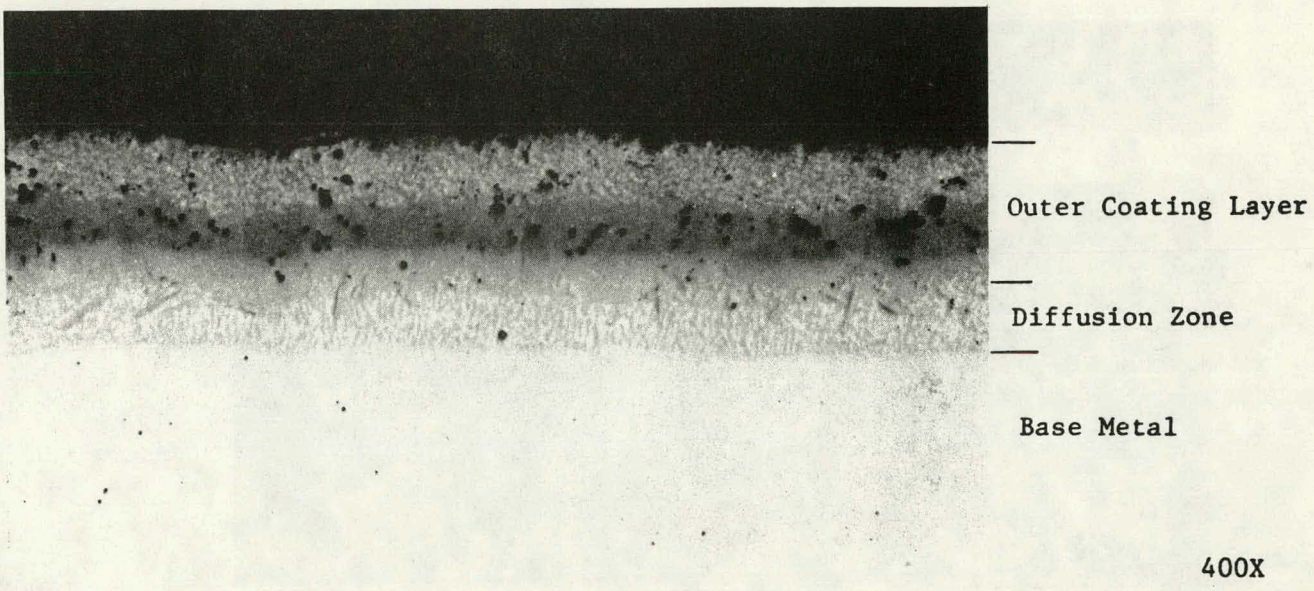

Figure 2.51 Photomicrograph Of The Aluminide Diffusion Coating On The Convex Surface Of A Rover Rotor Blade After The 1000 Hour Test Illustrating No Corrosion Scale

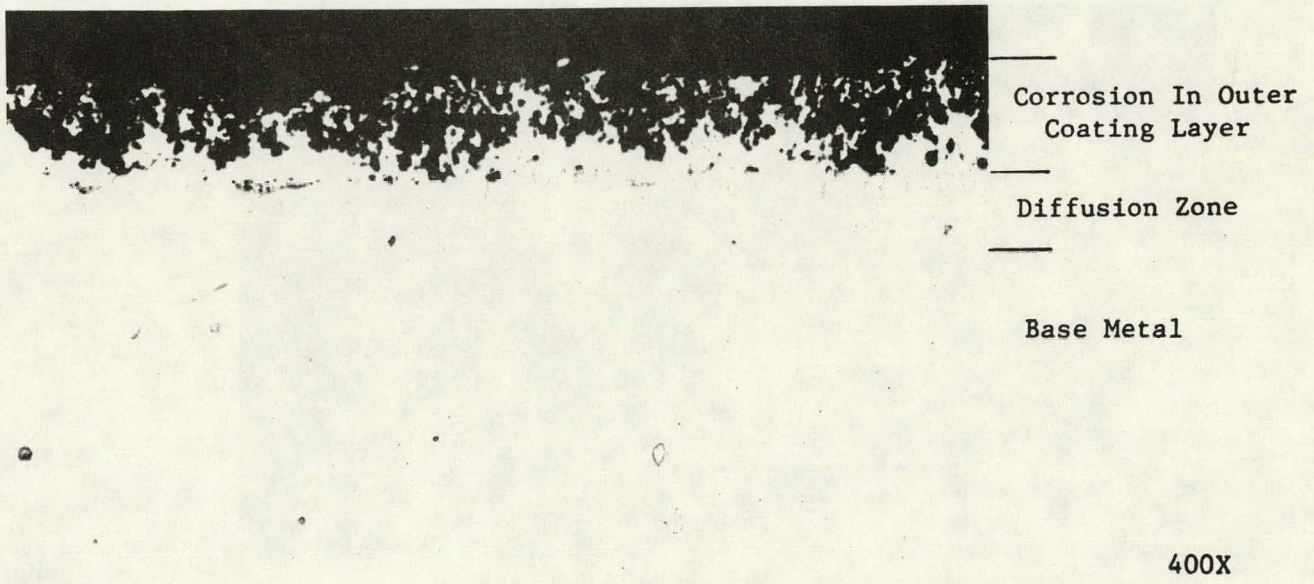

Figure 2.52 Photomicrograph Of The Aluminide Coating On The Convex Surface Of Rover Rotor Blade After The 1000 Hour Test Illustrating Corrosion In The Outer Coating Layer

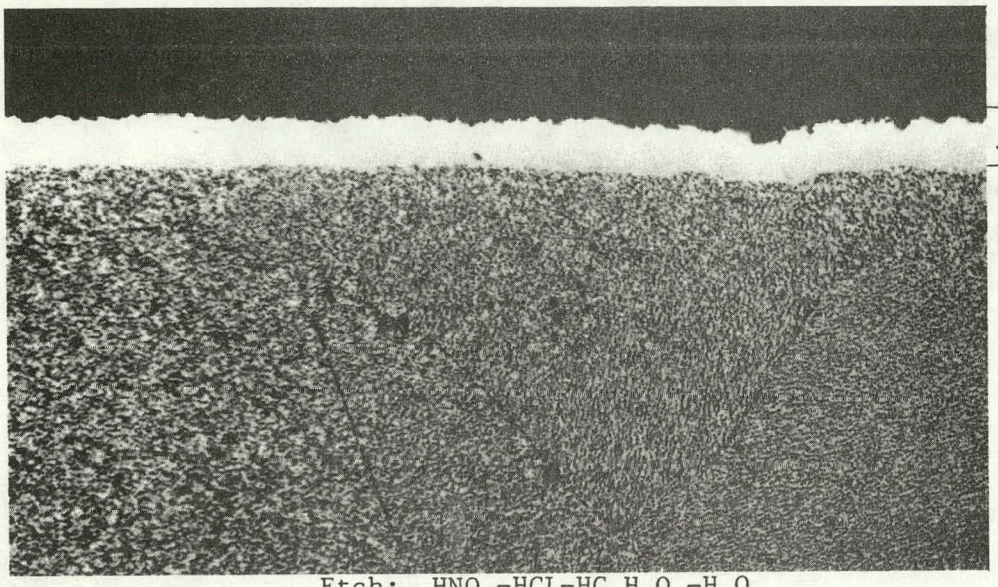

Etch: HNO_3-HCL-$HC_2H_3O_2$-H_2O 400X

Figure 2.53 Alloy Depleted Zone Along Concave Surface Of An Uncoated Rover Rotor Blade

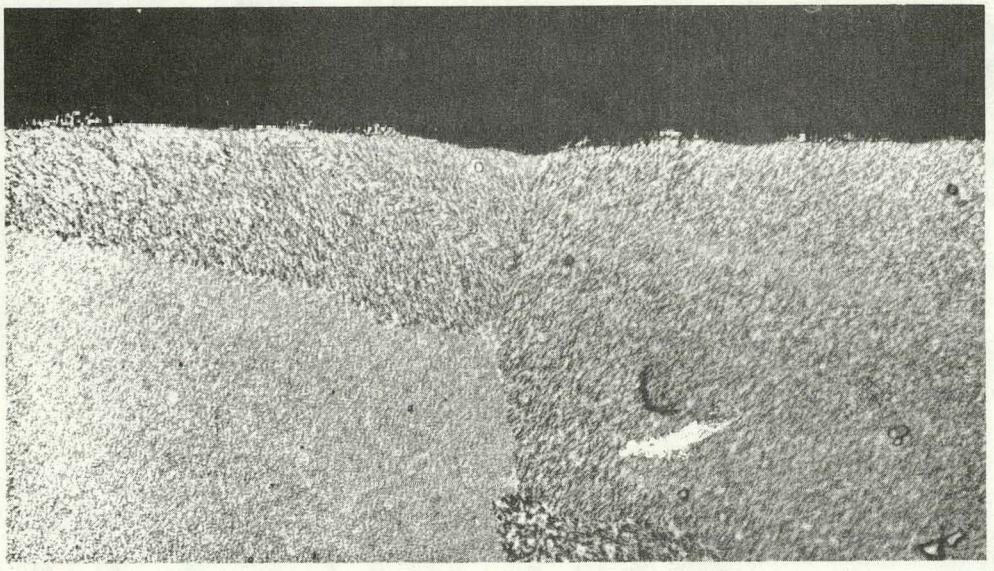

Etch: HNO_3-HCL-$HC_2H_3O_2$-H_2O 400X

Figure 2.54 Photomicrograph Showing The Microstructure Of An Uncoated Rover Rotor Blade On The Convex Surface Near The Leading Edge

Two corrosion resistant alloys, IN-738 (nickel base) and FSX-414 (cobalt base) were utilized as vane alloys. Five different coatings were applied to each alloy ranging from the straight aluminide diffusion coatings to the vapor deposited M-Cr-Al-Y coatings, where M was cobalt, nickel and iron.

A total of ten alloy/coating combinations (one of each combination) were subjected to metallurgical analysis. The vanes were cut in the chordwise direction at about half the airfoil height and subjected to metallurgical analysis. There was no erosion evident on any of the stator vanes. A fly ash deposit was present at the leading edge or on the concave surface near the leading edge on all the vanes subjected to metallographic analyses. This deposit (Figure 2.55) varied in thickness from 2.5 to 9 mils on the vanes examined.

Corrosion on the vanes was confined to a relatively small area on the convex surface around the point of maximum camber (Figure 2.56).

The most corrosion resistant coating was the Fe-Cr-Al-Y vapor deposited overlay (ATD-17). The maximum observed corrosion depth was only about 0.5 mil in this nominal 10 mil thick coating (Figure 2.57).

The maximum corrosion depth was evident in the Co-Cr-Al-Y vapor deposited overlay (ATD-12). This nominal 7 mil coating showed "spotty" corrosion to a maximum depth of about 5 mils (Figure 2.58).

The remaining coatings, both aluminide diffusion, and vapor deposited overlay types exhibited 1-3 mil deep corrosion (Figure 2.59). Only in the case of one shallow (1-2 mil) aluminide coating (RT-19) was any penetration of the base metal observed.

PHOTOGRAPH OF FLY ASH DEPOSIT ON ROVER VANE LEADING EDGE

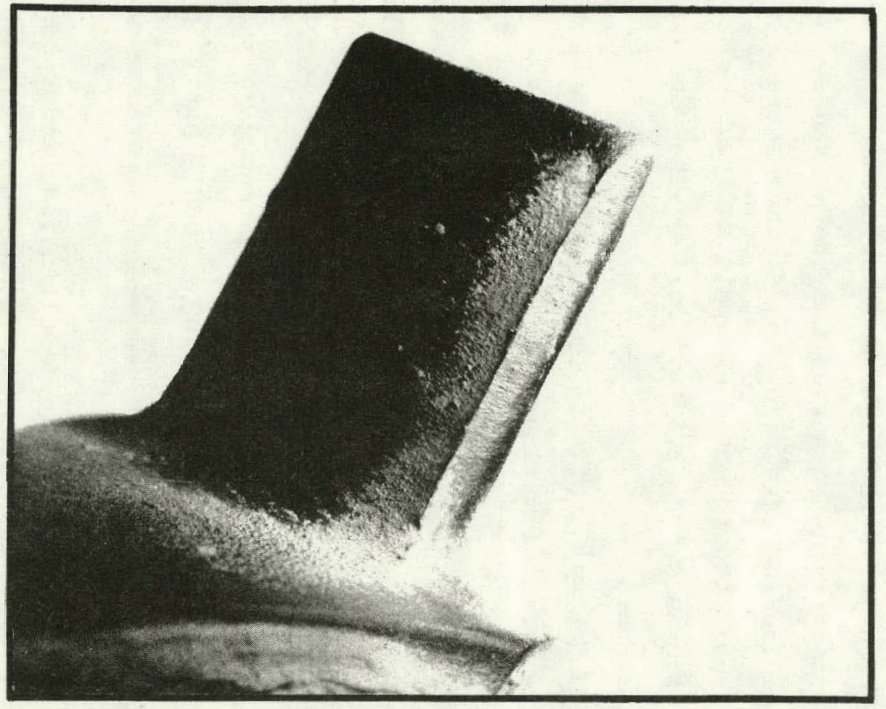

PFB-III-275

Figure 2.55

ROVER VANE, CONVEX (SUCTION) SURFACE COATED WITH Fe Cr AlY VAPOR DEPOSITED COATING

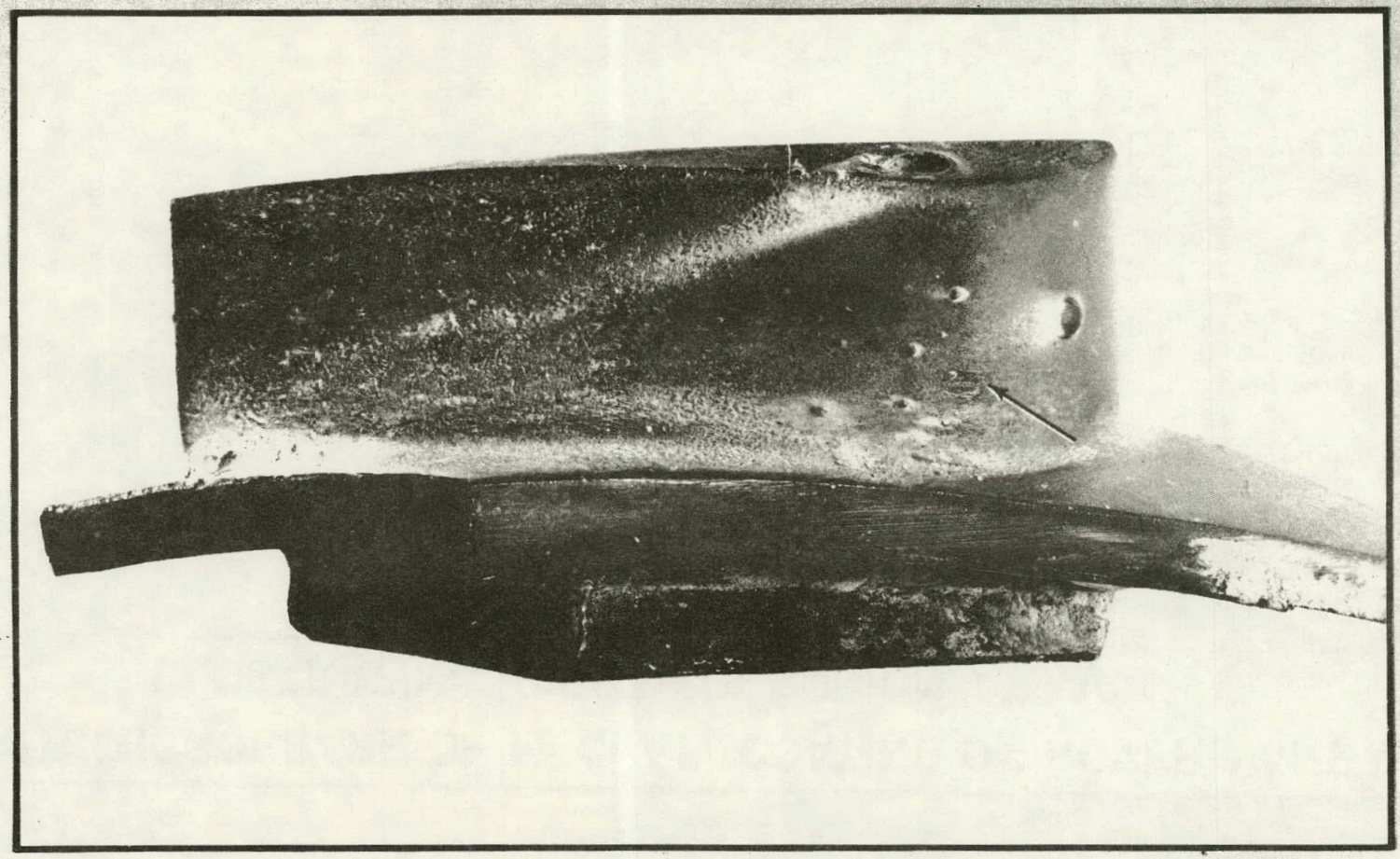

APPROX. 3 X

PFB-III-268-S

Figure 2.56

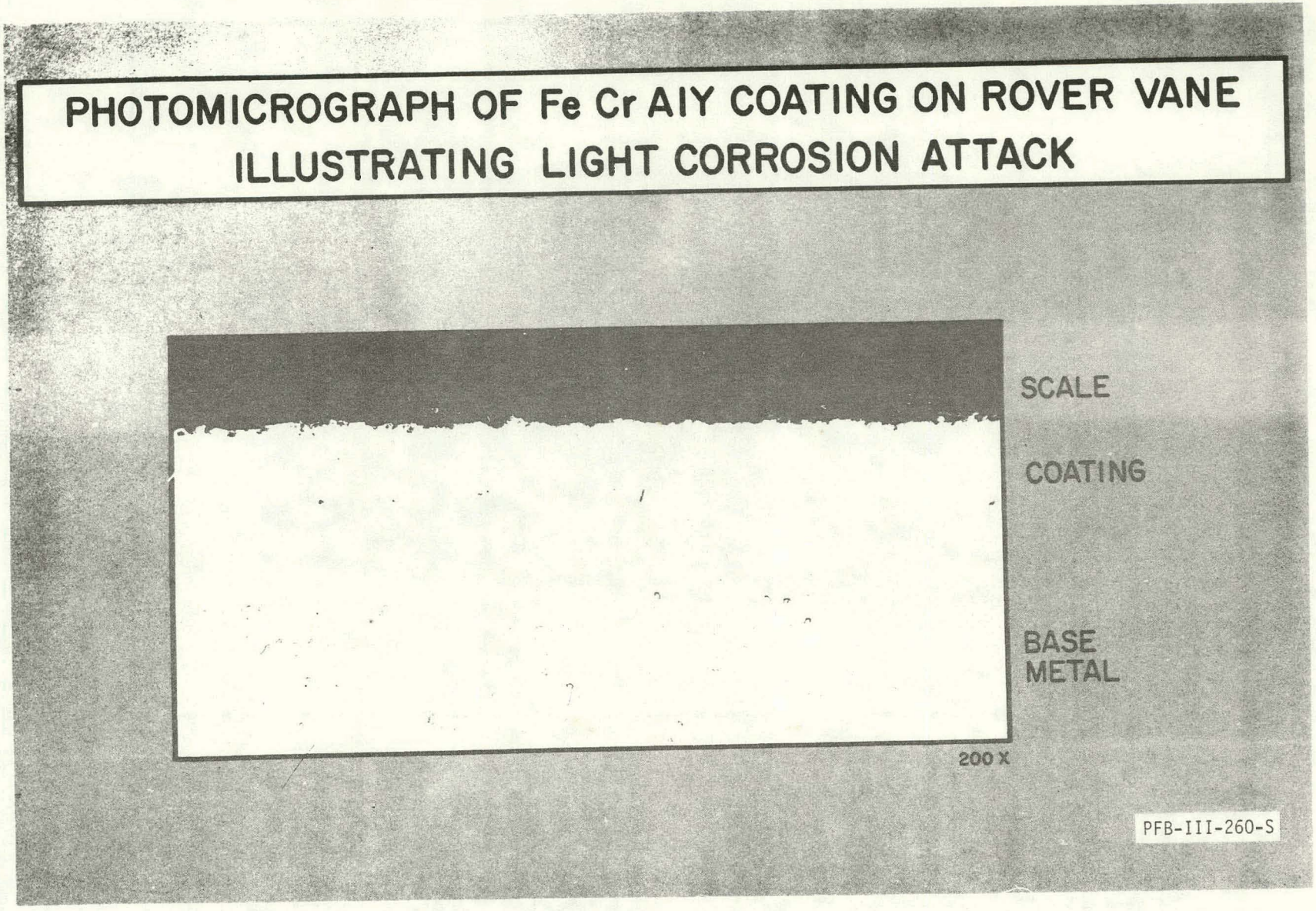
PHOTOMICROGRAPH OF Fe Cr AlY COATING ON ROVER VANE
ILLUSTRATING LIGHT CORROSION ATTACK
SCALE
COATING
BASE
METAL
200 X
PFB-III-260-S

Figure 2.57

PHOTOMICROGRAPH OF Co Cr AlY COATING ON ROVER VANE ILLUSTRATING "SPOTTY" CORROSION ON CONVEX SURFACE

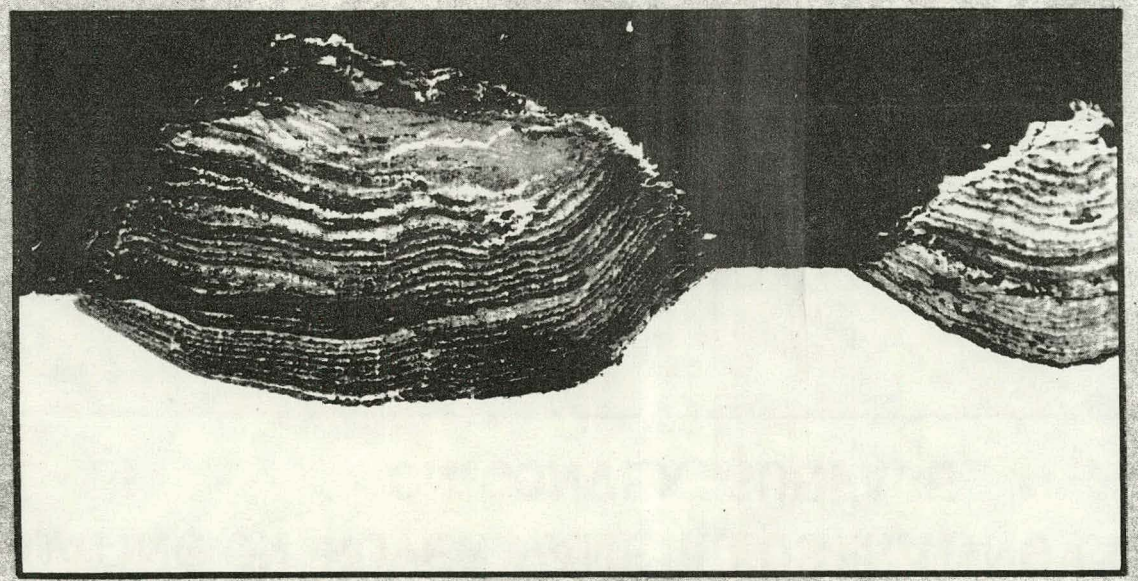

PFB-III-271-S

Figure 2.58

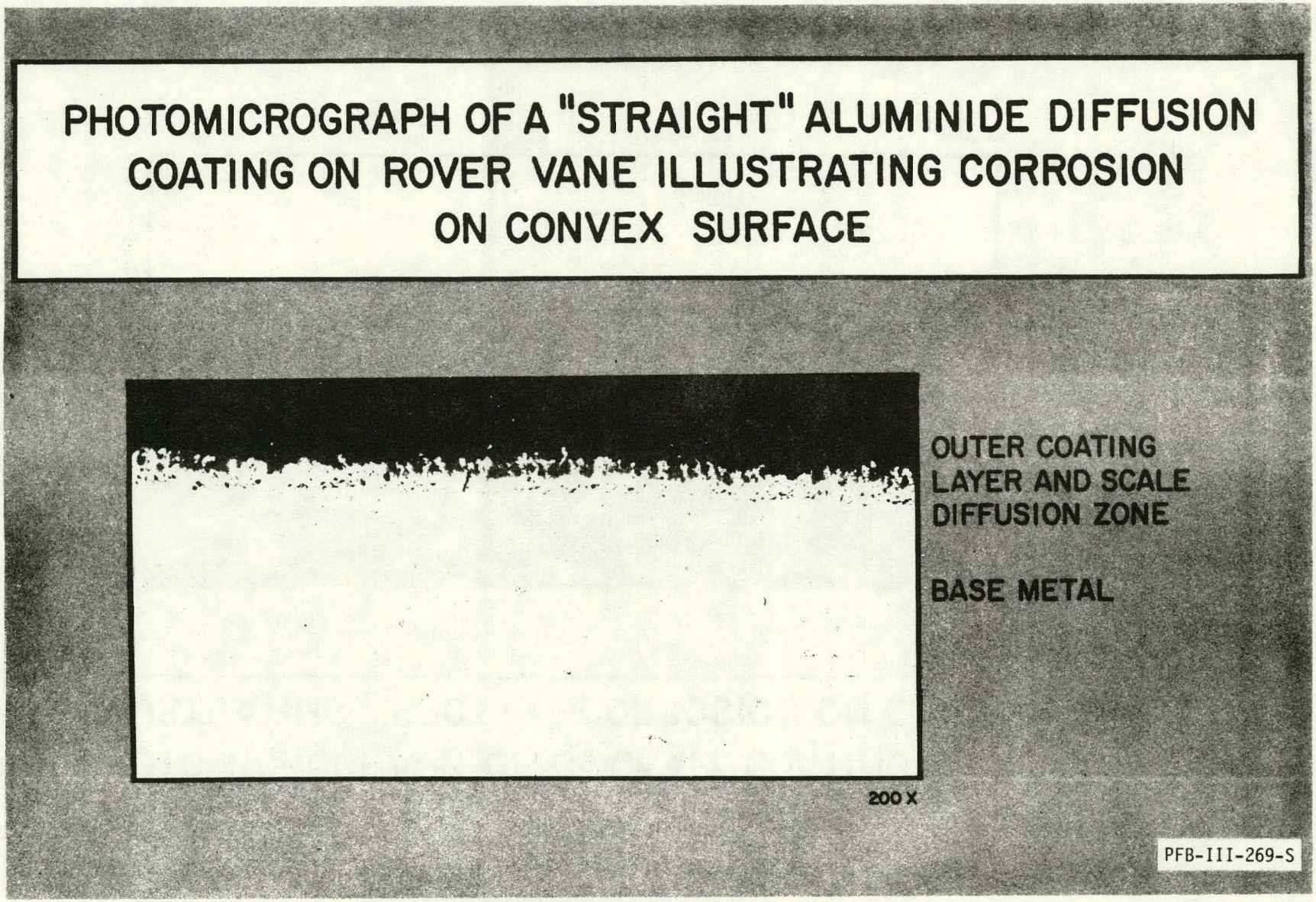
PHOTOMICROGRAPH OF A "STRAIGHT" ALUMINIDE DIFFUSION COATING ON ROVER VANE ILLUSTRATING CORROSION ON CONVEX SURFACE
OUTER COATING LAYER AND SCALE
DIFFUSION ZONE
BASE METAL
200 X
PFB-III-269-S

Figure 2.59

Section 3.0
PILOT PLANT FINAL DESIGN

The Pilot Plant is being constructed by converting an existing MOD POD 8 Total Energy Power Generating Station located at the Curtiss-Wright, Wood-Ridge, New Jersey Facility. The station consists of a gas turbine driven alternator and a waste heat recovery boiler, and currently provides the facility requirement for electric power and steam for process and heating. The gas turbine liquid/gas-fueled combustor will be replaced with a pressurized fluidized bed combustor capable of operating on crushed coal.

The steam produced in the waste heat recovery boiler as a product of the Pilot Plant will continue to be used for facility process purposes at Wood-Ridge, rather than powering a steam turbine electric generator set.

The Pilot Plant final design has been completed. Activity during the reporting annual period included updating of plant designs and specifications to reflect the additional stages of gas cleanup, design changes recommended by SGT/PFB technology tests, and refinements in design resulting from completion of final stress analyses for all design and off-design operating conditions.

An artist's concept of the design is shown in Figure 3.1.

3.1 OVERALL PERFORMANCE

3.1.1 Internal Design Conditions

The Pilot Plant internal design conditions were revised as follows to account for the information generated during the Technology Rig testing:

1. Increased pressure drops through the process to account for increased combustion bed density, additional high pressure drop separator, and increased tuyere pressure drop to prevent bed material siftback.

PRESSURIZED FLUIDIZED BED COAL FIRED COMBINED CYCLE POWER PLANT

CURTISS WRIGHT POWER SYSTEMS

DATA	PILOT PLANT
RATING, MW	13
HEAT RATE, BTU/KWHR	N/A
COAL FLOW, TONS/DAY	120
DOLOMITE FLOW, TONS/DAY	30
BED TEMPERATURE, °F	1650
BED PRESSURE, ATM.	7
BED DEPTH, FT.	16
BED SUPERFICIAL VELOCITY, FPS.	2.7
COMBUSTION EFFICIENCY, %	99.9

KEY

1. PFB combustor
2. Air cooled heat exchanger
3. Recycle cyclone
4. Collected solids return loop
5. Combustion gas clean-up system
6. Collected solids lockhopper
7. PFB ash discharge cooling column
8. Gas turbine/alternator module
9. Gas turbine compressor
10. Volutes for compressed air exit and heated gas return
11. Turbines to drive compressor and alternator
12. Gas turbine exhaust
13. Alternator
14. Turbine and alternator controls and switchgear
15. Waste heat recovery boiler
16. Coal supply conveyor
17. Bucket elevator for alternate supply
18. Coal supply surge bin
19. Coal milling and drying system
20. Cyclone separator for milled coal
21. Bag house for coal milling system
22. Milled coal storage bin
23. Coal storage injector
24. Coal primary injector
25. Dolomite storage silo
26. Dolomite storage bin
27. Dolomite storage injector
28. Dolomite primary injector
29. Control building
30. Combustion air inlet pipe
31. Heat exchanger air inlet pipe
32. Combustion air start-up heater
33. Gas turbine start-up combustor

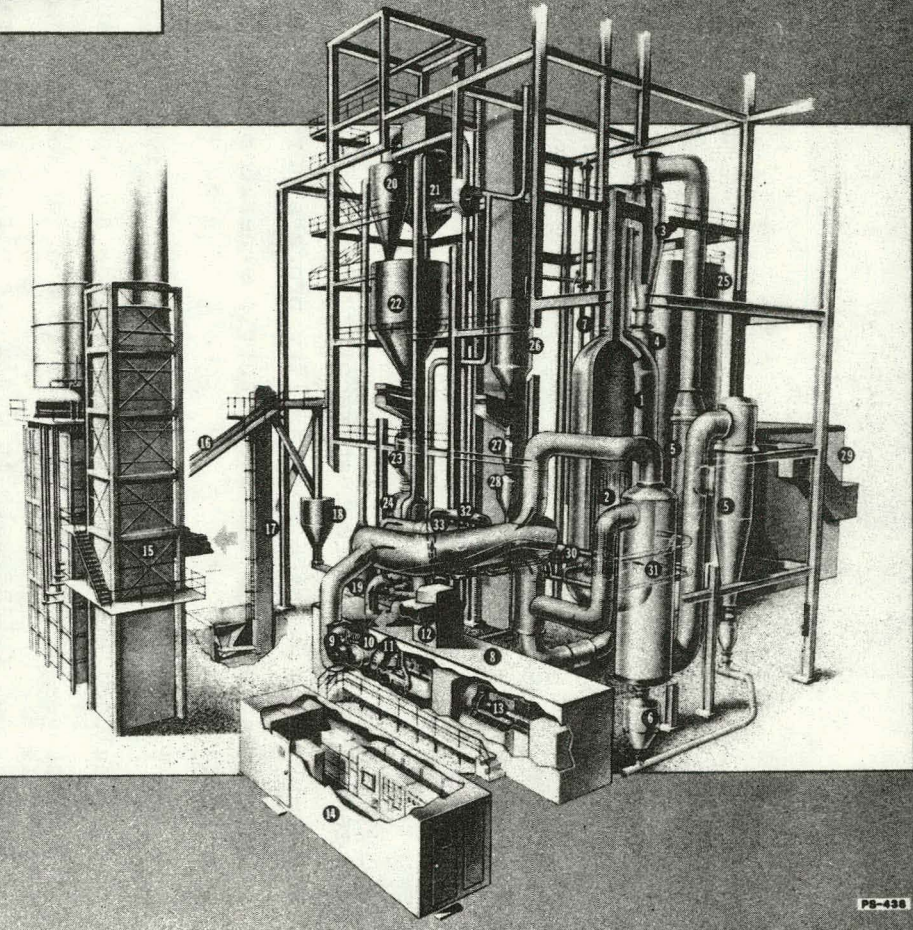

PS-438

Figure 3.1

2. Increased bed temperature from 1650°F to 1660°F to duplicate the bed conditions (with 93% heat exchanger effectiveness) of the commercial plant necessary for setting a turbine inlet temperature of 1660°F. This increase offsets the possible increased heat losses in the separator vessels and piping between the combustion bed outlet and turbine inlet stations plus the lower effectiveness of the present heat exchanger configuration.

The higher pressure drops resulted in gas turbine operation close to compressor surge. To achieve surge free operation, the compressor turbine flow capacity was increased approximately 2% and an air bleed was provided ahead of the power turbine.

The internal conditions are presented in Table 3.1.

Figures 3.2 to 3.5 present the turbine inlet temperature, exhaust gas temperature, exhaust gas flow and coal flow versus net gas turbine power output at various ambient temperatures.

TABLE 3.1

PILOT PLANT DESIGN - INTERNAL CONDITIONS

Compressor

Inlet Pressure, psia	14.55
Inlet Temperature, °F	59.0
Outlet Pressure, psia	104.20
Outlet Temperature, °F	511.0
Airflow, pps	119.03
Speed, rpm	8143

Combustor

Inlet Temperature, °F	511.0
Inlet Pressure, psia	101.57
Inlet Flow, pps	38.62
Coal Flow, pps	2.547
Sorbent Flow, pps	.943
Equivalent Ratio	.6941
Calcium/Sulfur Ratio	1.65
Outlet Temperature, °F	1660

TABLE 3.1 (Continued)

PILOT PLANT DESIGN - INTERNAL CONDITIONS

Combustor (Continued)

Outlet Pressure, psia	94.0
Outlet Flow, pps	41.223
Superficial Velocity, fps	2.7

Heat Exchanger

Inlet Temperature, °F	511.0
Inlet Flow, pps	72.718
Outlet Temperature, °F	1546.8
Effectiveness, %	90.1

Separators

Inlet Pressure, psia	94.0
Outlet Pressure, psia	89.5
Inlet Flow, pps	41.223

Compressor Turbine

Inlet Temperature, °F	1560
Inlet Pressure, psia	89.0
Inlet Flow, pps	113.942
Stator Cooling Flow, pps	3.238
Rotor Cooling Flow, pps	.833
Outlet Pressure, psia	29.5
Outlet Temperature, °F	1125.3

Turbine Bypass

Flow, pps	8.10

Power Turbine

Inlet Flow, pps	111.75
Inlet Temperature, °F	1115.8
Inlet Pressure, psia	29.28
Rotor Cooling Flow, pps	.60
Outlet Pressure, psia	16.04
Outlet Temperature, °F	921.5
Outlet Power, Kw	5664

Exhaust

Pressure, psia	15.06
Temperature, °F	933.8
Flow, pps	120.44

PFB PILOT PLANT

COMPRESSOR TURBINE INLET TEMPERATURE VS NET OUTPUT

Sea Level

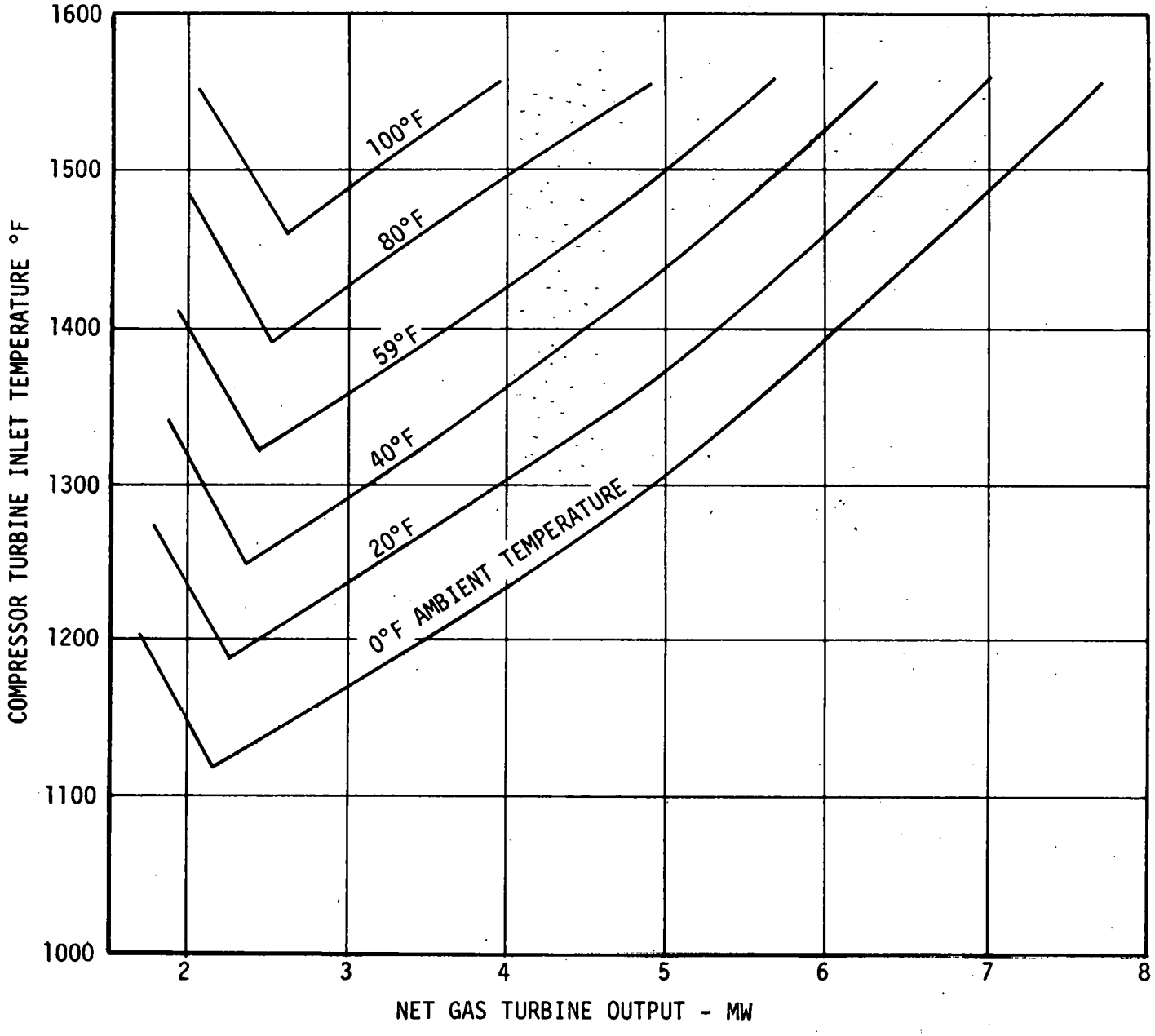

Figure 3.2

PFB PILOT PLANT

WASTE HEAT BOILER GAS INLET TEMPERATURE VS GENERATOR OUTPUT

ESTIMATED SEA LEVEL PERFORMANCE

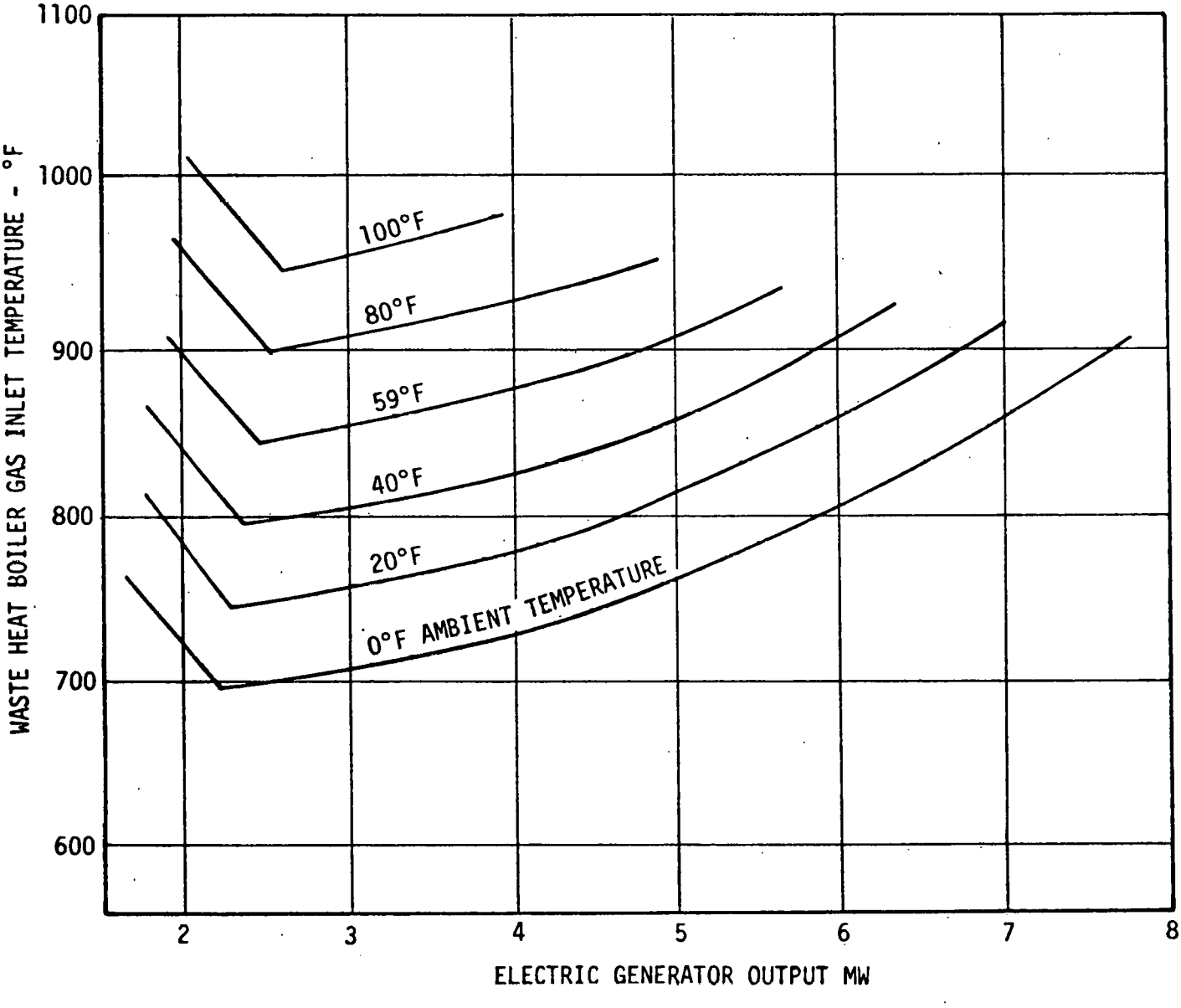

Figure 3.3

PFB PILOT PLANT

COAL FLOW VS NET OUTPUT

Sea Level

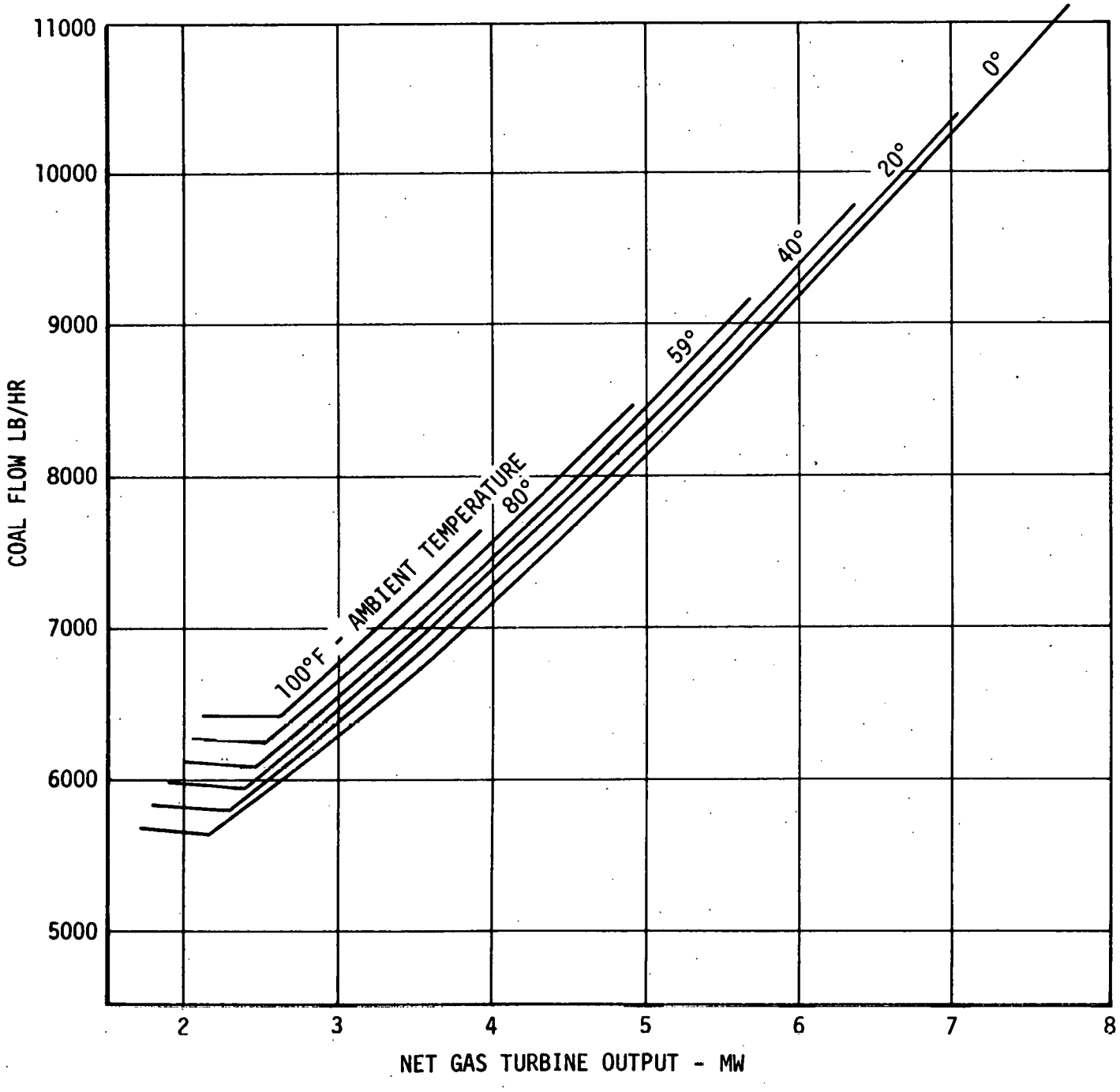

Figure 3.4

PFB PILOT PLANT

EXHAUST STACK GAS FLOW RATE VS GENERATOR OUTPUT

ESTIMATED SEA LEVEL PERFORMANCE

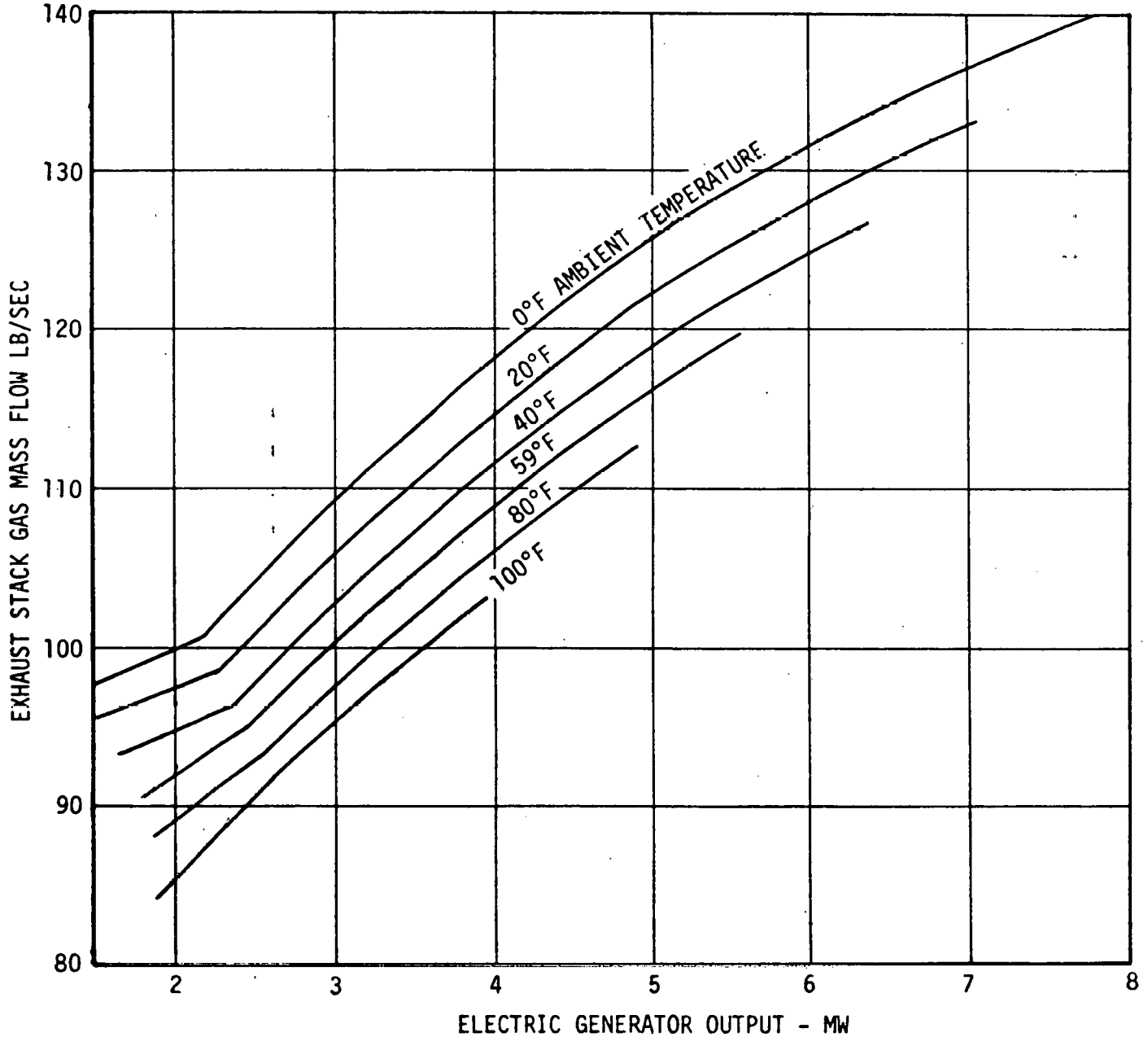

Figure 3.5

3.1.2 Start-up and Heat-up Procedure

The PFB will operate from idle speed to a gas generator speed of 7000 rpm with the power turbine bypass valve (No. 8) (Figure 3.6) and the starter burner inlet valve (No. 1) wide open. The power turbine isolator valve (No. 9) will be closed as the power turbine is not synchronized during this mode of operation. The engine is operating on the starter burner using liquid or gas fuel with no flow through the bed system with all other valves closed.

Throughout the bed heat-up cycle, the auxiliary heater airflow will be controlled by operating at a constant airflow to freeboard pressure ratio, using valve (No. 1) and the tube bypass valve (No. 2) will be adjusted to hold actual airflow ratio of 1.5 between the bed inlet air and the clean air entering the aerodyne. The bed temperature is controlled by either liquid fuel or coal flow to maintain a rate of temperature change of 100°F/hour. The gas generator speed of 7000 rpm is controlled by fuel flow to the starter burner.

The heat-up cycle will be initiated by opening the auxiliary heater inlet valve (No. 5), and the heat exchanger tube bypass valve (No. 2). As additional heat flux is required to heat up the bed, the auxiliary heater is ignited to an initial temperature of 600°F and then ramped at 100°F per hour to a maximum temperature of 1000°F. At this point, further increase in heat flux is accomplished by injecting liquid fuel into the bed to a maximum temperature of 1200°F. During oil injection into the bed, the auxiliary heater outlet temperature is maintained at 1000°F. At 1200°F, a fuel transfer from liquid fuel to coal is accomplished and the auxiliary heater is ramped down to 600°F. When the bed temperature reaches 1400°F, the auxiliary heater is shut down and inlet valve (No. 4) is opened. At a bed temperature of 1560°F, the alternator is synchronized at zero power by fully opening the power turbine isolation valve (No. 9) and partially closing the power turbine bypass valve (No. 8) until synchronization is completed. After the breaker points close, the power bypass valve is fully closed. The engine is now producing power at a bed temperature of 1560°F and a gas generator speed of 7000 rpm controlled by the starter burner. The heat-up cycle is completed by ramping the bed temperature to 1660°F.

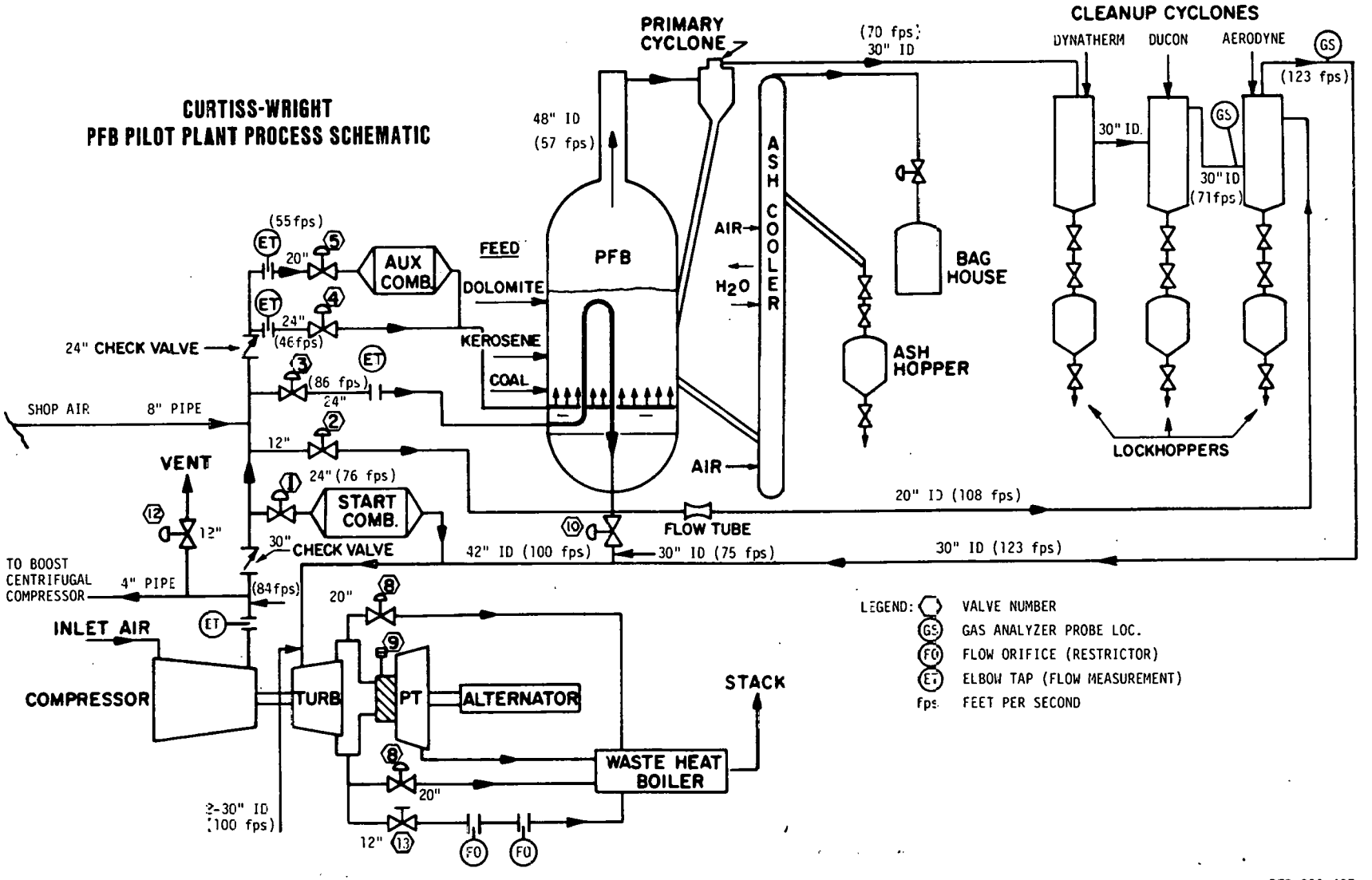
CURTISS-WRIGHT
PFB PILOT PLANT PROCESS SCHEMATIC
PRIMARY CYCLONE
(70 fps) 30" ID
CLEANUP CYCLONES
DYNATHERM
DUCON
AERODYNE
GS
(123 fps)
48" ID
(57 fps)
30" ID.
30" ID
(71fps)
ASH COOLER
AIR
H2O
BAG HOUSE
ASH HOPPER
LOCKHOPPERS
(55fps)
ET
20"
AUX COMB.
FEED
DOLOMITE
PFB
24"
(46fps)
24" CHECK VALVE
KEROSENE
COAL
(86 fps)
24"
SHOP AIR
8" PIPE
12"
AIR
VENT
24" (76 fps)
START COMB.
20" ID (108 fps)
FLOW TUBE
30" CHECK VALVE
42" ID (100 fps)
30" ID (75 fps)
30" ID (123 fps)
TO BOOST CENTRIFUGAL COMPRESSOR
4" PIPE
(84fps)
20"
INLET AIR
COMPRESSOR
TURB
PT
ALTERNATOR
STACK
WASTE HEAT BOILER
20"
12"
FO
LEGEND:
VALVE NUMBER
GAS ANALYZER PROBE LOC.
FLOW ORIFICE (RESTRICTOR)
ELBOW TAP (FLOW MEASUREMENT)
fps FEET PER SECOND
PFB-III-497

Figure 3.6

Part throttle operation is initiated by activating the load control which is set at a demand load greater than that required for 7000 rpm operation. The load demand increases coal flow which raises the bed temperature above its preset limit which opens the heat exchanger tube inlet valve (No. 3) allowing air to flow through the heat exchanger tube thereby maintaining the bed temperature at 1660°F. The increased airflow through the tube causes valve (No. 2) to close to hold constant aerodyne flow and when valve (No. 2) is fully closed valve (No. 10) is activated to meter the clean air entering the aerodyne to the required ACFM ratio of 1.5 between dirty and clean air in the 3rd stage cyclone. As the demand for heat exchanger tube air is increased resulting in higher heat outputs, the starter burner fuel flow requirement is decreased until its minimum fuel air ratio is reached at which point the burner will be shut off. The superficial velocity control is now transferred from the starter burner inlet valve (No. 1) to the heat exchanger bypass valve (No. 2). At this point the system is under load control, the bed temperature will now be controlled by the heat exchanger tube inlet valve (No. 3) and the heat exchanger bypass valve (No. 2) will control the superficial velocity.

Component operating pressures, temperatures, etc. were calculated for the various settings in the warm-up and part throttle points that are listed below.

Start-up and Heat-Up Procedure (1 through 12 at 7000 rpm)

Point No. 1 - Starter Burner On - No Bed Flow - Power Turbine Bypass Valve Open

Point No. 2 - Starter Burner On - Bed Flow - No Tube Flow - Freeboard Temperature 200°F

Point No. 3 - Starter Burner On - Auxiliary Heater 600°F - Freeboard Temperature 400°F - No Tube Flow

Point No. 4 - Starter Burner On - Auxiliary Heater 1000°F - Freeboard 800°F - No Tube Flow

Point No. 5 - Starter Burner On - Auxiliary Heater 1000°F - Freeboard 1200°F Bed Liquid Fuel - No Tube Flow

Point No. 6 - Starter Burner On - Auxiliary Heater 600°F - Freeboard 1200°F Bed Coal - No Tube Flow

Point No. 7 - Starter Burner On - Auxiliary Heater Off - Freeboard 1400°F Bed Coal - No Tube Flow

Point No. 8 - Starter Burner On - Freeboard 1560°F - No Tube Flow - Non-Synch.

Point No. 9 - Starter Burner On - Freeboard 1560°F - No Tube Flow - Power Turbine Isolator Valve Open - Power Turbine Bypass Valve Partially Open - Synchronized at Zero Power

Point No. 10 - Starter Burner On - Freeboard 1560°F - No Tube Flow - Power Turbine Bypass Valve Closed

Point No. 11 - Starter Burner On - Freeboard 1660°F - No Tube Flow

Point No. 12 - Starter Burner Off - Synchronized at 1.938 Mw Part Throttle Open Valve No. 3

Point No. 13 - 7180 rpm - Minimum rpm not on Surge Control

Point No. 14 - 60% Rated Load

Point No. 15 - 80% Rated Load

Point No. 16 - 100% Rated Load

3.2 DYNAMIC SIMULATION STUDY

Operation of the computer program developed to simulate dynamic behavior of the PFB Pilot Plant continued. Initial simulator operation included definition of critical system failure modes. In particular, the process control response of the power turbine subsystem required definition. The current design utilizes a valve (No. 9) to isolate the power turbine and generator from the gas turbine exhaust and valve (No. 8) to bypass the gas turbine exhaust into the waste heat boiler (Figure 3.6). System failure modes investigated were:

1. Inadvertent opening or failsafe opening of 8 causing gas turbine exhaust area to increase and resulting in rotor overspeed.

2. Inadvertent or failsafe closing of valve (No. 9) causing gas generator exhaust pressure to exceed design limitation of the exhaust structure.

3. Loss of electrical load due to breaker relay trip causing power turbine, gearbox, and generator to overspeed.

The preliminary results of the investigation of these failure modes are presented in the following paragraphs:

1. Turbine Bypass System Valve (No. 8)

   Failure of valve (No. 8) to open position will result in a sudden increase in gas turbine exhaust area and subsequent gas turbine overspeed condition. Figure 3.7 presents rotor speed response versus time for failure of a single 16 in. valve at its nominal actuation rate of 60 deg/sec. Indicated is the requirement for control system response to prevent the overspeed event.

PFB DYNAMIC SIMULATOR

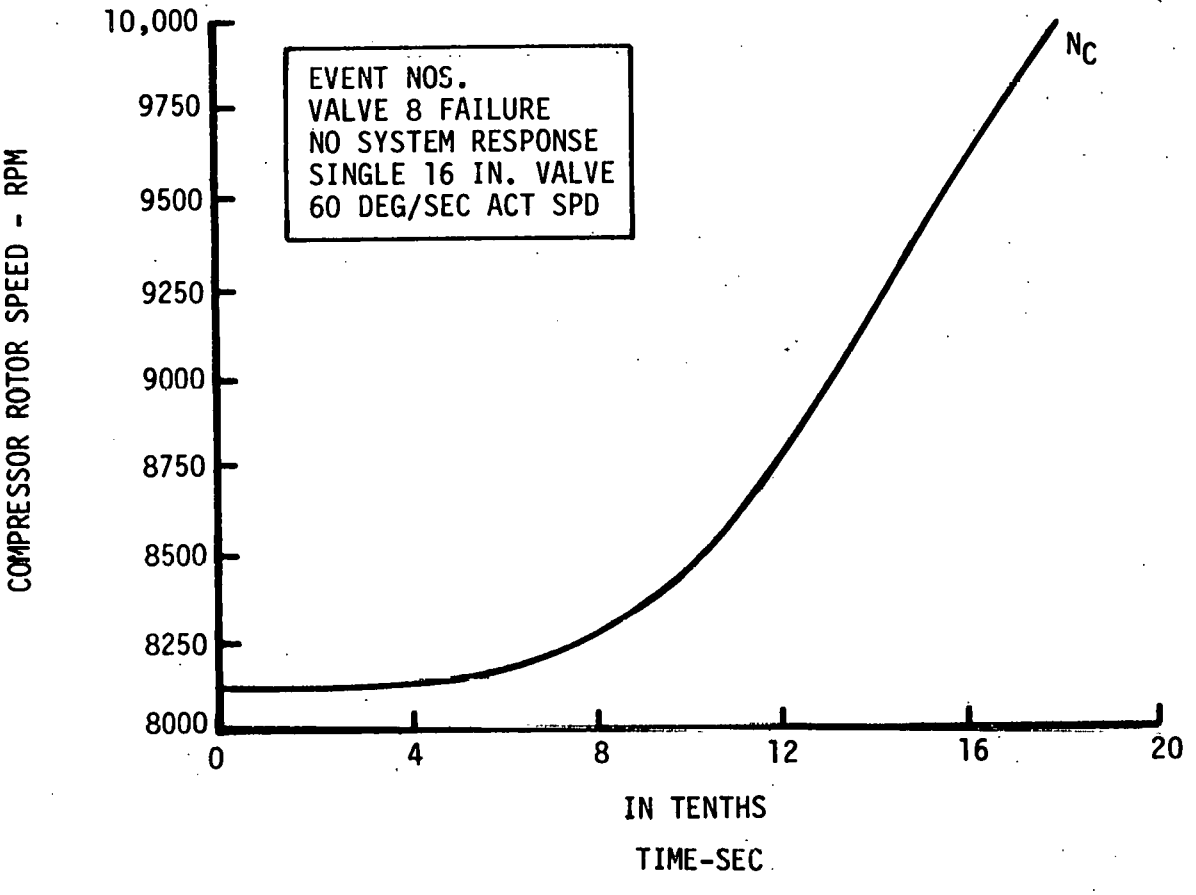

Figure 3.7

To reduce gas turbine exhaust area, the power turbine isolator valve control logic was revised to respond to a gas turbine rotor overspeed trip and loss of signal to valve (No. 8).

Power turbine isolator valve (No. 9) receives the actuation signal when 104% of gas turbine rotor speed (N_c) is detected and a positive valve (No. 8) actuation rate is sensed. Valve (No. 9) then modulates to hold design gas generator rotor speed (see Figures 3.8 and 3.9).

An alternative to this control scheme would be a 50 degree failsafe stop position for valve (No. 8). Analysis of this control mode has shown gas turbine rotor speed overshoot is minimized by limiting valve (No. 8) travel (see Figure 3.10).

Additional studies have included control parameter optimization such as, valve actuation speed, actuator signal log times, valve failsafe position, and modulator proportional gain. Results indicate the relationship of valve (No. 8) and valve (No. 9) actuation speed to be the dominant control parameter.

2. Power Turbine Isolator Valve (No. 9)

Failure of valve (No. 9) to its closed position under full load would result in excessive gas generator exhaust pressure and possible compressor surge. Movement toward surge, indicated by a decrease in N_c, and a pressure pulse at the compressor-turbine exit are overcome by actuation of valve (No. 8) to its full open position (see Figures 3.11 and 3.12). Again, the dominant control variable is the relationship of valve actuation speeds rather than actuation speed itself.

3. Breaker Relay Trip

Loss of electrical load at breaker trip requires control system response to protect power turbine and generator from overspeed.

PFB DYNAMIC SIMULATOR

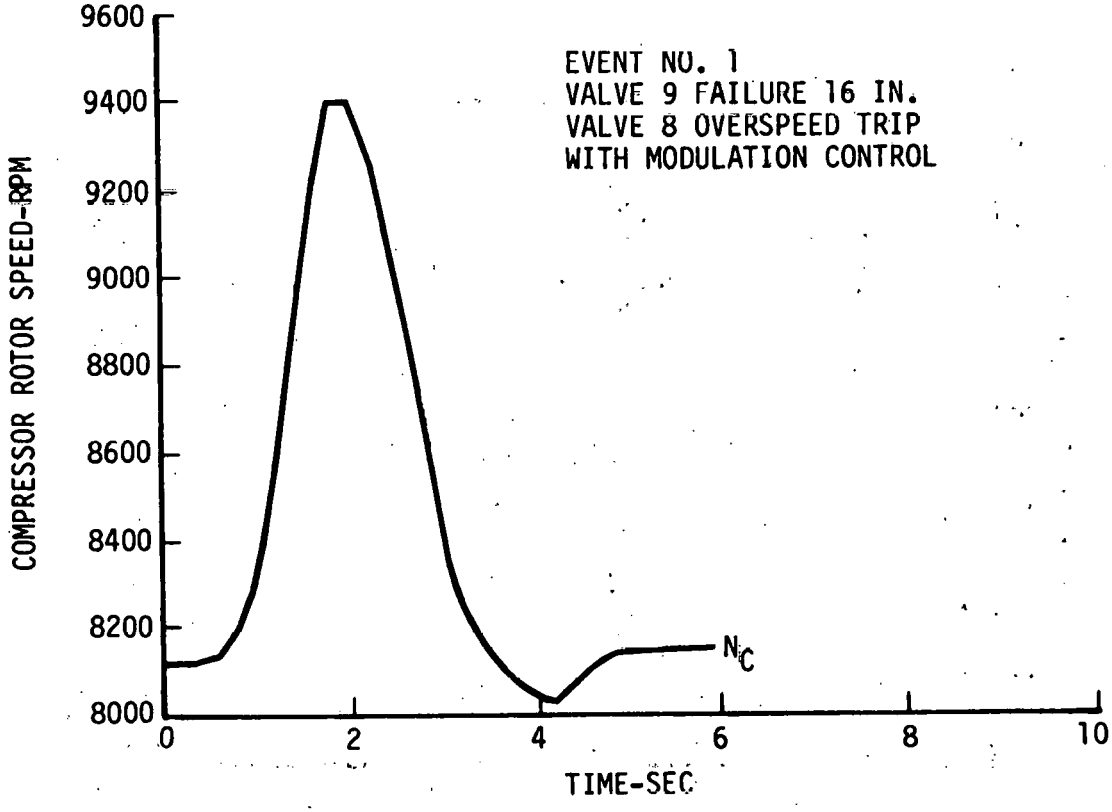

Figure 3.8

PFB DYNAMIC SIMULATOR

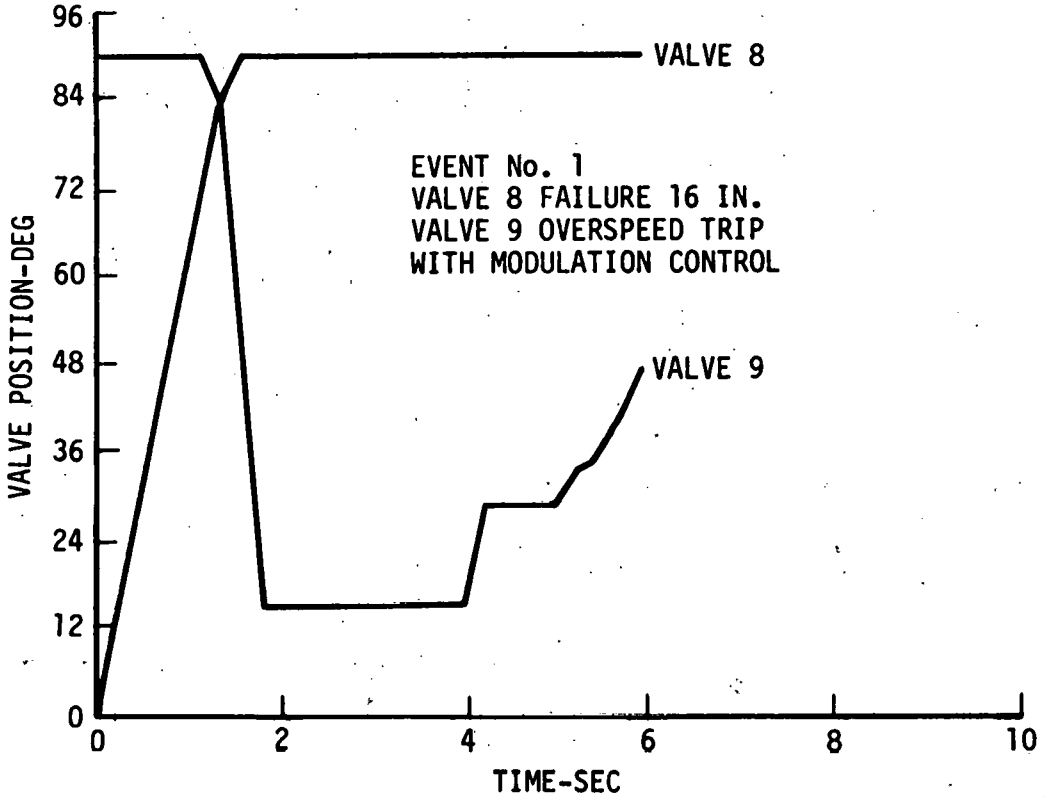

Figure 3.9

PFB DYNAMIC SIMULATOR

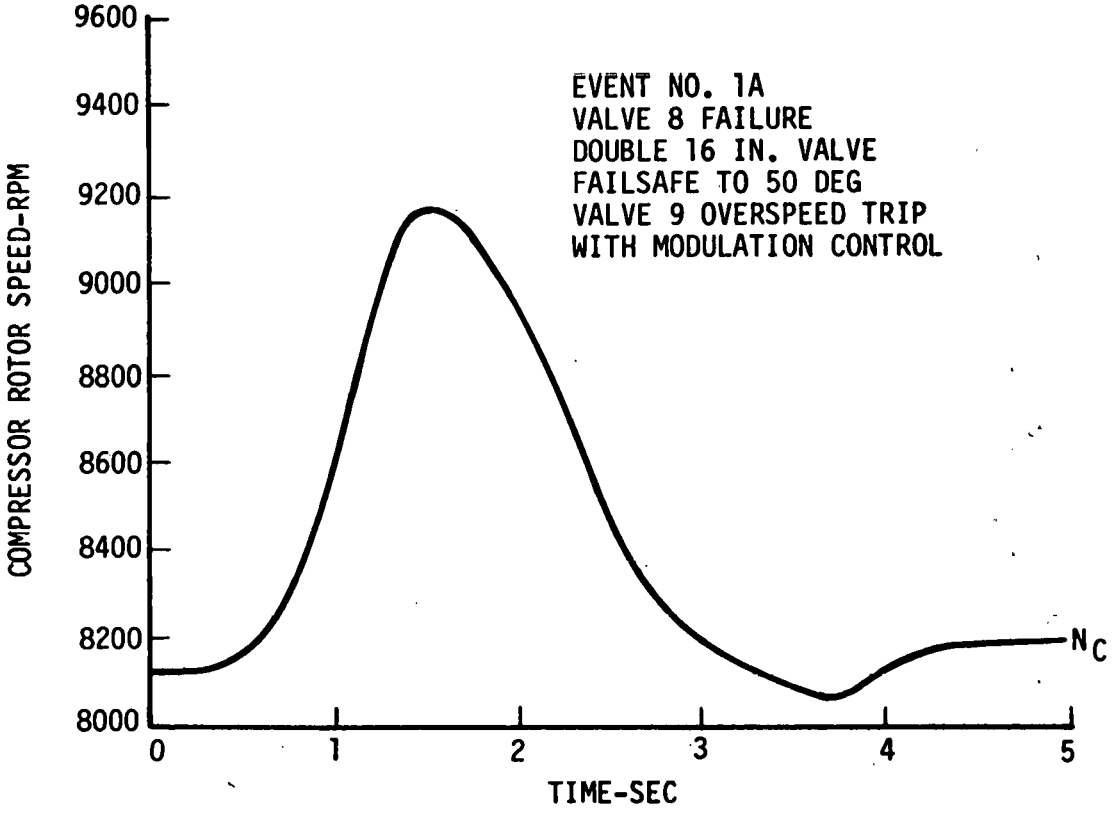

Figure 3.10

PFB DYNAMIC SIMULATOR

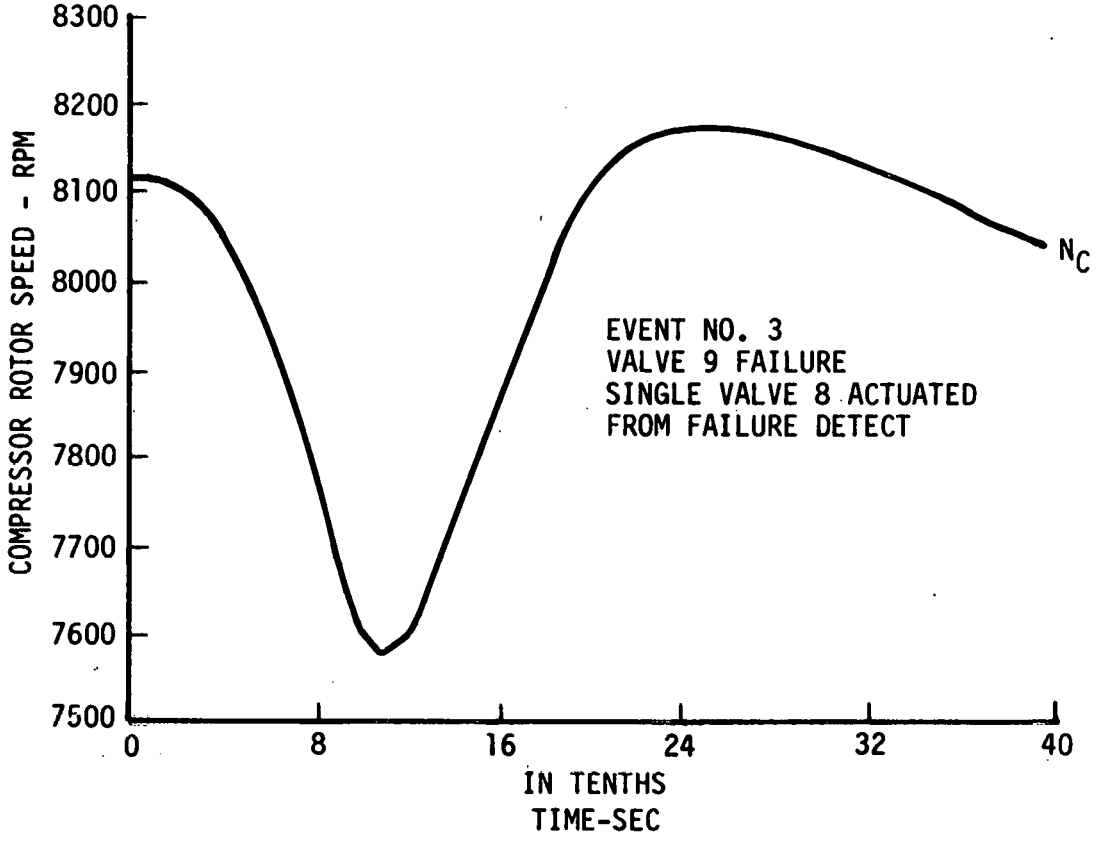

Figure 3.11

PFB DYNAMIC SIMULATOR

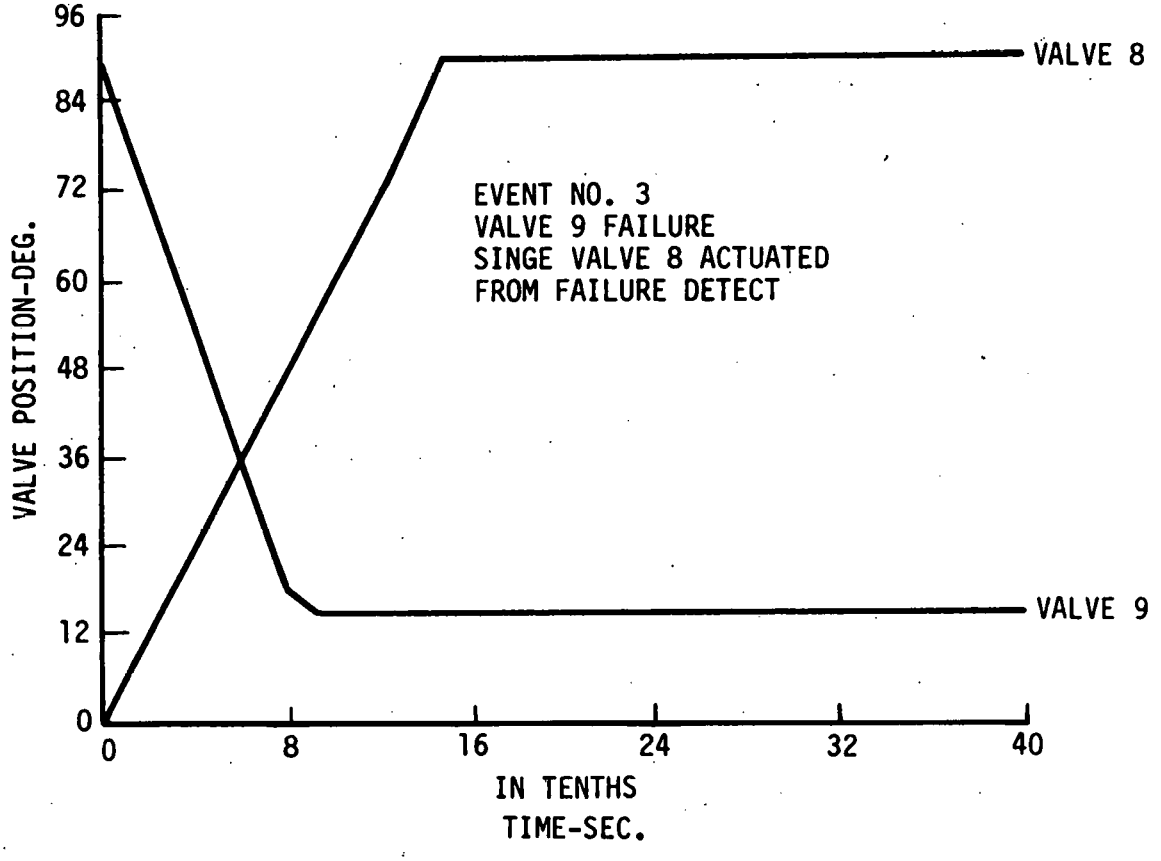

Figure 3.12

Since the power turbine is instantaneously unloaded, the power turbine isolator valve (No. 8) must close to limit flow and the turbine bypass system valve (No. 8) must open to satisfy the gas turbine exhaust area requirement. Valve actuation times are determined by overspeed limit considerations with modulation control determined by gas turbine rotor speed and/or compressor surge characteristics (see Figure 3.13 and 3.14). Optimization of valve response time requirements precluded use of the blowoff valve system to provide adequate compressor surge margin during the first second of the breaker trip event.

An alternative solution to the breaker trip event would have valve (No. 8) actuated by gas turbine exhaust pressure, i.e., acting as a pressure relief valve. Response characteristics for this event including compressor surge margin were determined and again, actuation time and valve (No. 8) trip level must be optimized to eliminate blowoff valve system operation.

In the event valve (No. 8) failed to function, the surge margin control, sensing a signal failure to valve (No. 8), would actuate the blowoff valve and modulate to a predetermined surge margin. In effect, the gas turbine experiences a snap deceleration, the check valve closes, and PFBC blows down through the compressor-turbine. Variations in surge margin, blowoff valve actuation signal lag time, blowoff valve actuation speed, and check valve location were examined to determine optimum control system response.

These preliminary control system studies have identified the power turbine subsystem as a critical region requiring valves with high actuation speeds and appropriate control logic redundancy to handle system failure modes.

PFB DYNAMIC SIMULATOR

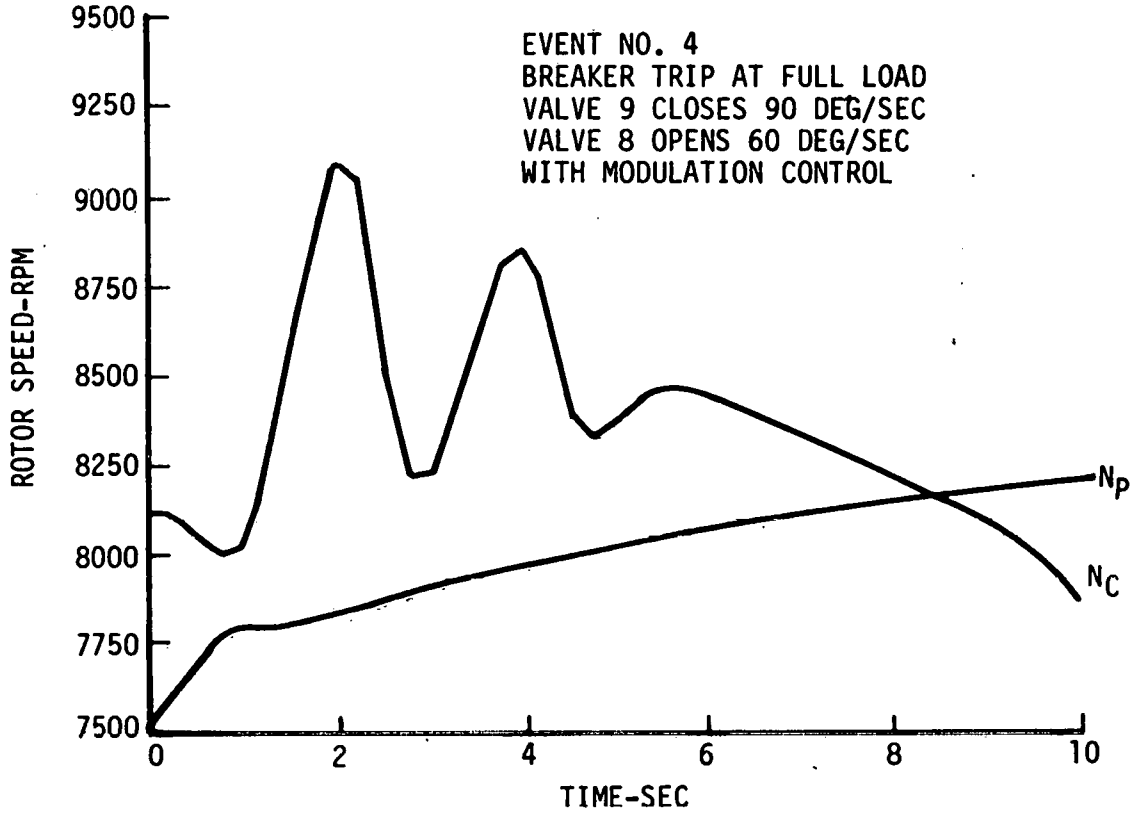

Figure 3.13

PFB DYNAMIC SIMULATOR

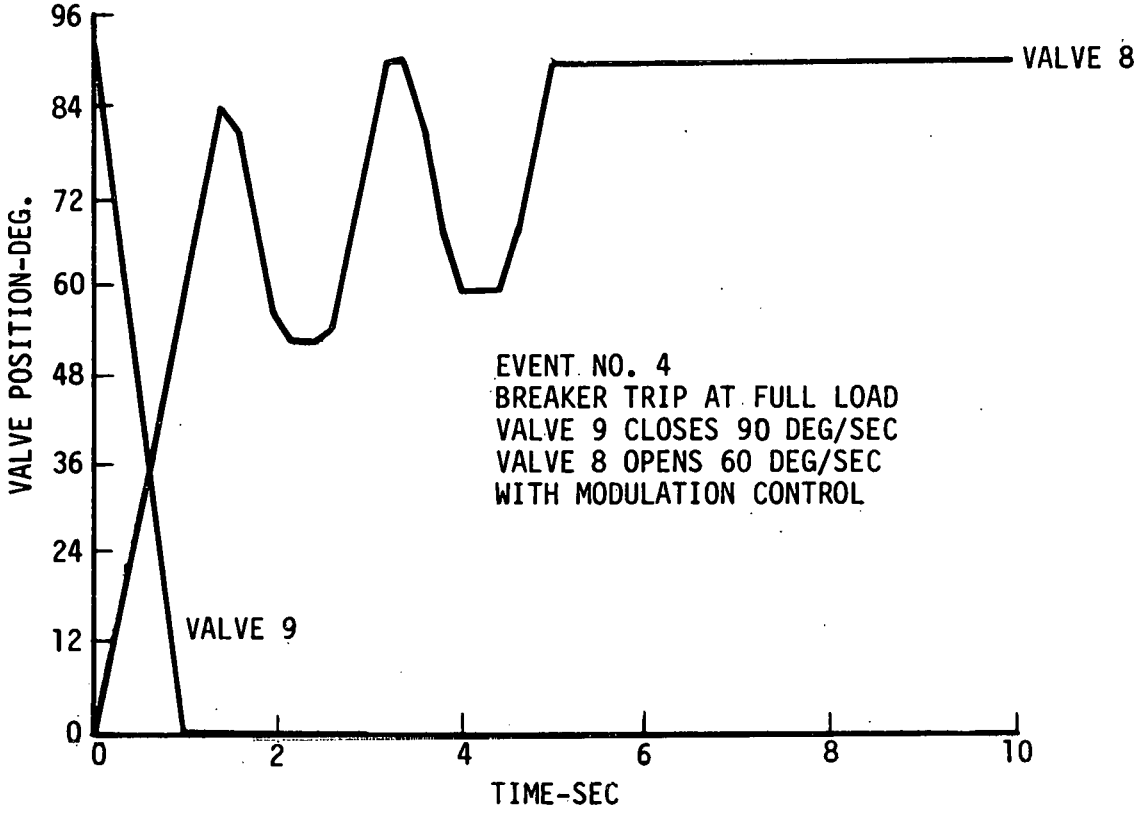

Figure 3.14

3.3 PFB PROCESS

3.3.1 PFB Combustor

The design concept for the PFB combustor is a 15' O.D. single wall pressure vessel lined with refractory insulation and with bayonet type (concentric flow) heat exchanger tubes mounted vertically in the active bed region.

PFBC Shell Penetrations - Penetrations into the PFB combustor occur at several elevations required to provide the vessel with cooling air and fluidizing air. Service ports are also provided to remove potential windbox siftback dust. An ASME Pressure Vessel Code, Section 8, Division 1, analysis was made to determine if adequate reinforcement exists around these openings when their relative proximity is considered. All ASME code criteria have been met with the existing design.

PFBC Lifting Fixtures - Lifting fixtures have been designed for the PFB combustor shell to make a horizontal lift, rotate the shell into the vertical and install it into the supporting tower. This gear consists of cables, spreader bars, eyebolts, lugs, etc. Dynamic load factor used for analysis of the hardware (exclusive of slings) was 0.50. All parts stressed meet the ASME code allowable of 17.5 ksi for the fixture material (SA-515 Gr 70) being used.

PFBC Lateral Support at Approximate 118 Ft Elevation - As accomplished for the Technology Rig a lateral support at the top of the PFBC is to be installed to preclude vibratory rocking of the vessel during system operation. This support system consists of cabling and lugs between supporting tower and the upper vessel flange. A 50 kip design load was used to stress the components of this 90° opposed cabling system, and this will preclude lateral motion of the PFBC at this elevation.

Fluidizing and Cooling Air Inlet Piping Bellows - Fatigue life data for the air inlet bellows and rated pressure movements are available for standard ambient operating conditions. However, the bellows conducts compressor discharge

air and is required to operate at 506°F, therefore, a component life for this application had to be established. A reasonable estimate of the upper bound for the number of cycles required would be 10 full range cycles/week for 30-year unit life, or 15,600 cycles. Stress analysis reveals that the available cycles exceeds 10^5. By analogy it can be concluded that the fluidizing air inlet bellows is also satisfactory. Pressure cycling of these bellows has little or no influence on this result as the Δp across the bellows wall is less than 6 psi due to the construction used.

Coal Supply Guns - There are four vertical and eight horizontal coal supply guns. The upper PFB vessel was modified to provide eight additional horizontal coal supply ports below the existing eight. The vertical coal gun was modified so that it was concentric with a tuyere.

3.3.2 Recycle Cyclone Loop

The design permits the removal of the entire recycle loop which consists of the cyclone, cyclone tee, upper ash return spool assembly, trickle valve assembly, and the lower ash return spool assembly. A process pipe spool assembly has been designed which connects from the outlet of the freeboard/primary cyclone tee to the inlet process piping connected to the 1st stage hot gas cleanup system. A lap joint flange was provided at the lower end of the freeboard/primary cyclone tee to permit alignment for the substituting process pipe spool.

The recycle loop was modified to permit removal of cyclone returns above the trickle valve by providing a 30° take-off port. A take-off port was also provided below the trickle valve so as to bleed off a percentage of the cyclone returns.

Recycle Cyclone - The recycle cyclone was updated to reflect the design tested in the Technology Rig. The length of the cylinder barrel was increased from 90.5" to 102". The throat was modified from an 18.38" X 55.14" ellipse to a rectangular throat 18.625" X 44.25".

3.3.3 Improved Hot Gas Cleanup

A new site plan as shown in Figure 3.15, incorporates the latest configuration tested in the PFB Technology Unit for hot gas cleanup. The facility piping design has been modified for the new hot gas cleanup devices. Piping mounts and guides for the configuration have been finalized.

The new hot gas cleanup system consist of 3 stages, the 1st stage is a Dynatherm, the 2nd stage is a Ducon cyclone and the 3rd stage is a clean-air Aerodyne. The process piping was sized for minimum pressure drop. The process piping in the hot gas cleanup system up to the inlet to the clean-air Aerodyne is refractory lined. All of the process piping leaving the heat exchanger plenum, the clean-air line to the Aerodyne and the clean-air Aerodyne outlet process piping is metal lined, refractory insulated piping. The construction of the metal lined refractory insulated piping is similar to the SGT/PFB Technology Rig which has 3000 hours of running time.

A separate hot gas cleanup system is provided for handling PFB fluidizing and combustion gas during the start-up mode when there is no dilution by clean bed cooling air. This system will also have the capacity to accept full design point combustion flow for continuous operation with the main cleanup system decoupled.

3.4 GAS TURBINE POWER TRAIN

The 1st stage turbine stator vane was restaggered to increase the throat area from 120.65 square inches to 123.84 square inches to match required flow conditions.

Final heat transfer analysis of the fishmouth seals at the turbine stator vane assembly necessitated a redesign. Both inner and outer fishmouth assemblies were redesigned to allow thermal growth between the cooler structural member and the hot liner shielding the insulation. A radial centering device was incorporated which keeps the fishmouth assembly concentric with the engine centerline but still permits the radial thermal growth.

PILOT PLANT SITE PLAN

CLEAN-UP SYSTEM DYNATHERM DUCON, CLEAN AIR AERODYNE

(D.O.E. CONTRACT EX 76-C-01 - 1726)

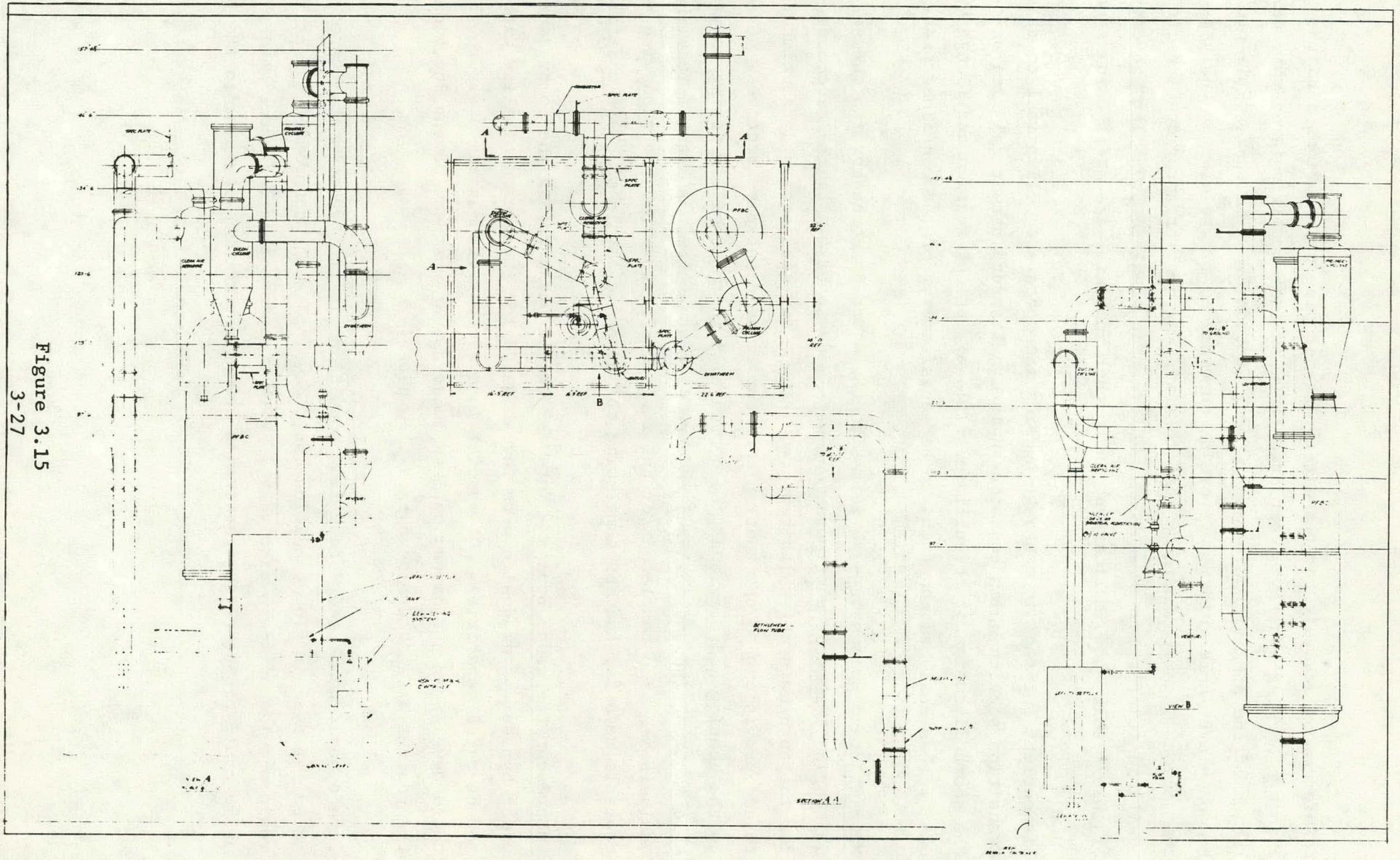

Figure 3.15
3-27

Reinforcement analysis for the air-in/air-out pipe penetrations into the air exchange housing shell was completed based on the simplified area rule calculation of the ASME Pressure Vessel Code, Section 8, Division 1. This provided the only available guideline short of an extended finite element analysis of the region. Results indicate that the existing geometry provides a ratio of available reinforcement/required reinforcement equal to 3.0. The conservatism of this result, and implications on further analysis, are still being studied.

Air outlets for the air exchange housing incorporate an elliptical to circular transition section which contains an internal strut (structural tie) across the short dimension of the ellipse. This elliptical section and flange were also stress analyzed and found to be satisfactory for the contained pressure.

Main Start-up Combustor - Revisions to the start-up combustor (which uses the J65 engine combustor configuration) were made to eliminate the accommodations for the turbine section (thereby requiring a new aft centerbody section) and to add provisions to the housing to mount to adjacent pipe sections. Changes to the housing had previously been modeled into the facility piping as variable section pipe and analyzed as part of that system. A lateral buckling analysis was also completed for the revised aft centerbody section with acceptable results, thereby completing the stress analysis of these modifications.

Compressor Emergency Bypass - Internal static pressures in the compressor emergency bypass system design were investigated for their compatibility with component rated capacities. Of special interest was the maximum pressure that could develop in a Flexspan bellows located just upstream of the junction of the compressor and turbine bypass flow pipes.

Both dynamic and steady-state flow conditions in the bypass system were investigated. A dynamic flow condition could develop in the compressor bypass from a rapid opening of the bypass valve. With a rapid opening, a shock wave pressure pulse could propagate supersonically downstream through the pipe to the bellows.

With 100 psia upstream of the bypass valve and near atmospheric pressure downstream, a pressure pulse of this type would have an elevated pressure behind the shock wave of over 30 psia. This would exceed the permissible pressure difference of 3 psi at the Flexspan bellows. To produce this condition, however, would require a very rapid valve opening, within a time interval of about 0.1 second or less. This type of pressure pulse would travel very rapidly down the pipe and therefore persist at any one location for only a very short time, of the order of milliseconds. Because of the relatively slow-acting valve used in the bypass system (1 second or more) and the very short time interval of the passage of a shock wave pressure pulse, if one were produced, dynamic over-pressure conditions of that type were not considered to be a potential problem.

Steady-state operation was investigated for the most severe flow condition conceivable, which consists of full bypass flow simultaneously in both the compressor and turbine bypass pipes. This condition is possible if power to certain control valves should fail. Starting from a normal 100% power operating condition and switching suddenly to a full compressor and turbine bypass condition, the maximum static pressure difference across the Flexspan bellows from inside to outside was estimated to be 4.4 psi. Therefore, to reduce the pressure differential to a value below 3 psi, a flow restriction in the piping was eliminated from the design. The 42-inch diameter pipe located between the junction box of the two bypass flows and the vaned elbow of the main exhaust duct was removed, and the junction box was placed directly on the exhaust duct elbow.

3.5 CONTROLS AND INSTRUMENTATION

Operational experience gained from the continued running of the PFB/SGT Technology Rig has been integrated into the Pilot Plant design to reflect improvements in reliability, operation, etc. Included in the changes to the Process and Instrumentation Diagram (P&ID) were:

1. Added redundant pressure probes in the PFBC to provide cross-check capability to prevent reading errors due to line or probe plugging.

2. Provided for additional hot gas cleanup stages with associated instrumentation, valves, particulate sampling facilities, etc.

3. Reviewed dual start-up fuel capability of system components for start-up operation on either gas or liquid.

Other revisions have also been incorporated into the P&ID's. The actuation media of the power turbine isolation valve has been changed from pneumatic to hydraulic to simplify mounting (see Figure 3.16). This has led to modification to the valve controls. The addition of gas fuel for the start-up combustor will require a change to the finalized fuel system.

The purge air system capacity has also been updated as follows to reflect the additional air requirement for the redundant pressure probes and coal guns.

Transport Air at 275 psig *

1.	Dolomite	100 SCFM
2.	Coal	270 SCFM
3.	Pressurizing-Intermittent Demand (Continuous) (Equivalent)	75 SCFM
	Total	445 SCFM

Purge and Cooling Air at 125 psig

1.	Coal Gun Cooling Air, 16 at 40 SCFM	640 SCFM
2.	Dolomite Gun Cooling Air, 4 at 25 SCFM	100 SCFM
3.	Oil Gun Cooling Air, 2 at 25 SCFM	50 SCFM
4.	Pressure Probes Type 1, 15 at 13.2 SCFM	198 SCFM
5.	Pressure Probes Type 11, 11 at 3.3 SCFM	36 SCFM
6.	Grab Sampler Single, 4 at 3.3 SCFM	13 SCFM
7.	Gas Emission Probes, 3 at 3.3 SCFM	10 SCFM
	Total	1,047 SCFM

* 275 psig was established as the minimum in order to accommodate sonic venturi tubes in the future.

POWER TURBINE ISOLATOR VALVE HYDRAULIC SYSTEM

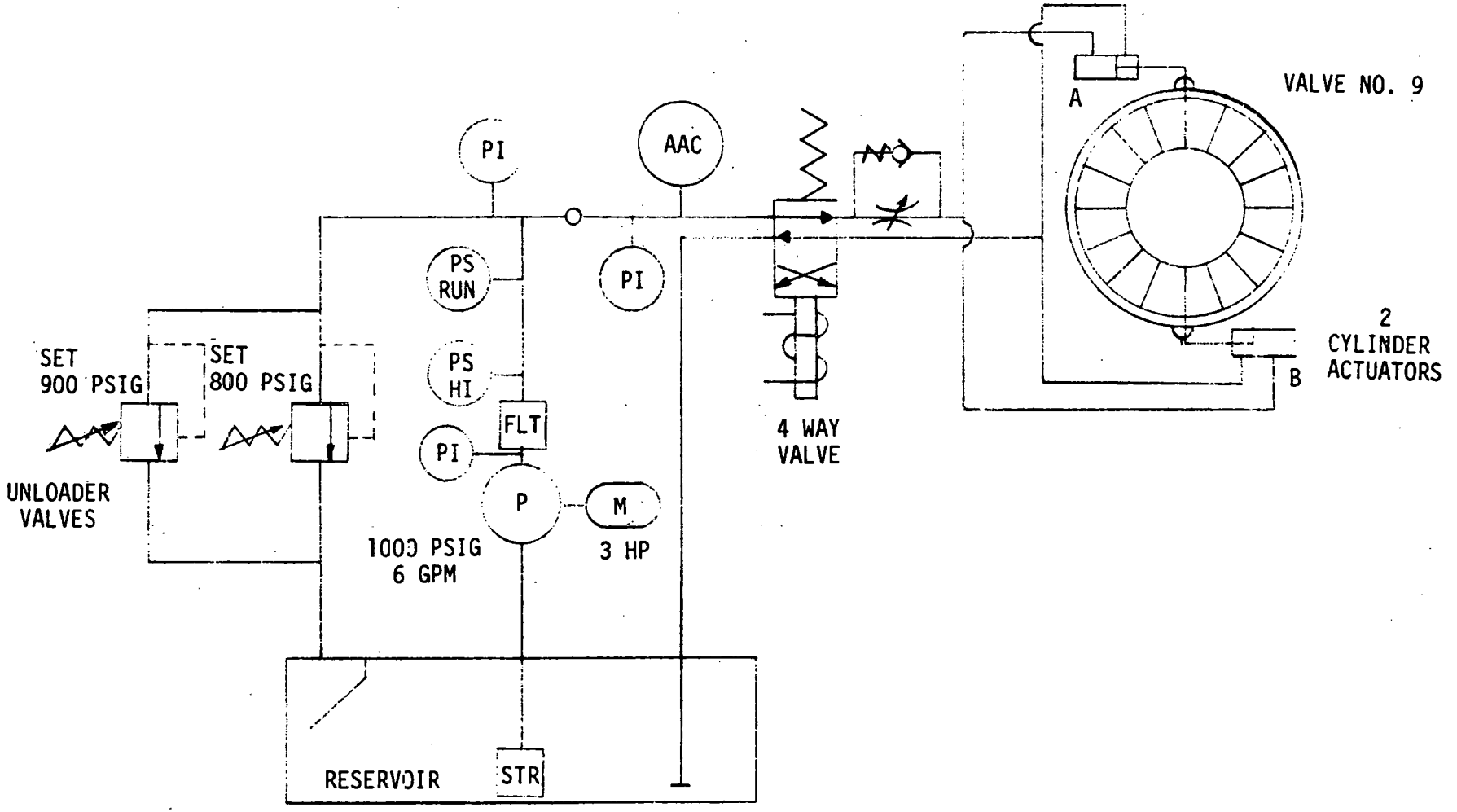

PFB-III-467

Figure 3.16

3.6 GROUNDING AND CATHODIC PROTECTION SURVEY

Stone & Webster conducted a preliminary grounding and cathodic protection survey of the Pilot Plant site at the Wood-Ridge, New Jersey Facility. Soil resistivity, structure-to-soil potential, and resistance-to-earth measurements were made about the site. Analysis of the measurements taken indicate the following:

1. Soils can be classified as very corrosive.

2. Resistance-to-earth of the existing boiler house grounding system is low (0.22 ohms).

3. Existing metallic structures about the PFB Pilot Plant site are not being afforded cathodic protection.

Based on the above, a recommendation is being studied that cathodic protection systems be designed and installed to provide complete corrosion control for all PFB plant substructures. Cathodic protection is an electrical means of arresting corrosion. In general, there are two types of cathodic protection systems, galvanic and impressed current. Both systems utilize anodes to discharge protective current to structures being afforded cathodic protection. When the protective current is equal to or greater than the natural corrosion current of the structure, corrosion is mitigated.

Structures that would be afforded cathodic protection include the grounding system, substructure piping, buried tanks, and above ground storage tank bottoms. It was also recommended that the PFB grounding system be interconnected to the existing boiler house grounding as well as to all contiguous substructures.

The following observations were made from the survey:

Soil Resistivity Measurements - Seven soil resistivity measurements were taken about the PFB Pilot Plant site. These measurements were used as input to the Stone & Webster soil resistivity analysis computer program which outputs the average (Wenner), cumulative (Moore), and layer (Barnes) soil resistivities.

Soil resistivities are one index of galvanic corrosion potential. A correlation between soil resistivity and galvanic corrosion potential is as follows:

Soil Resistivity (ohm-cm)	Classification
0 - 1,000	Extremely Corrosive
1,000 - 2,000	Very Corrosive
2,000 - 10,000	Corrosive
Greater than 10,000	Progressively Less Corrosive

The data from the survey for the layer (Barnes) resistivities vary from extremely corrosive to progressively less corrosive; however, the majority of the resistivities can be classified as very corrosive. The soil resistivities for the given layers are as follows:

Layer (Feet)	50% Soil Resistivity (ohm-cm)
0-5	2850
5-10	1650
10-15	1325
15-20	1325

These resistivity values indicate that, in accordance with the classifications previously listed, the majority of the soils at the PFB Pilot Plant site can be classified as very corrosive.

Structure-to-Soil Potential Measurements - Sixteen structure-to-soil potential measurements were taken about the PFB Pilot Plant site using a copper-copper sulphate ($Cu-CuSO_4$) reference electrode.

Structure-to-soil potential measurements are another index of galvanic corrosion potential. Metallic structures which are more negative in a galvanic series tend to corrode to metallic structures which are more positive. Potential measurements taken about the PFB Pilot Plant site indicate a propensity for galvanic corrosion with potentials varying between -0.22 volt and -0.66 volt.

Resistance-to-Earth Measurements - Two resistance-to-earth measurements were made on the existing boiler house grounding system. Measurements were made using the three terminal method. The approximate resistance-to-earth of the existing boiler housing grounding system was measured at 0.22 ohms. This low resistance value indicates that no special grounding provisions for the Pilot Plant will be required. It was recommended, however, that the proposed grounding system be interconnected with all existing contiguous substructures, including the boiler house grounding system and all other grounding systems.

3.7 FAILURE MODE AND EFFECTS ANALYSIS

During this period the PFB Pilot Plant FMEA has been completed with emphasis placed on the new technology components involved in the plant along with interface areas with the Total Energy System and the feed systems.

The level of detail achieved in the FMEA analysis for the Pilot Plant is to the subsystem - level 2. Typical functional level breakdown structures are shown in Figures 3.17 through 3.22, where the initial level is the Pilot Plant Power Generating System. Some of the systems such as the coal preparation system represents a collection of equipment which is either existing or commercially available and represents "off-the-shelf" technology and componentry. Therefore, these systems, where reliability and safety can be expected to have matured, were not broken down to the subsystem - level 2 for FMEA study.

FUNCTIONAL LEVEL BREAKDOWN STRUCTURE - COAL FEED SYSTEM

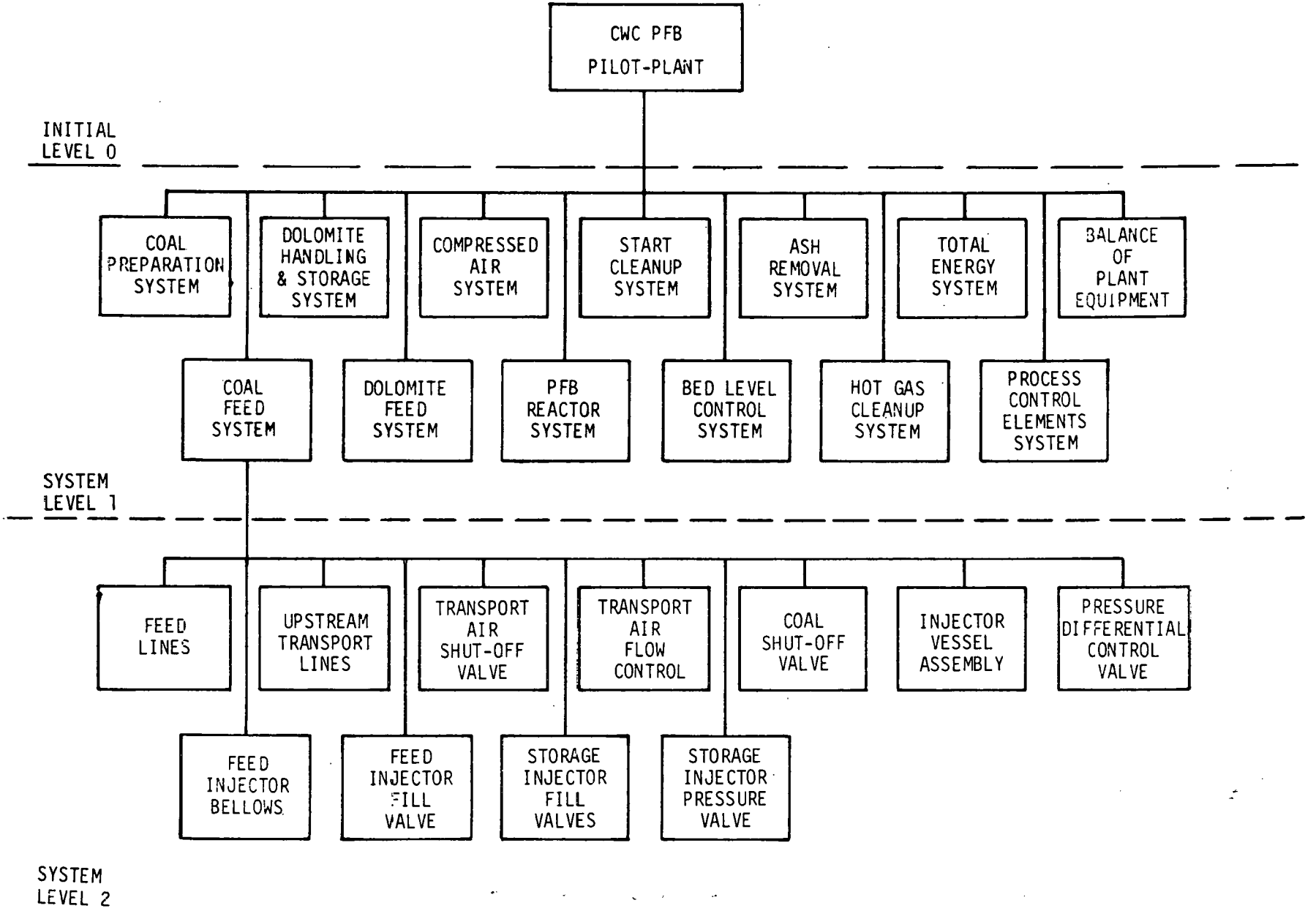

Figure 3.17

FUNCTIONAL LEVEL BREAKDOWN STRUCTURE - PROCESS CONTROL VALVE SYSTEM

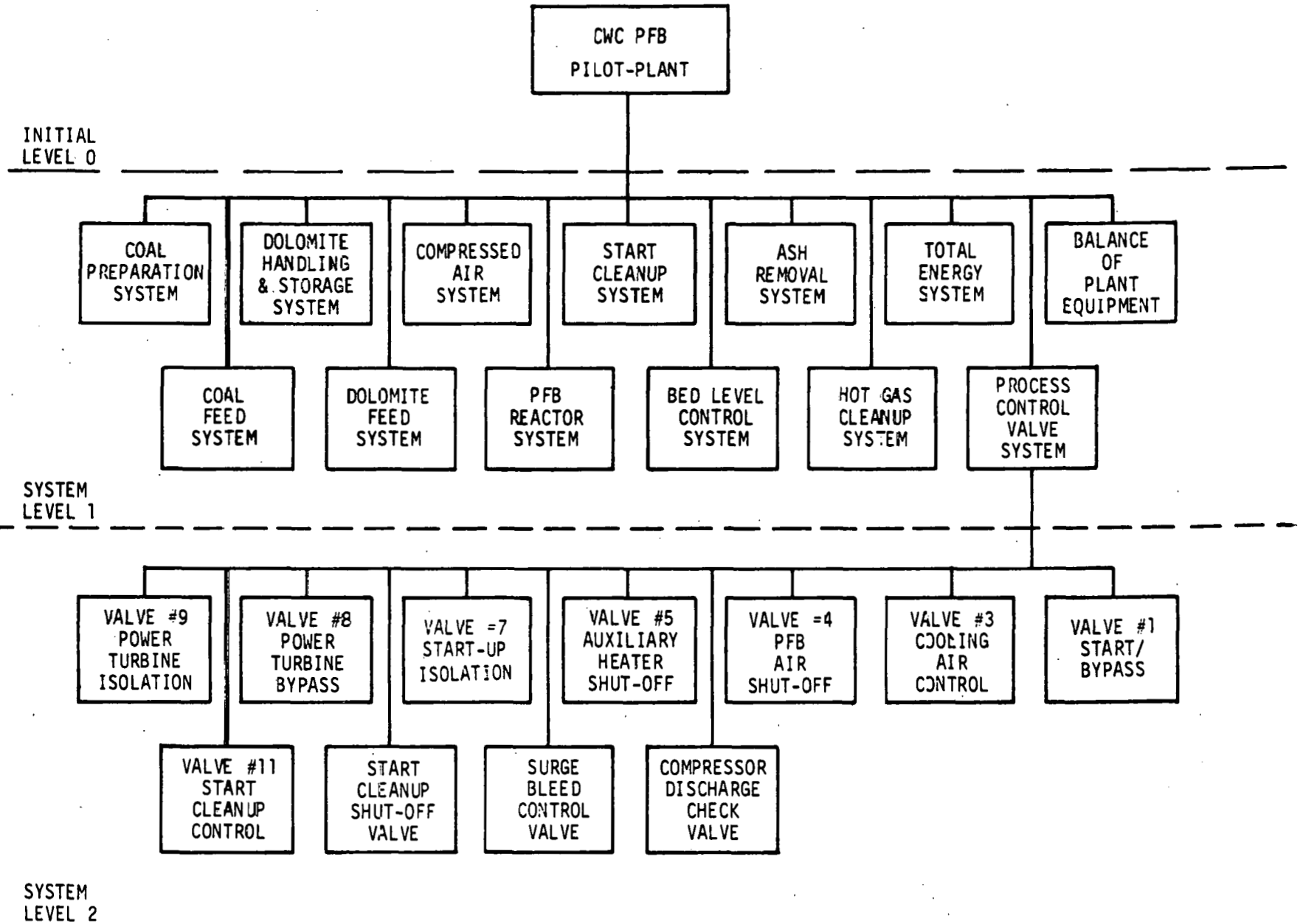

Figure 3.18

FUNCTIONAL LEVEL BREAKDOWN STRUCTURE - PFB REACTOR SYSTEM

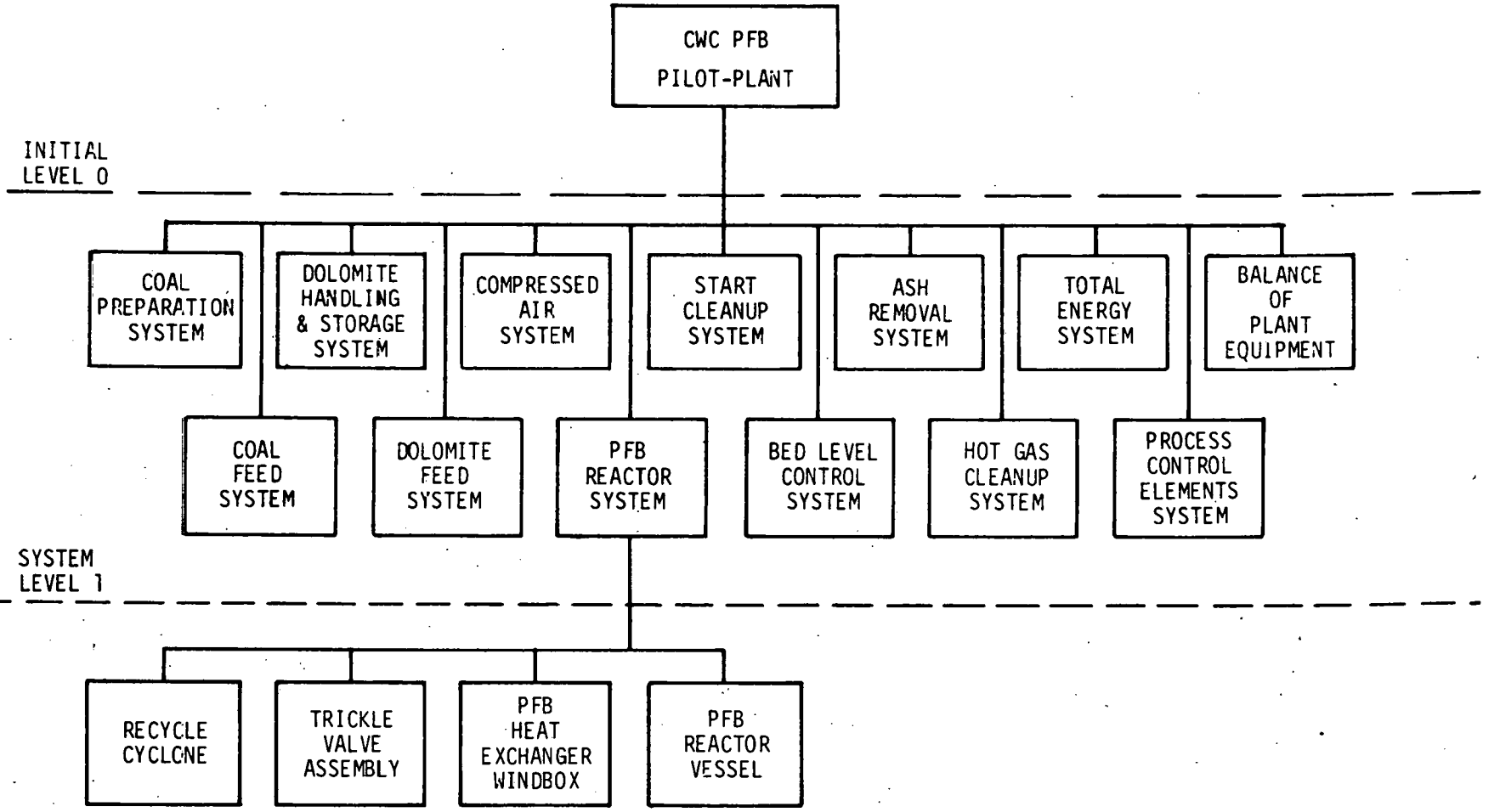

Figure 3.19

FUNCTIONAL LEVEL BREAKDOWN STRUCTURE - BED LEVEL CONTROL SYSTEM

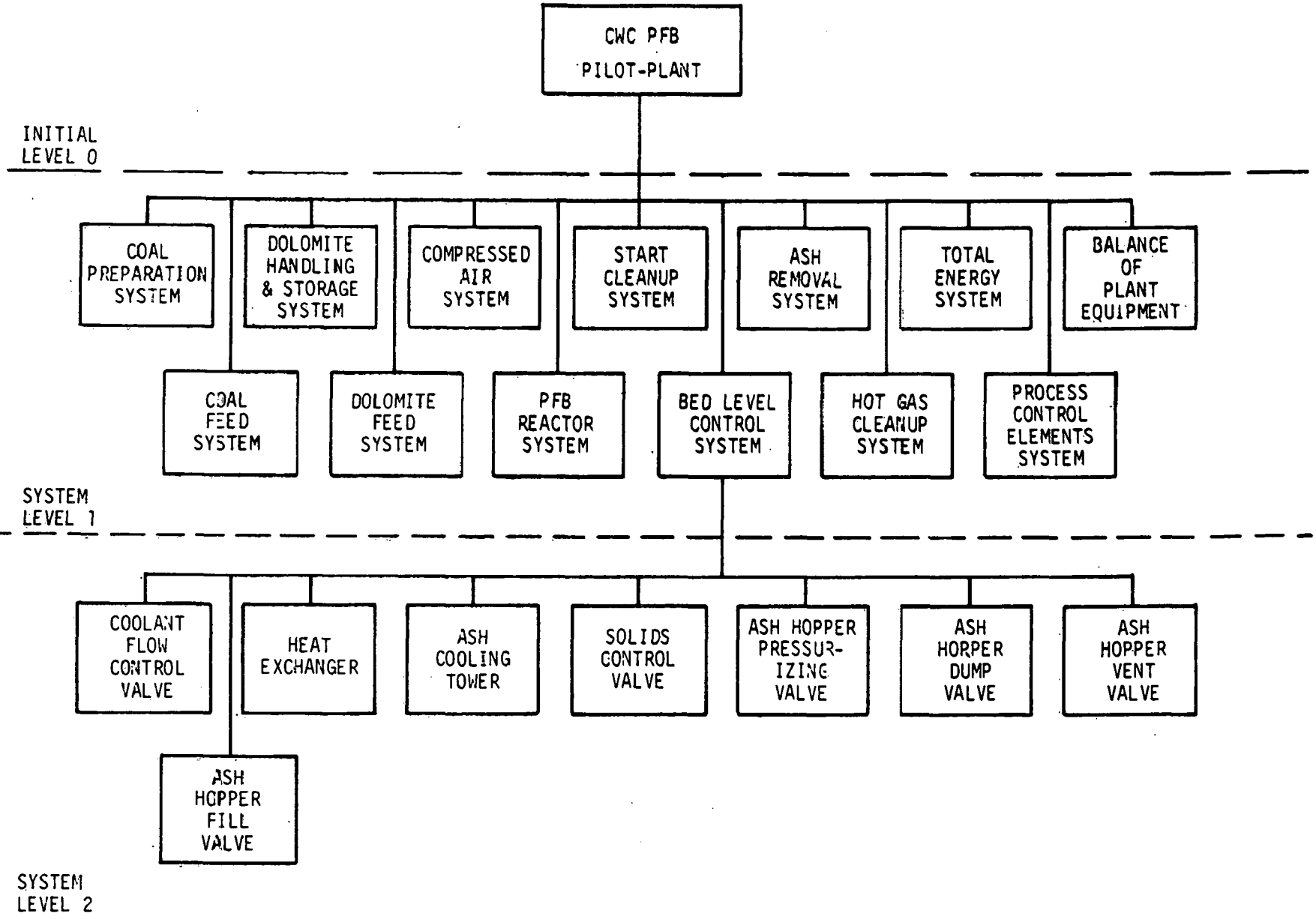

Figure 3.20

FUNCTIONAL LEVEL BREAKDOWN STRUCTURE - HOT GAS CLEANUP SYSTEM

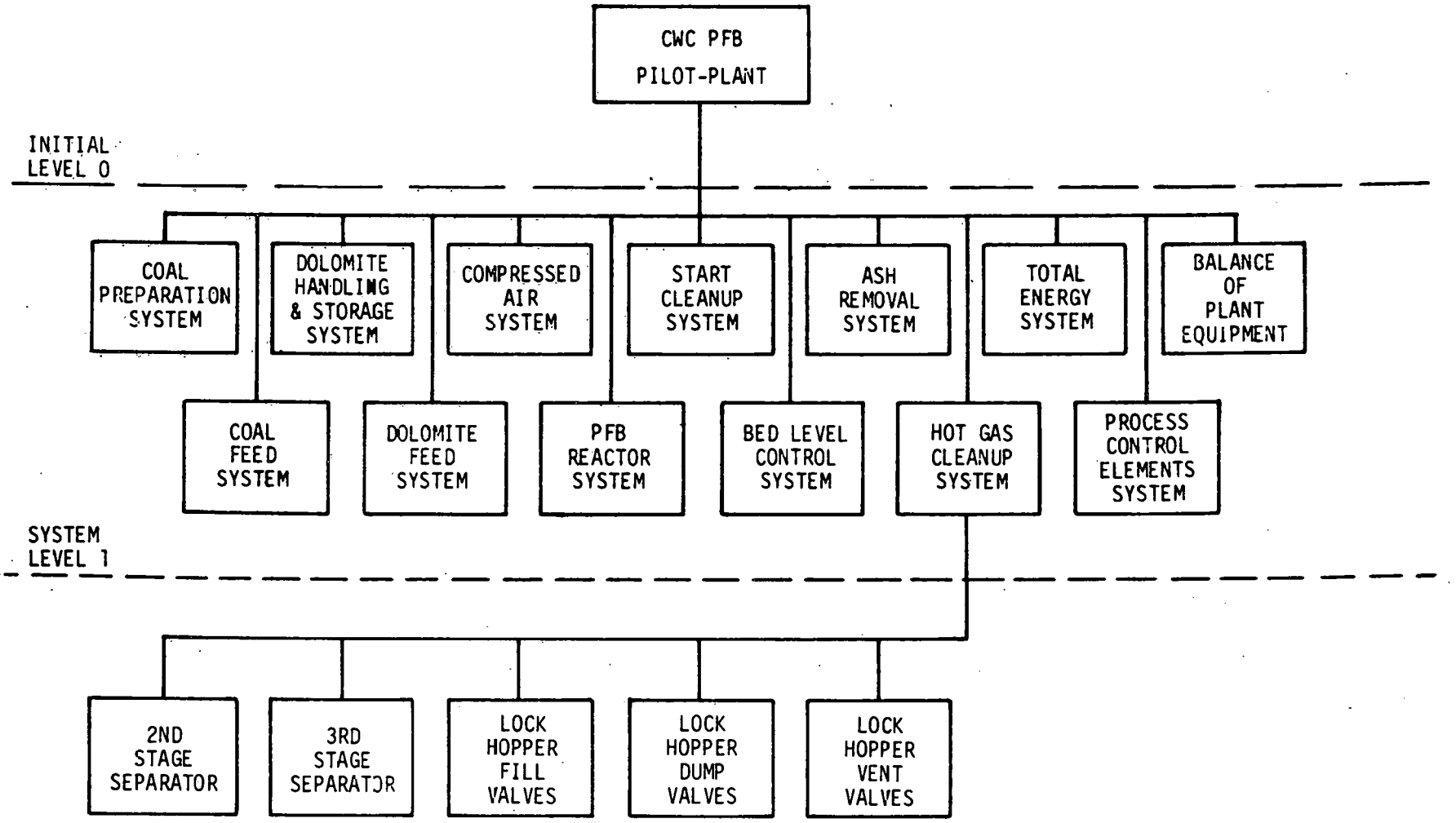

Figure 3.21

FUNCTIONAL LEVEL BREAKDOWN STRUCTURE - TOTAL ENERGY SYSTEM

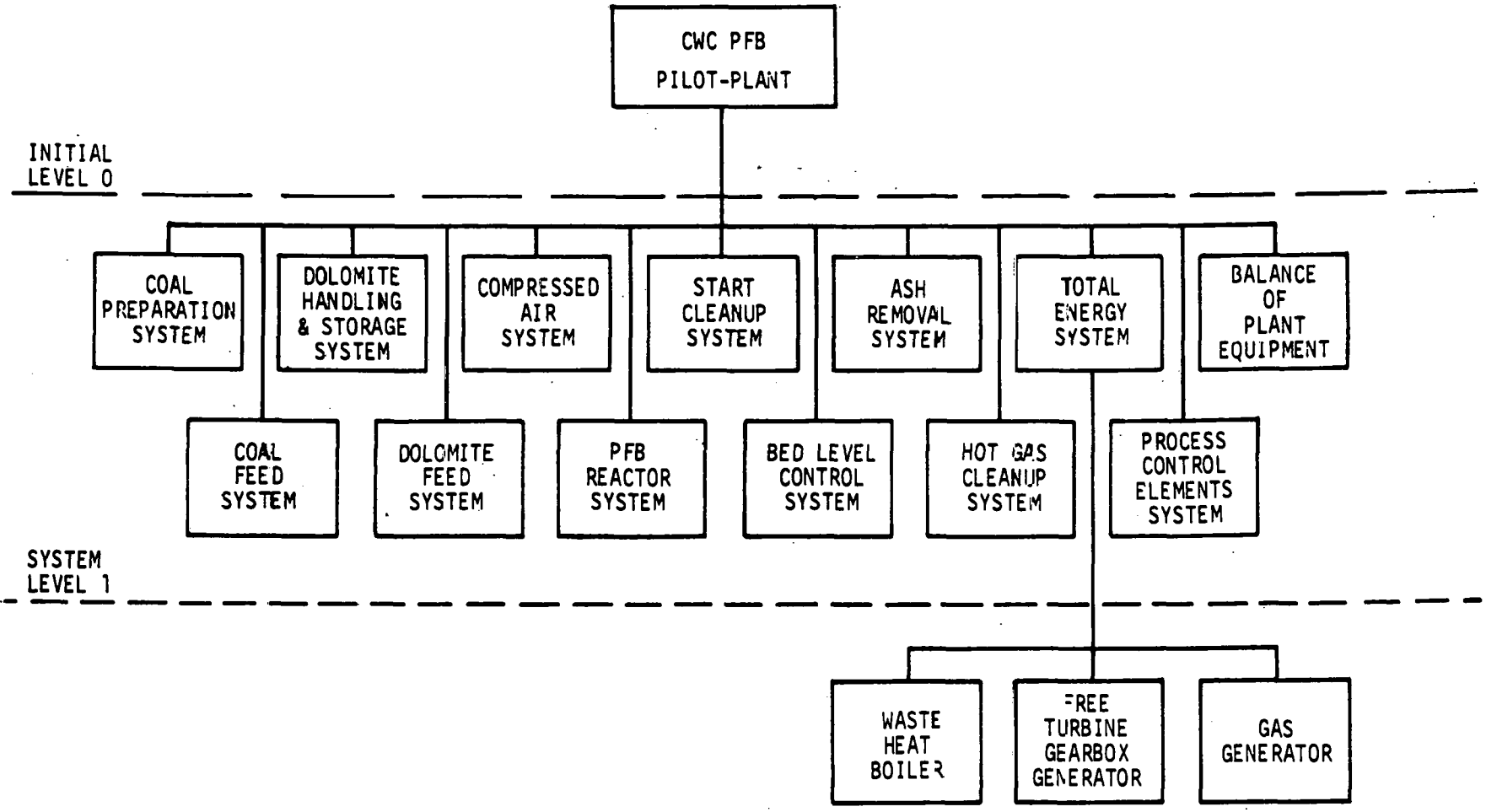

Figure 3.22

Hazardous failure modes have been substantially eliminated by the cycle selection of the PFB air heater design. In contrast to boiler/steam systems, system pressures are limited by the capability of the gas turbine in the existing Total Energy System. The capability of auxiliary sources of high-pressure air is small relative to the volume and flow areas of the PFB air heater.

System temperatures are effectively limited by the massive thermal inertia of the PFB and the air-to-air heat exchanger which assures close control of temperature in response to changes in fuel flow and airflow.

The PFB air-heater design is particularly insensitive to small leaks and also eliminates the waterside corrosion of heat exchanger tubes.

Categorizing the class of failure modes has been accomplished using the following definitions:

Class 1: A Class 1 failure mode represents a potential threat to human life or systems at level 1 or higher. A summary of Class 1 failure modes for the Pilot Plant is shown in Figure 3.23.

Class 2: A Class 2 failure mode represents a potential threat to major equipment at level 1 or lower and should result in extended periods of level 0 inoperability.

Class 3: A Class 3 failure mode represents a potential threat to level 0 operability and may result in extended periods of level 0 inoperability.

Class 4: A Class 4 failure mode should have little or no effect on operability at level 1 or higher.

It should be noted that the class of a failure mode is assigned with regard to its effect or hazard level and without regard to likelihood of occurrence.

SUMMARY OF CLASS 1 FAILURE MODES

System	Item	Failure Mode and Effect Summary	Planned or Implemented Corrective Action	Class
Coal Feed	Feed Lines	Rupture of feed line(s) causes a reversal of pressure differential in the lines with reverse flow of hot combustor products from the PFB. This flow will exit at the break along with fresh coal and transport air creating a potential for an open fire. If the phenomenon takes place near the injector vessel, a potential for fire exists.	Due to a large number of failure modes in the coal feed system with a similar effect, quick-acting shut-off valves will be installed in the feed lines. Controls logic design will operate these valves, and injector vessel shut-off valves when line Δp and line flow reverses. SGT/PFB testing is being conducted to evaluate parameters for sensing such as line pressure, temperature, etc.	1
	Transport Air Supply Lines	Line rupture or massive leak causes reverse flow of hot combustor products from the PFB into the area of the injector vessel, creating potential for fire.	Same as feed lines.	1
	Injector Vessel Pressure Relief Valve	Failure of the pressure relief valve vents the vessel to atmospheric and may "suck" hot combustor products into the injector vessel with a potential for fire.	Same as feed lines. Also relief valve flow area may be sized to allow injector pressurizing valve to maintain injector pressure at safe levels.	1
	Injector Expansion Bellows	Rupture of the bellows causes loss of injector pressure and flow of PFB combustion products into injector vessel.	Same as feed lines.	1

Figure 3.23 (Sheet 1 of 4)

SUMMARY OF CLASS 1 FAILURE MODES

System	Item	Failure Mode and Effect Summary	Planned or Implemented Corrective Action	Class
Coal Feed	Primary Injector Feed Valve	Opening of the valve during the feed cycle of the primary injector has the same effect as the rupture of the bellows with the potential for fire.	Same as feed lines. Also interlock will be provided to prevent opening of valve when storage injector is at low pressure. Valve will be a failsafe closed valve.	1
	Storage Injector Fill Valve	Opening of the valve during the fill cycle of the primary injector has the same effect as failures of the expansion bellows or the primary injector fill valve with the potential for fire.	Same as feed lines. Also interlock will be provided to prevent opening of valves when storage injector is under pressure. Valve will be a failsafe closed valve.	1
Bed Level Control	Ash Hopper Dump Valve	Opening of the valve during the fill cycle causes an immediate and large dump of bed ash since the bed level control system is vented to atmosphere. If the water in the water-cooled ash cooler H/E is converted to steam, the heat exchanger may overtemp and fail the ash cooler.	The dump valves will incorporate redundancy and each will be failsafe closed. As well, the valves will be interlocked to prevent opening while hopper is under pressure.	1
Hot Gas Cleanup	Lock Hopper Dump Valve	Valve opening during lock hopper fill vents process to atmosphere through the ash transport system. The lock hoppers are unlined and will heat up very quickly.	Lock hopper dump valves will be redundant and failsafe closed. Also the valves will be interlocked to prevent opening while lock hopper is under pressure.	1

Figure 3.23 (Sheet 2 of 4)

SUMMARY OF CLASS 1 FAILURE MODES

System	Item	Failure Mode and Effect Summary	Planned or Implemented Corrective Action	Class
Total Energy System	Electrical Generator, Gearbox, Power Turbine	A loss of electrical load due to a breaker relay trip causes the power turbine, gearbox and generator to accelerate immediately toward overspeed which could terminate in the release of high energy rotating parts.	Several systems have been investigated for protection of the rotating machinery during loss of load. The current design utilizes a Valve No. 9 to isolate the power turbine and generator from the gas generator exhaust and Valve No. 8 to bypass the gas generator exhaust into the waste heat boiler. The CWC PFB Dynamic Simulator has been used to establish required system time response characteristics to avoid hazardous rotor overspeeds. Valves are redundant and failsafe open to assure availability at breaker trip.	1
Process Control	Valve No. 8 Power Turbine Bypass	Inadvertent opening or failsafe opening at design causes the gas generator exhaust area to increase. Rotor speed increases and should reach overspeed condition.	Valve must be a failsafe open valve to assure availability during the breaker trip. Valves are redundant and completely independent to achieve a smaller increase in area when one valve fails open. Valve No. 9 closes on a gas generator overspeed trip to reduce the gas generator speed. Also Valve No. 8 position will be interlocked with Valve No. 9 to prevent opening Valve No. 8 with a control while Valve No. 9 is open. The CWC PFB Dynamic Simulator has been used to establish Valve No. 9 valve response characteristics to Valve No. 8 opening.	1

Figure 3.23 (Sheet 3 of 4)

SUMMARY OF CLASS 1 FAILURE MODES

System	Item	Failure Mode and Effect Summary	Planned or Implemented Corrective Action	Class
Process Control (Cont.)	Valve No. 8 Power Turbine Bypass	Closing of the Valve No. 8 during start-up mode causes gas generator exhaust pressure to exceed the capability of the exhaust structure risking a possible rupture.	Valve No. 8 is redundant and each is a failsafe open valve. They have independent muscle and signal. Each is interlocked to prevent closing while Valve No. 9 is closed.	1
	Valve No. 9	Inadvertent or failsafe closing of Valve No. 9 causes gas generator exhaust pressure to exceed the design limitation of the exhaust structure, with a resultant danger of rupture. The valve must be a failsafe closed valve to assure availability during breaker trip.	A control system signal will be provided to open Valve No. 8 when Valve No. 9 leaves the open position. Valve time response characteristics required will be determined by the PFB Dynamic Simulator. An alternative/ supplementary rupture disc is under investigation in the event time response characteristics of Valve No. 8 are marginal.	1

Figure 3.23 (Sheet 4 of 4)

Design margins or failsafe devices or other features do not affect the class of a failure mode. It should also be noted that the actual effect and therefore, a failure class is a matter of judgment in many cases. Therefore, it may not be assumed that the occurrence of any class type failure will result in the effect associated with that class of failure and thus class designation of a failure mode is inherently conservative.

SGT/PFB Technology Unit - Over 3000 hours of actual PFB experience have been accumulated on the SGT Technology Unit for the Pilot Plant. The SGT rig has been operating at the Curtiss-Wright Corporation, Wood-Ridge Facility since July 1977. Most of the Pilot Plant systems, including the coal-feed system, PFB combustor, hot gas cleanup system, bed level control system, process control energy conversion system, but with the exception of the Total Energy System, are represented by SGT rig hardware. The Total Energy System which will be modified for use with the Pilot Plant, has been operational as a power generating system since 1970. This operating experience (SGT Technology Unit and Total Energy System) was utilized in the Pilot Plant FMEA analysis.

Section 4.0

PHASE III - CONSTRUCTION

Early in this reporting period, funding approval was received from DOE for procurement of long-lead items consisting of raw material and certified drawings of subcontractor equipment. These items have an impact on the Critical Path Schedule, Figure 4.1, for the construction phase of the Pilot Plant Program.

Advertising for subcontractor bidders for Pilot Plant Construction Bid Packages was initiated during the latter part of this reporting period. Advertisements were placed with Engineering News Record, Electric World, and Dodge Reports. A minimum of 30 days are provided for bidders to submit their interest and qualifications.

4.1 LONG-LEAD EQUIPMENT

Certified engineering design drawings for the major equipment components to be installed within the Pilot Plant structure will pace completion of the structural design. In order for work to proceed in a timely manner and within established schedules, purchase orders for the engineering design of the equipment have been placed for the following:

1. Coal Handling System
2. Dolomite Handling System
3. Ash Handling System
4. Coal and Dolomite Feed System
5. Coal Crushing and Drying System
6. Lower Vessel Lifting Rig
7. Facility Electric Elevator

PHASE III PFB PILOT PLANT CONSTRUCTION
SIMPLIFIED CRITICAL PATH SCHEDULE

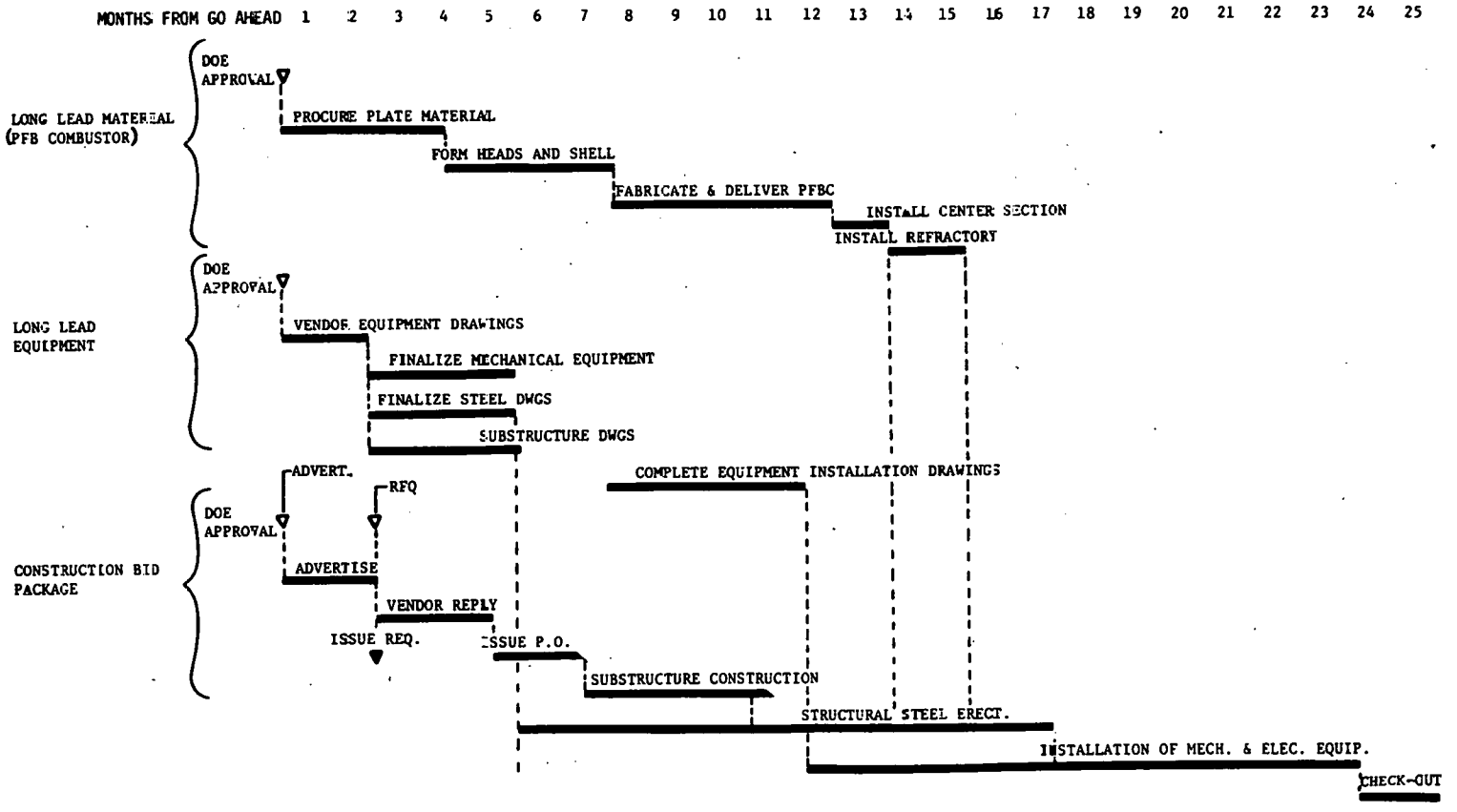

Figure 4.1

PFB-II-306

Although these purchase orders only released the engineering design, they contain the requirements for the procurement of the hardware by amendment at a later date. The terms of these purchase orders provide for a fixed hardware price through February 4, 1980 and include an escalation index through May 1980. Other significant items include warranty, terms of payment and performance bond coverage through acceptance.

4.2 LONG-LEAD RAW MATERIALS

The following items of long-lead material for the PFB combustor and major process components (Figure 4.2) were released to fabrication during this period:

1. Hemihead for Upper Vessel
2. ASME Head for Lower Vessel
3. ASME Head for Recycle Cyclone
4. Flanges for Upper and Lower Vessels
5. Van Stone Flange for Recycle Cyclone
6. Fineline (Controlled Quality) Plate for PFB Combustor Vessel
7. Alloy Plate for Recycle Cyclone
8. Tooling for Welding Hemihead

A photograph of the ASME head for the lower vessel is shown in Figure 4.3.

4.3 LONG-LEAD PROCESS DEVELOPMENT

The objective of the 5" diameter heat exchanger tubular samples processed during the reporting period was to initially demonstrate that the new resistance welding equipment process and tooling will produce resistance welds with sufficient shear strength to prevent the occurrence of excessive braze joint gaps by shifting or loosening of the channels to be brazed.

The welding power source was a 75 KVA link portable tack welding machine. Air pressure was tapped directly into the shop lines approximately 120 psi.

PILOT PLANT PFB
LONG LEAD COMPONENTS

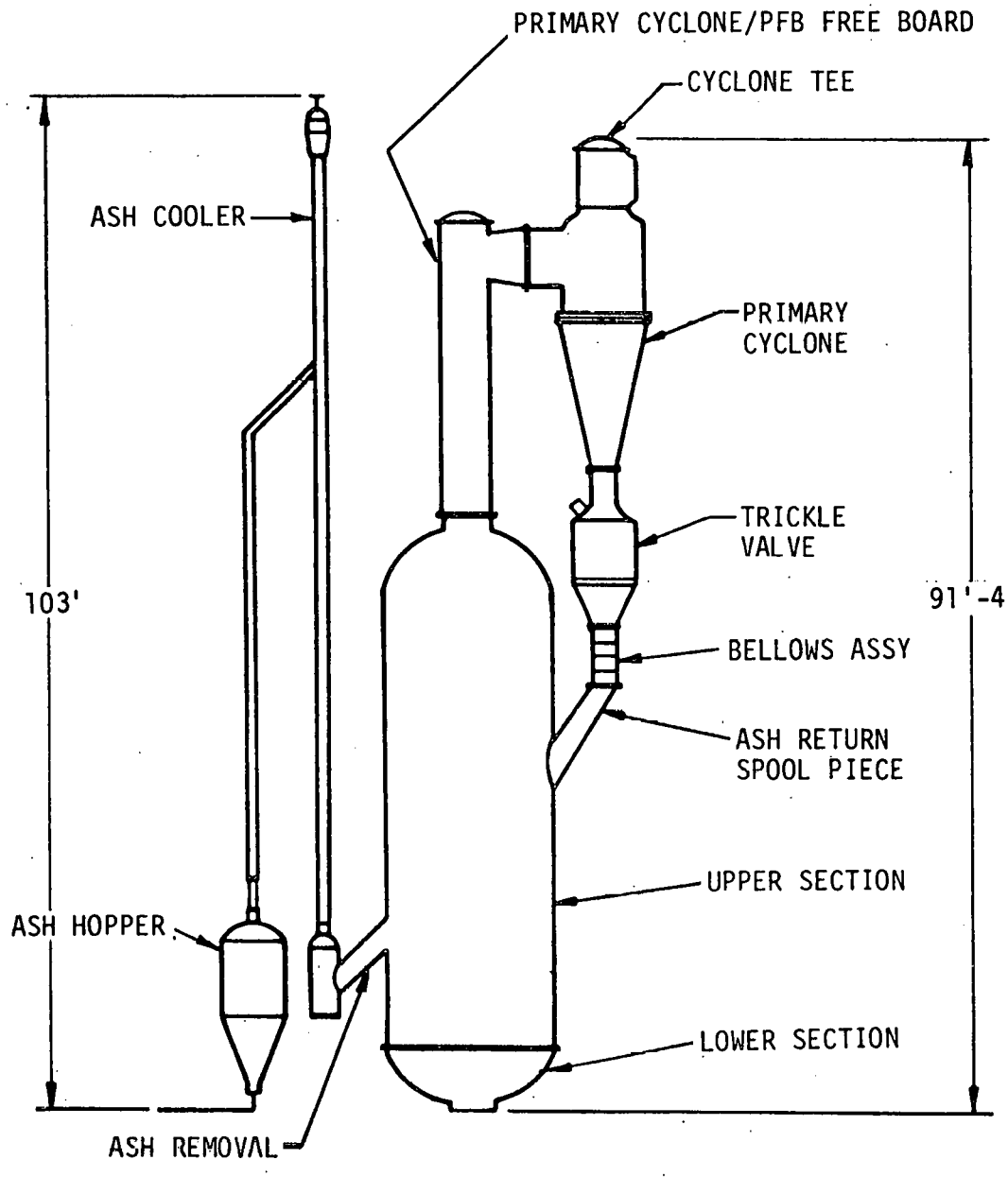

CURTISS-WRIGHT CORPORATION

Figure 4.2 PFB-II-226

PFB VESSEL LOWER HEAD

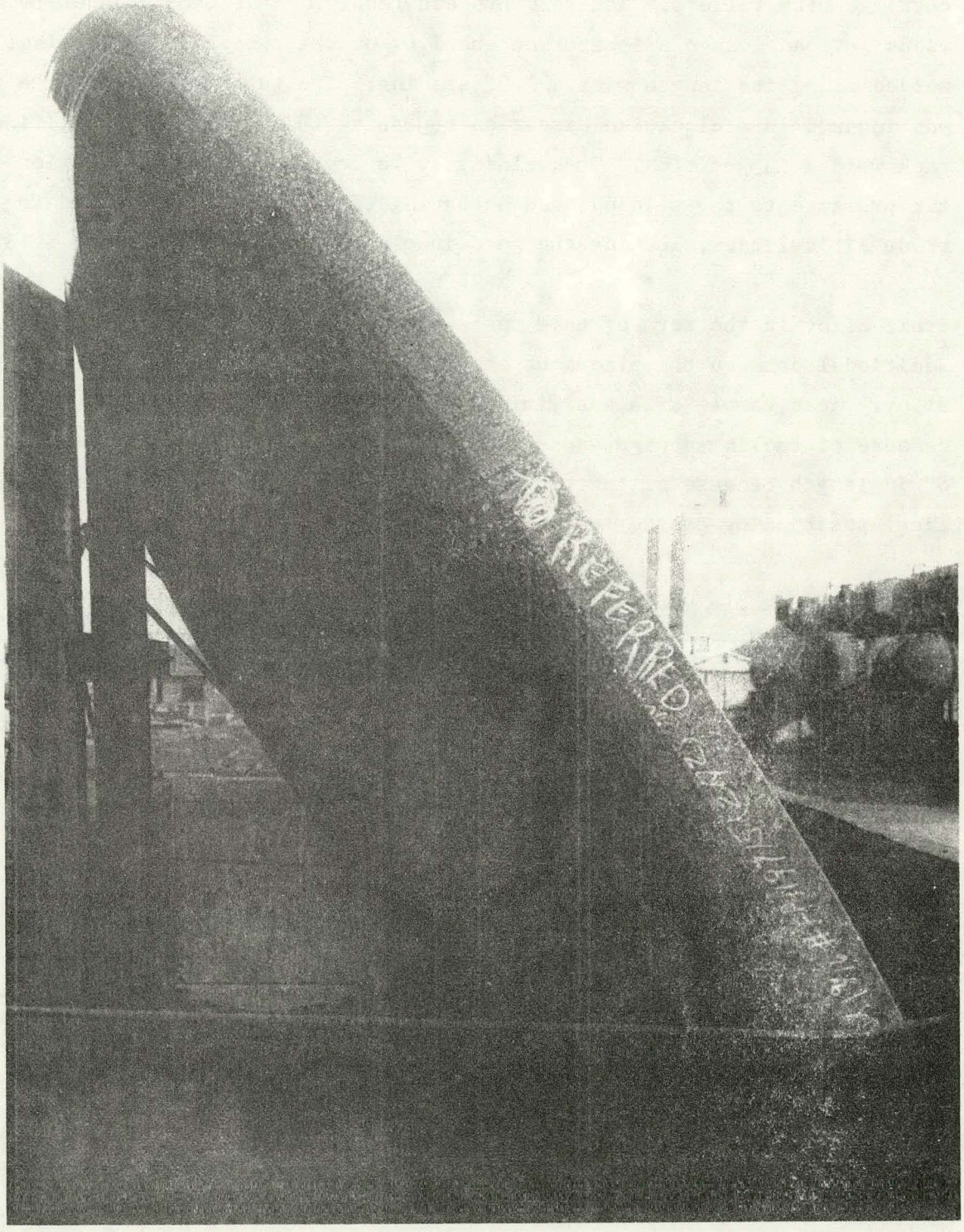

Figure 4.3

These air lines were attached to the welding head, mounted on one end of an 8' long shaft that located in the I.D. of the 5" tube, that in turn rested on a carriage with rollers. The weld process required that each channel be individually loaded into a locator on the I.D. of the tube and longitudinally spot welded along its length with a 1.5" spacing. The tube sample would be rotated and indexed in a clockwise direction repeating this cycle until all fins were tack welded in position. The welding cycle began with the application of the air pressure to the welding head actuating the following wheels and the electrode air cylinder, locking the head in place ready for resistance welding.

Braze alloy in the form of tape was added to the fins, to collect some limited additional data on the placement and application of No. 150 nicrobraze eutectic alloy. Test sample size was limited to 12" in length for resistance welding because of tooling design and available tubing material. Braze samples were 8" in length because of the vacuum braze furnace work load area and the vertical positioning of the test samples for gravitational braze flow.

The initial sample was tack welded and brazed. One-third of the fins showed no evidence of spot welds. Examination of this sample indicated poor surface finish on the I.D. of the tube.

Sample 1-2 was processed with the I.D. of the tube machined to improve the pitted I.D. surface finish, and manual tungsten arc tack welds made at each end of all channels. All fins brazed to the tube and there was no evidence of poor resistance welds. Sample 1-3 incorporated an improved holder and resistance welding electrode design that demonstrated improved shear strength values (Table 4.1). Sample 1-4 was deliberately made with braze defects for the non-destructive testing (NDT) ultrasonic technique (UT) development program. The remaining Samples 1-5, 1-6 and 1-7 were processed during this period and demonstrated acceptable resistance welds.

TABLE 4.1

TUBE/FIN TACK WELD SHEAR STRENGTH VALUES

	Original Electrodes and Holder	New Electrodes and Holder
Sample 1-1	470 Pounds	480 Pounds
Sample 1-2	435 Pounds	510 Pounds
Sample 1-3	420 Pounds	600 Pounds
Average	441 Pounds	530 Pounds

Since there was no comprehensive NDT method developed at this time for determining whether the samples had 90% braze coverage, multiple destructive cross-sections were made and the individual braze joints examined (Figure 4.4). Sections where alloy had not flowed and filled the joints, i.e., gap measurements, were recorded from .001" to .004" on all samples.

Small areas on these samples processed exhibited this intermittent braze condition and accentuated the need for a non-destructive UT test method to completely examine the braze quality. The other data accumulated on Sample 1-7 and others was the width of the braze joint interface for each channel. This measurement is critical to the effectiveness of the heat transfer of each channel. Measurements taken on Sample 1-7, Table 4.2, indicated all brazed channels exceeded a width of .100".

TUBE SPOT WELDING AND BRAZE DEVELOPMENT -
CROSS-SECTION OF TUBE SHOWING BRAZED FINS

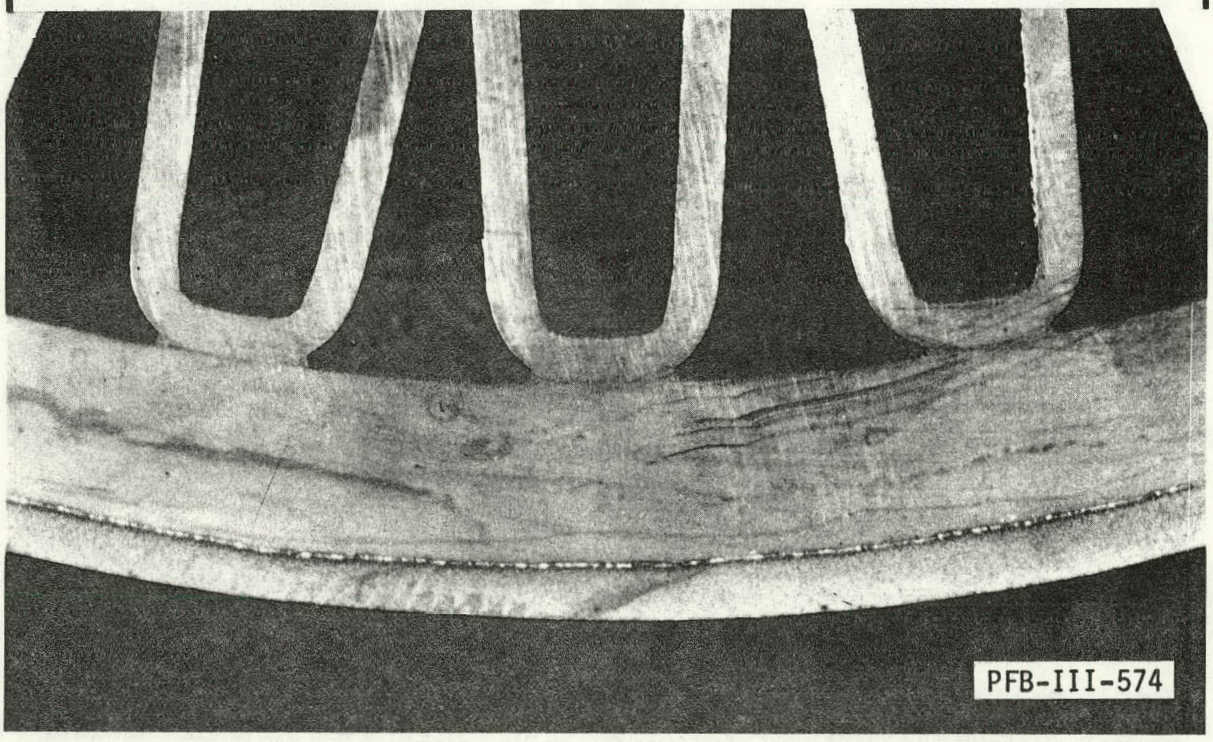

Figure 4.4

TABLE 4.2

FINE BRAZE MEASURED CROSS-SECTIONAL INTERFACE

Fin (Channel Number)	Average * Interface Width
1	.157
2	.445
3	.147
4	.164
5	.145
6	.165
7	.176
8	.169
9	.163
10	.159
11	.163
12	.154
13	.144
14	.155
15	.158
16	.157
17	.163
18	.166
19	.163
20	.163
21	.155
22	.160
23	.168
24	.170
25	.157
26	.170
27	.171
28	.157
29	.159
30	.176
31	.154
32	.154
33	.156
34	.161
35	.160
36	.159

* Average of four measurements taken along length of 8" sample tube.

*U.S. GOVERNMENT PRINTING OFFICE: 1981-740-145/2804